SURFACE-DIRECTED ASSEMBLY OF FIBRILLAR EXTRACELLULAR MATRICES

A Doctoral Thesis

Presented to

The Academic Faculty

by

Jeffrey R. Capadona

In Partial Fulfillment

of the Requirements for the Degree

Doctor of Philosophy in Chemistry

Georgia Institute of Technology

May 2005

SURFACE-DIRECTED ASSEMBLY OF FIBRILLAR EXTRACELLULAR MATRICES

Approved by:

Dr. David M. Collard, Chair
School of Chemistry and Biochemistry
Georgia Institute of Technology

Dr. Andrés J. García, Co-Chair
Woodruff School of Mechanical Engineering
Georgia Institute of Technology

Dr. Marcus Weck
School of Chemistry and Biochemistry
Georgia Institute of Technology

Dr. Loren Williams
School of Chemistry and Biochemistry
Georgia Institute of Technology

Dr. Elliot L. Chaikof
Chief of Vascular Surgery
Emory University

Date Approved: April 11, 2005

FOR MY FAMILY

Without the love of a family, there is nothing else.

“Good, Better, Best! Never let it rest until your Good is Better, and your Better is BEST.” -Grandpa Startz

Thanks you for helping me become “my best.”

ACKNOWLEDGMENTS

Earning my Ph.D. was a very challenging race that would have been impossible to complete without the love and support of several people. I would like to thank Professor David Collard, my advisor, for recognizing my goals for my Ph.D. during my recruitment, and providing me with not just the opportunity, but the guidance and knowledge to surpass my goals and prepare me for my future. I would also like to thank my “co-advisor”, Professor Andrés García for several things. You have been everything that I could ask for in a true mentor and friend. Thank you for your compassion, dedication, and for challenging me to become my best by never giving up on even the most difficult tasks. You will be the measure of all future bosses. Susi (Coons) Moore, I would not be a “chemist” if it was not for your help in the early stages of graduate school, thank you. I also have to thank all past and present members of the García lab. Ben and Nate, my office mates, thanks for making every day exciting and for the continuous “stimulating” conversations, countless welcomed distractions and mind-numbing music; beware of the eels. Kristin, thanks for always taking the lead with the ebeam, and not killing me every time I broke it. Catherine, thanks for your silent leadership in the lab, and your help with the numerous adventures in radio-labeling. Charlie, thanks for testing the limits of my compulsive cleanliness disorder and for introducing me to bar poker. Jen, thanks for keeping me on my toes with your sarcastic wit. Tim, thanks for working crazy hours and

keeping me driven late into the night. It would have been harder to work those hours in an empty lab with no one but Zuma. Lindsay and Kellie, thanks for keeping the lab in order and making every day events manageable. Heung-soo, thanks for helping me with the trouble-shooting of numerous experiments.

A special heart felt THANK YOU to two of the best friends I could ask for, Colin and Denise. You have gone beyond the call of friendship on so many occasions. Most notably, by opening your house and giving me a HOME during the final weeks/months of this process. Thanks for being the truest friends in every sense of the word. I would not have made it without your support and company.

Most significantly, I must acknowledge the support and love my whole family has provided throughout the years. Thank you Mom, Dad, Jenny, and Kris for believing in me when I did not, and for never doubting that I could do it. I am eternally grateful to my best friend and soul mate, my wife, Lynn Anne. Lynn, you are my reason and motivation for everything that I do. Without you I would never had been able to jump any of the hurdles of graduate school. Life is not about what you accomplish, or how hard you work… It is about what you take the time to enjoy. Thank you for being my biggest distraction and helping me truly enjoy every moment of our life. It became very evident in the final months of graduate school when you were 700 miles away, that even when you were not here to feed my body, phone calls, cards, pictures, and memories of you fed my soul. You are my everything. Wife, you are my life!

This work was funded by the National Science Foundation (CAREER BES-0093226) and the Georgia Tech/Emory NSF ERC on the Engineering of Living Tissues (EEC-9731643).

TABLE OF CONTENTS

LIST OF FIGURES

LIST OF SYNTHETIC SCHEMES

SUMMARY

Biologically-inspired materials have emerged as promising substrates for enhanced repair in various therapeutic and regenerative medicine applications, including nervous and vascular tissues, bone, and cartilage. These strategies focus on the development of materials that integrate well-characterized domains from biomacromolecules to mimic individual functions of the extracellular matrix (ECM), including cell adhesive motifs, growth factor binding sites, and protease sensitivity. A vital property of the ECM is the fibrillar architecture arising from supramolecular assembly. For example, the fibrillar structure of fibronectin (FN) matrices modulates cell cycle progression, migration, gene expression, cell differentiation, and the assembly of other matrix proteins. Current biomaterials do not actively promote deposition and assembly of ECM. In this research, we describe the rational design and investigation of non-fouling biomimetic surfaces in which an oligopeptide sequence (FN13) from the self-assembly domain of FN is tethered to non-fouling substrates. This surface modification directs cell-mediated co-assembly of robust fibrillar FN and type I collagen (COL) matrices reminiscent of ECM, and increases in cell proliferation rates. Furthermore, the effect of this peptide is surface-directed, as addition of the soluble peptide has no effect on matrix assembly. We have also identified a critical surface density of the immobilized peptide to elicit the full activity. These results contribute to the development and design of biomimetic surface modifications that direct cell function for biomedical and biotechnology applications.

CHAPTER 1

SPECIFIC AIMS

The focus of this project was to engineer biomaterial surfaces that modulate cell-mediated assembly of extracellular matrices (ECM) in order to direct cell function. The ECM plays a central role in tissue morphogenesis, homeostasis, and repair,[1] and ECM characteristics are therefore worthy of mimicking to provide control of cellular activities on synthetic substrates. Biological macromolecules provide innovative recognition and structural motifs that have been engineered into substrates to create novel bio-functional mimetic materials.[2,3] However, current materials displaying ECM characteristics, including cell adhesive motifs[2,3] and growth factor binding sites[4] do not reconstitute the fibrillar supramolecular structure of the natural ECM. A vital property of the ECM is the fibrillar architecture arising from its supramolecular assembly. The architecture of the natural ECM is responsible for its dynamic properties. For example, the fibrillar structure of fibronectin (FN) matrices modulates cell cycle progression, migration, gene expression, cell differentiation, and the assembly of other matrix proteins.[1,5-7] Current biomaterials do not actively promote deposition and assembly of ECMs. **The objective of this project was to engineer surfaces that promote the cell-mediated assembly of fibrillar FN. Our central hypothesis was that a short peptide sequence (FN13) from the self-assembly domain of FN tethered to synthetic surfaces will promote cell-mediated fibrillar FN matrix assembly which will in turn**

direct cellular activities. This hypothesis was based on previous studies that have demonstrated that FN13 mediates assembly of FN and collagen (COL) matrices when added to the culture media of several cell types. A significant advantage to our experimental system over previous studies is the use of model surfaces of self-assembled monolayers (SAMs) of alkanethiols on gold. This system allows for the controlled presentation of immobilized ligands on a non-fouling background, and coupled with robust biochemistry and bioengineering approaches, allows for rigorous analysis of the hypothesis.

AIM 1: INVESTIGATE FIBRONECTIN ADSORPTION AND CELL ADHESION TO MODEL NON-FOULING SUPPORTS.

FN adsorption and cell adhesion to CH_3/EG_3 mixed SAMs were investigated using ultra-sensitive techniques. Differences in cell adhesion profiles arise from differences in the densities of adsorbed FN.

AIM 2: ENGINEER MODEL BIOMIMETIC SURFACES THAT PROMOTE FIBRILLAR FN MATRIX ASSEMBLY.

The densities of tethered peptides were evaluated using ELISA and ellipsometry. Both methods indicated that coating concentration (over a fixed time interval) controlled tethered peptide surface density, and that only background levels adsorbed non-specifically. FN matrix assembly was visualized by immunofluorescence staining, and quantified biochemically using Western blot analysis of detergent-insoluble fractions. FN13-tethered surfaces showed the highest levels of assembled FN matrix compared to surfaces with tethered

peptides presenting scrambled sequences, and the current state-of-the-art adhesive peptide sequence, arginine-glycine-aspartic acid (RGD).

AIM 3: COMPARE CELL FUNCTIONS FOR CELLS CULTURED ON FN13-TETHERED SUPPORTS TO CELLS CULTURED ON RGD-TETHERED AND UNMODIFIED SUPPORTS.

Only cells cultured on FN13-tethered surfaces assembled robust matrices with co-assembled FN and type I collagen. The FN13-induced FN matrices were surface directed in that only surface bound peptides (not soluble in culture media) promoted FN matrix assembly. Assembled FN matrices were completely composed of cell- secreted FN, opposed to FN from the culture media. Cells cultured on these FN13-induced FN matrices also showed the highest levels of cell proliferation.

THESIS OUTLINE

This thesis addresses the Specific Aims outlined above, and is organized in the following manner. Chapter 2 provides background and significance of the field specific to this project. Chapter 3 addresses topics in Specific Aim 1 and the findings described here were used in designing experiments to investigate Specific Aims 2 and 3. Chapter 4 presents results addressing topics in Specific Aims 2 and 3. Chapter 5 discusses the over all conclusions from the thesis work and identifies possible future directions for the project.

REFERENCES

1. Adams,J.C. & Watt,F.M. Regulation of Development and Differentiation by the Extracellular-Matrix. *Development* **117**, 1183-1198 (1993).

2. Hubbell,J.A. Materials as morphogenetic guides in tissue engineering. *Curr. Opin. Biotechnol.* **14**, 551-558 (2003).

3. Langer,R. & Tirrell, D.A. Designing materials for biology and medicine. *Nature* **428**, 487-492 (2004).

4. Zisch,A.H., Lutolf,M.P., & Hubbell,J.A. Biopolymeric delivery matrices for angiogenic growth factors. *Cardiovasc Pathol* **12**, 295-310 (2003).

5. Sakai,T., Larsen,M., & Yamada,K.M. Fibronectin requirement in branching morphogenesis. *Nature* **423**, 876-881 (2003).

6. Sottile,J., Schwarzbauer,J., Selegue,J., & Mosher,D.F. 5 Type-I Modules of Fibronectin Form A Functional Unit That Binds to Fibroblasts and Staphylococcus-Aureus. *J. Biol. Chem.* **266**, 12840-12843 (1991).

7. Sechler,J.L. & Schwarzbauer,J.E. Control of cell cycle progression by fibronectin matrix architecture. *J. Biol. Chem.* **273**, 25533-25536 (1998).

CHAPTER 2

BACKGROUND AND SIGNIFICANCE

Biomaterials are central to numerous biomedical and biotechnological applications including contact lenses, vascular grafts, heart valves, and total joint replacements. Initially, biomaterials were adopted from other areas of science and technology without significant redesign for medical use.[1] These early biomaterials include silicones, polyurethanes, Teflon, nylon, titanium, and stainless steel. While these early biomaterials filled a gap in medical technology, several limitations still existed. Most significantly, immune responses to implanted materials resulted in chronic inflammation and poor host integration.[2-6] Next generation biomaterials consisted of polymers designed specifically for use as biomaterials. Polyesters and polyamides were designed to decrease host immune responses and degrade *in vivo* through hydrolysis. While these materials improved on select functions compared to their earlier counterparts, these polymers lack the ability to direct cell function and mimic the natural extracellular environment. Recent advances in biomaterial science include the development of *biomimetic* materials.[7-10] This class of biomaterials incorporates bioactive motifs from biological macromolecules to control cell function. While some of these recently developed biomaterials mimic the natural extracellular matrices (ECM) through the incorporation of numerous bioactive domains, they do not mimic the spatial and temporal resolution of the natural ECMs. There is an evident need for further advances.

EXTRACELLULAR MATRIX: NATURE'S BIOMATERIAL SCAFFOLD

Native Extracellular Matrix

The ECM is a dynamic network of proteins and polysaccharides secreted and assembled locally by cells.[11] ECMs are constantly undergoing remodeling to maintain the structure and presentation of protein ligands and growth factors. The complex organization of matrix-assembled proteins provides structural support to cells within tissues while also providing signaling cues vital for cellular regulation, development, migration, proliferation, shape and function.[11-18] Important structural proteins of the ECM include collagen (COL) and elastin, while the adhesive components include fibronectin (FN), vitronectin (VN), and laminin (LN). Each of these ECM proteins has domains to which cells adhere. Cells adhere to the ECM using a class of transmembrane proteins called integrin.

FN was the first identified cell-adhesive protein, and is one of the best characterized.[19-23] FN is a large multi-domained glycoprotein found on cell surfaces, in blood and body fluids, and in the ECM (**Figure 2.1**). FN is secreted by cells as a large soluble dimer (220 kDa each), and is assembled within the ECM into a fibrillar high molecular weight insoluble multimer.[24] As demonstrated in a FN-knockout study in mice, FN is essential for embryonic development.[25] Furthermore, integrin (specifically, $\alpha_5\beta_1$) mediated adhesion to FN regulates osteoblast survival and expression of osteoblast-specific genes and matrix mineralization, as well as myoblast differentiation, *in vitro*.[26-28] Matrix assembled FN modulates cell cycle progression, migration, gene expression, cell differentiation, and the assembly of other matrix proteins.[11-18,29]

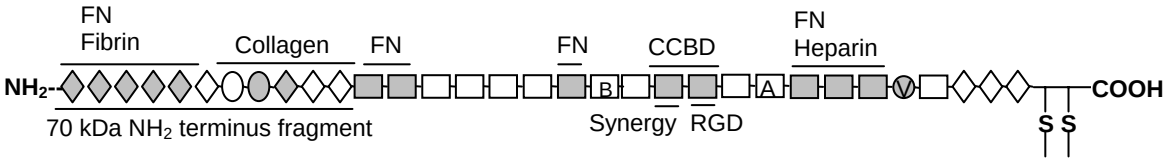

FIGURE 2.1 Schematic model of FN domain structure. This cartoon illustrates the organization of repeating structural domains I (◇), II (⬭) and III (▭),and the variable region, V, (○), the amine and carboxy termini and the disulfide-bridge site of dimerization. Highlighted domains include binding sites for fibrin, collagen, FN (self-assembly), and heparin, as well as the central cell binding domain (CCBD) that includes the RGD binding motif and the PHSRN synergy site. Also highlighted, with shading are domains that have identified roles in FN matrix assembly.

FN Matrix Assembly

The ECM plays a central role in tissue development, homeostasis, blood clotting, wound healing, and cancer metastasis.[30-33] A critical property of ECMs is the assembly of supramolecular structures. The architecture of the natural ECM is responsible for its dynamic properties.[30] Matrix assembled FN modulates cell cycle progression, migration, gene expression, cell differentiation, and the assembly of other matrix proteins.[11-18,29] Matrix assembly of FN involves a complex series of cell mediated events (**Figure 2.2**) that begins with the cellular secretion of soluble FN dimers, and involves the binding of multiple integrin receptors ($\alpha_5\beta_1$, and $\alpha_v\beta_3$) to them.[19,24,34,35] Through cytoskeletal induced tension and receptor motility, FN is assembled into a network of insoluble fibrils stabilized through disulfide cross-linking.[35-38] Cell-induced tension on FN creates conformational changes within individual domains.[39] The conformational changes within FN expose normally buried amino acid sequences, often called "cryptic domains." These newly exposed domains are critical for the presentation of integrin binding sequences and FN-FN binding domains; which are responsible for the robustness of ECMs formed by co-assembled proteins.[40-44]

The development of recombinant FN proteins and the use of integrin- and FN-blocking antibodies has been significant in the isolation of FN self-assembly domains (**Figure 2.1**). Several regions of FN play a role in the assembly of fibrillar FN matrices.[24,45] The first five type I repeats,[15,46] the RGD cell-binding domain,[35] the synergistic cell adhesive region,[34,47] the alternatively spliced V region,[48] the heparin II binding domain,[49] the type $I_{7\text{-}9}$ COL binding domain which

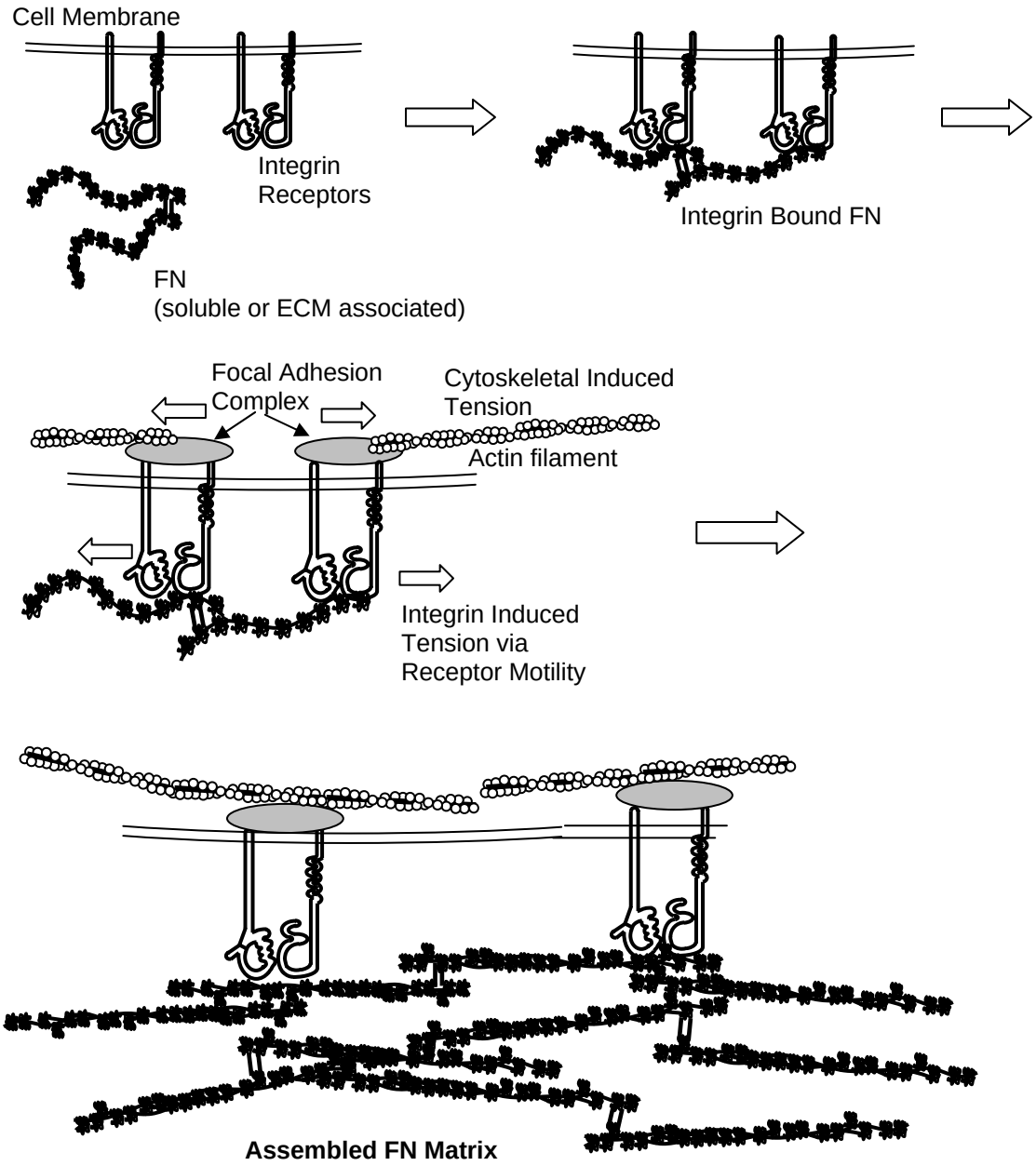

FIGURE 2.2 Cell induced FN matrix assembly. This cartoon depicts the systematic assembly of FN matrices, which begins with integrin binding to FN dimers. Integrin binding of FN initiates intracellular focal adhesion formations, followed by integrin motility along assembled actin filaments creates tension on FN fibrils that exposes cryptic FN-FN binding domains. Finally, exposure of FN-FN binding domains creates high molecular weight multimers of cross-linked FN fibrils.

stabilizes FN fibrils,[50] and an FN-FN binding site in a 14-kDa FN fragment containing the first two type III repeats have all been identified to influence FN matrix assembly.[51,52] The smallest identified sequence of amino acids within FN shown to promote FN matrix assemble is a 13-amino acid stretch (FN13) spanning between the type II_2 and I_7 repeats.[53] Culture media supplemented with several of these sequences regulate cell functions such as matrix assembly, adhesion, migration, proliferation, and the co-assembly of other matrix proteins such as COL.[16,53,54]

ECM MIMETIC MATERIALS

The most significant recent advances in the development of biomaterials have been the development of *biomimetic* materials. These biologically inspired materials are characterized by their ability to interact specifically with their environment to elicit a natural biological response. Biomimetic materials have emerged as promising substrates for enhanced repair in various therapeutic and regenerative medical applications, including nervous and vascular tissues, bone, and cartilage.[55,56] These strategies focus on the development of materials which integrate well-defined domains from biomacromolecules to mimic individual functions of the ECM, including cell adhesive motifs,[10] growth factor binding sites,[57] and protease sensitivity.[58]

Materials Presenting Cell Adhesive Motifs

Pioneering work has identified domains of adhesive proteins present in the ECM, such as the arginine-glycine-aspartic acid (RGD)[59] motif present in FN, the tyrosine-isoleucine-glycine-serine-arginine (YIGSIR) sequence in laminin,[60] and the glycine-phenylalanine-hydroxyproline-glycine-glutamate-arginine (GFOGER) oligo-peptide in collagen (COL).[61,62] Since then, numerous groups have covalently attached or physisorbed these bioadhesive peptides to substrates and scaffolds to promote receptor-mediated cell adhesion and migration in various cell types.[1,8,63-66] The density and distribution of adhesive ligands are important for cell adhesion, integrin clustering, cell migration, and differentiation.[67-71] Numerous studies have shown that there is a critical density of RGD peptide on non-adhesive backgrounds for initial cell attachment.[72-75] Massia and Hubbell have shown that 4×10^5 molecules of RGD per cell were required to promote cell adhesion, integrin clustering and focal adhesion.[73] Peptide density-dependent responses are also important for cell activity and differentiation in numerous cell types including osteoblasts and myoblasts.[70,76-78] Rezania and Healy have shown that surface-bound RGD-containing peptides enhance mineralization of osteogenic cells compared to control RGE-presenting surfaces, and unmodified surfaces.[70]

Although short bioadhesive peptides attached to synthetic surfaces increase cell adhesion, the biological activity of these peptides is significantly lower than that of complete proteins due to the absence of complementary domains.[79,80] Furthermore, short amino acid sequences (RGD) lack cellular

specificity due to its presence in numerous adhesive proteins,[59] and the ability of numerous cell types to recognize that sequence with multiple integrin receptors. Furthermore, the deposition of ECM is significantly reduced in cells cultured on substrates functionalized with increasing densities of RGD containing peptides.[81]

Materials Presenting Growth Factors/ Growth Factor Binding Sites

Growth factors are extracellular polypeptide signaling molecules that stimulate cell proliferation and differentiation. Natural ECMs bind soluble growth factors and regulate their stability, presentation, and delivery to cells.[31,32,82] The biological activity of the growth factor depends on its presentation in space and time.[63] Biomaterials can mimic this event using three different strategies, (1) direct immobilization,[83-85] (2) tethering via immobilized heparin,[86-88] and (3) immobilization via a heparin bridge to heparin binding motifs[89,90] (for review[57]). While some researchers rely on proteolytic release of immobilized growth factors from biomaterial surfaces,[85,91-93] others have shown that immobilized growth factors are as active as the soluble form.[84,87,94] Growth factor ligands immobilized through heparin binding domain, or programmed to release enzymatically most closely resemble the mechanism of the natural ECM.[32,82] The incorporation of growth factors within scaffolds by any of the above-mentioned techniques have been instrumental in enhancing cellular responses to biomaterials.

Materials Incorporating Protease Sensitive Sites

Major enzymes, including matrix metalloproteinase, regulate the ECM structure by removing excess components, remodeling the structure, and releasing growth factors during growth, morphogenesis, and tissue repair.[95,96] Cells migrate through the ECM via the proteolytic degradation of matrix proteins to clear pathways for movement.[8] Proteolytic cleavage domains incorporated into the framework of biomaterials allow cells to mimic this behavior, while promoting cell infiltration and migration.[58,97-100] Cell adhesive ligands can also be incorporated[55,75,101] into materials with proteolytic domains, which serve the role of releasing growth factors to migrating cells.[102] The extent of migration and cell infiltration depends on the protease-substrate activity, adhesion ligand concentration, and the density of cross-links in the material.[103]

While there have been numerous attempts to mimic the functions of the ECM, little work has been directed towards promoting the assembly of cell mediated matrices. Pernodet and colleagues have developed sulfonated polystyrene surfaces which mediate FN fibrillogenesis.[104] While it is evident that the FN in this study was fibrillar, there was no investigation of its biochemical integrity, or the ability of the FN to mediate cellular responses. Cellular assembled ECMs incorporate all of the previously mentioned bioactive domains (**Figure 2.1**) while controlling the spatial distribution of each element to optimize cell function. Synthetic biomaterials prepared to date do not mimic the complete function of the natural ECM. Even though considerable advances have been

made to mimic specific functions of the natural ECM, there is clearly a need for further advances to recreate the functions of natural ECMs.

CELL ADHESION TO SYNTHETIC MATERIALS

Cell adhesion to synthetic surfaces is critical to numerous biomedical and biotechnological applications.[3,105,106] Biomaterials elicit host responses when implanted into living tissues (for review[2]). In most instances, specific binding of cellular receptors to proteins adsorbed onto material surfaces mediate cell-material interactions. For example, many proteins, including immunoglobulins, fibrinogen, and FN, adsorb onto implant surfaces upon contact with physiological fluids.[107-109] These adsorbed proteins mediate the adhesion and activation of platelets, neutrophils, and macrophages which in turn modulate subsequent inflammatory responses.[110-112] Because of the central role of protein adsorption in cell adhesion, inflammation, and tissue formation, extensive research efforts have focused on the control of protein adsorption to synthetic surfaces.

Protein Adsorption to Synthetic Surfaces

Numerous studies have shown that the type, quantity, and structure of adsorbed proteins are influenced by the underlying substrate.[113-118] Surfaces that readily adsorb proteins from solution often offer little control over the type or quantity of protein adsorbed, resulting in lack of specificity. Passively adsorbed proteins undergo a range of processes including a dissociation from the surface

and return to solution, change in orientation, changes in conformation/structure with retention of biological activity, conformational changes resulting in loss of activity, or exchange with other proteins from the solution.[119] García et. al. have shown that substrates with controlled surface chemistries modulate the functionality of adsorbed FN.[116,118] These changes in adsorbed FN structure modulate cell adhesion and higher order cell activities, including myoblast and osteoblast proliferation and differentiation.[28,118,120,121] While passive adsorption of proteins to coat surfaces can offer control over the presentation of proteins to cells in a controlled *in vitro* experiment, protein coated surfaces may elicit a wide range of responses *in vivo*. Non-fouling chemistries offer an alternative strategy for biomaterial surface modifications to both create protein resistant surfaces, and to decrease host responses to implanted devices.

Non-Fouling Protein Resistant Surfaces

Surface chemistries that prevent protein adsorption and render surfaces non-adhesive have emerged as promising biomaterial modifications for minimizing host-implant inflammatory responses and providing a non-specific background for the presentation of bioactive motifs to elicit specific cellular responses.[75,122-130] It is generally accepted that surfaces that readily adsorb proteins will support cell adhesion while surfaces that resist protein adsorption will prevent cell attachment. As a general rule, hydrophobic surfaces promote protein adsorption while hydrophilic surfaces resist protein adsorption. Common methods to create non-fouling protein resistant materials include adsorption or

grafting of carbohydrates (agarose[131], mannitol[132]), proteins (albumin[133]), or synthetic polymers (poly-(ethylene glycol (EG_n),[134] polyacrylamide[135]) onto the surfaces of the material. Each of these techniques has distinct advantage and disadvantages. For example, albumin adsorption to surfaces represents a simple method to decrease initial cell adhesion, but adherent cells are able to remodel surface proteins and deposit their own adhesive matrix proteins.[131] Albumin can also be displaced from surfaces by other adhesive proteins in solution. While carbohydrates often offer longer stability in their ability to retain non-fouling properties,[132,136] small molecule synthesis of these complex functional groups is often more laborious than the simple repeating units of non-fouling polymers (i.e. EG_n, $(OCH_2CH_2)_n$). However, monolayers of short EG containing alkanethiols lose their ability to resist protein adsorption and cell adhesion after seven days in culture.[132] Like most other polyethers, EG containing polymers are subject to oxidative degradation and chain cleavage.[137] Over time, this decrease in EG chain length results in decreases in the ability to resist both protein deposition and cellular infiltration. Increasing the number of EG repeat units significantly increases the stability of EG functionalized materials. While surface modifications have been very successful *in vitro* to prevent protein adsorption and cell adhesion, there is often little correlation between *in vitro* and *in vivo* studies. For example, Park et. al. showed that grafting EG polymers to several biomaterials (including Nitinol stents, glasses, and silicon rubber) reduced protein adsorption and platelet adhesion by nearly 95% compared to unmodified surfaces *in vitro*.[138] However, in the same study, only moderate

improvements were evident *in vivo* (~30% decreases in platelet adhesion). The authors attribute these discrepancies to the extent of tissue damage during implant surgery. While it is important to have flexibility in choosing the correct non-fouling chemistry for the desired application, EG functionalized materials are often considered the standard in protein resistant non-fouling surface modifications for their ease of synthesis and robust non-fouling properties, and are currently used in several *in vivo* applications.[114,129,139,140]

MODEL SUBSTRATES: SELF-ASSEMBLED MONOLAYERS

Model substrates with well-controlled surface properties represent useful tools for the analysis of surface-protein-cell interactions. In particular, self-assembled monolayers (SAMs) of alkanethiols on gold have provided a robust system to systematically investigate the effects of surface chemistry on protein adsorption without altering other surface properties such as roughness.[114,119,141-147] ω-functionalized, long-chain alkanethiolates ($HS\text{-}(CH_2)_n\text{-}\mathbf{X}$, $n \geq 10$) spontaneously assemble from solution onto gold surfaces to form stable, well-packed and ordered monolayers.[148-151] The physicochemical properties of these monolayers are controlled by the tail group, **X**.[152,153] Through the use of straight forward synthetic chemistry, the terminal **X** group of the alkanethiols can be modified to create model systems to study interaction such as wetting,[151,154-157] surface initiated polymerization,[158,159] protein adsorption,[132,160-163] fibrin polymerization,[164] and cell attachment and adhesion.[128,134,165-168] Recently, SAMs have also been used as model systems for the design of biosensors, and

nanoscale switchable surfaces.[169-175] The simplicity of creating surfaces presenting wide ranges of chemistry makes SAMs an attractive method for studying interfacial interactions for numerous applicatoins.

Quantification of Surface Ligand Density

Due to both the organic composition of SAMs and the reflective gold substrates, numerous analytical techniques are available to quantify the density of SAM surface ligands (peptides/ proteins) on the surface. The most common methods to measure surface ligand density include ellipsometry, surface plasmon resonance (SPR), enzyme linked immunosorbent assays (ELISA), direct radiolabeling of ligands, and fluorescent labeling. Ellipsometry and SPR are powerful analytical techniques that were quickly adapted to SAMs because of the reflective nature of the gold substrates. Ellipsometry is used to measure the film thickness of dried samples by characterizing the change in refractive index of the surfaces after exposure to protein (or peptide) solutions. Changes in film thickness can be reproducibly measured with sensitivity of less and 1 Å. Whitesides and colleagues used this method exclusively in early studies characterizing proteins adsorption to SAM surfaces.[146] This method takes representative scans of small sample areas and assumes uniform distribution of ligands on the SAM surface. Because the samples are removed from solution, rinsed, and dried prior to analysis, weak and reversibly bound ligands may not be detected, which can lead to inaccurate measurements. However, with know elliptical constants this technique offer the ability to convert changes in film

thickness to absolute surface density on an undisturbed (without labeling the protein of interest).[176]

SPR is an attractive method for the analysis of ligand density since measurements can be made in real time in solution.[177] Samples are inserted into a flow chamber where they are exposed to ligand containing solutions. These chambers allow for the instantaneous measurements of adsorbates, and are powerful tools for measuring the kinetics of binding phenomena. However, surfaces that are determined to be protein resistant using these techniques are often shown to support cell adhesion.[126,161] These inconsistencies were most likely due to instrumental limitations. The sensitivity of SPR is ~2.0 ng/cm^2.[127]

García et. al. have previously reported using radio-labeled FN that 0.2 ng/cm^2 is sufficient to mediate robust cell adhesions.[120,163,178] While direct radio-labeling of ligands yields the most sensitive measurements (sensitivity of >0.01 ng/cm^2).[178-180] High background signals (i.e. low signal-to-noise) can be associated with ^{125}I measurements if remaining free iodine is not removed from the ligand solution since iodine also has a high affinity for gold.

Another technique commonly used to measure surface ligand density is ELISA. While this technique offers high specificity and accuracy of measurements, it provides only a relative measure of ligand density. In addition, when measuring the density of small peptide ligands, it is possible for the antibodies to saturate the surface before the significantly smaller immobilized ligands (Capadona, unpublished results). However, ELISAs are ideal for

surveying multiple samples in short time intervals, and are thus an attractive technique.

Finally, detection of fluorescently labeled ligands is a promising area that is currently being expanded. While labeling of ligands with fluorescent tags prior to introduction to the surfaces yields high specificity and throughput, the limitations to this system include auto-quenching of fluorescence, decrease sensitivity (compared to radio-labeling), and difficulties in accurately determining a standard. Furthermore, labeling small peptides with large fluorescent tags may also alter the surface-tethering (Capadona, unpublished results). While no single technique is ideal for all applications, there are significant advantages to the flexibility of several distinct methods of analysis of surface associated ligands.

EG_n-Containing SAMs and Protein Resistance

While numerous functional groups can be used to minimize protein adsorption to SAM surfaces, the EG_n group remains the standard for comparison (for summary/ review[181]). Extensive effort has focused on the characterization of the non-fouling properties of EG_n functionalized surfaces; including the mechanism for protein resistance. Andrade and coworkers have proposed that surfaces modified with EG_n retain protein resistance through "steric stabilization."[182,183] In aqueous solutions, the EG_n chains are highly solvated due to the high binding affinity for water,[184] and it is this interfacial layer of water that is suspected to repel soluble proteins. Through molecular modeling, and by controlling the surfaces packing density of EG_n functionalized alkanethiols in

monolayer, Grunze and Whitesides have shown that helical orientation of EG_n in monolayer influences the protein resistant properties by increasing the EG_n-water binding.[184-186] This unique property of EG_n functionalized alkanethiols allows for low surfaces densities of EG_n to retain the non-fouling surface properties.[114,146] These dynamic interactions between EG_n, water, and proteins create a powerful tool to control protein adsorption.

REFERENCES

1. Langer,R. & Tirrell,D.A. Designing materials for biology and medicine. *Nature* **428**, 487-492 (2004).

2. Anderson,J.M. Biological responses to materials. *Annu. Rev. Mat. Res.* **31**, 81-110 (2001).

3. Ziats,N.P., Miller,K.M., & Anderson,J.M. In vitro and in vivo interactions of cells with biomaterials. *Biomaterials* **9**, 5-13 (1988).

4. Bauer,T.W. & Schils,J. The pathology of total joint arthroplasty - II. Mechanisms of implant failure. *Skel. Radiol.* **28**, 483-497 (1999).

5. Albrektsson,T., Branemark,P.I., Hansson,H.A., Kasemo,B., Larsson,K., Lundstrom,I., Mcqueen,D.H., & Skalak,R. The Interface Zone of Inorganic Implants In vivo - Titanium Implants in Bone. *Annal. Biomed. Eng.* **11**, 1-27 (1983).

6. Ryd,L., Albrektsson,B.E.J., Carlsson,L., Dansgard,F., Herberts,P., Lindstrand,A., Regner,L., & Toksviglarsen,S. Roentgen Stereophotogrammetric Analysis As A Predictor of Mechanical Loosening of Knee Prostheses. *J. Bone Joint Surg.-British Volume* **77B**, 377-383 (1995).

7. Sakiyama-Elbert,S.E. & Hubbell,J.A. Functional biomaterials: Design of novel biomaterials. *Annu. Rev. Mat. Res.* **31**, 183-201 (2001).

8. Hubbell,J.A. Materials as morphogenetic guides in tissue engineering. *Curr. Opin. Biotechnol.* **14**, 551-558 (2003).

9. Lutolf,M.P. & Hubbell,J.A. Synthetic biomaterials as instructive microenvironments for morphogenesis in tissue engineering. *Nat. Biotech.* **23**, 47-55 (2005).

10. Langer,R. & Tirrell,D.A. Designing materials for biology and medicine. *Nature* **428**, 487-492 (2004).

11. Staffan Johansson in Molecular Components and Interactions, Edn. 2 68-94 (Harwood Academic Publishers GmbH, Netherlands; 1996).

12. Sakai,T., Larsen,M., & Yamada,K.M. Fibronectin requirement in branching morphogenesis. *Nature* **423**, 876-881 (2003).

13. Zhu,X.Y., Ohtsubo,M., Bohmer,R.M., Roberts,J.M., & Assoian,R.K. Adhesion-dependent cell cycle progression linked to the expression of cyclin D1, activation of cyclin E-cdk2, and phosphorylation of the retinoblastoma protein. *J Cell. Biol.* **133**, 391-403 (1996).

14. Boudreau,N., Myers,C., & Bissell,M.J. From Laminin to Lamin - Regulation of Tissue-Specific Gene-Expression by the Ecm. *Trends Cell. Biol.* **5**, 1-4 (1995).

15. Sottile,J., Schwarzbauer,J., Selegue,J., & Mosher,D.F. 5 Type-I Modules of Fibronectin Form A Functional Unit That Binds to Fibroblasts and Staphylococcus-Aureus. *J. Biol. Chem.* **266**, 12840-12843 (1991).

16. Sechler,J.L. & Schwarzbauer,J.E. Control of cell cycle progression by fibronectin matrix architecture. *J. Biol. Chem.* **273**, 25533-25536 (1998).

17. Bourdoulous,S., Orend,G., MacKenna,D.A., Pasqualini,R., & Ruoslahti,E. Fibronectin matrix regulates activation of Rho and Cdc42 GTPases and cell cycle progression. *J. Cell Biol.* **143**, 267-276 (1998).

18. Corbett,S.A., Wilson,C.L., & Schwarzbauer,J.E. Changes in cell spreading and cytoskeletal organization are induced by adhesion to a fibronectin-fibrin matrix. *Blood* **88**, 158-166 (1996).

19. Hynes,R.O. (Springer-Verlag, New York; 1990).

20. Hynes,R.O., Schwarzbauer,J.E., & Tamkun,J.W. Fibronectin: a versatile gene for a versatile protein. *Ciba Found. Symp.* **108**, 75-92 (1984).

21. Schwarzbauer,J.E., Patel,R.S., Fonda,D., & Hynes,R.O. Multiple sites of alternative splicing of the rat fibronectin gene transcript. *EMBO J.* **6**, 2573-2580 (1987).

22. Schwarzbauer,J.E., Paul,J.I., & Hynes,R.O. On the origin of species of fibronectin. *Proc. Natl. Acad. Sci. U. S. A* **82**, 1424-1428 (1985).

23. Mosesson,M.W. & Umfleet,R.A. Cold-Insoluble Globulin of Human Plasma .1. Purification, Primary Characterization, and Relationship to Fibrinogen and Other Cold-Insoluble Fraction Components. *J. Biol. Chem.* **245**, 5728-& (1970).

24. Wierzbicka-Patynowski,I. & Schwarzbauer,J.E. The ins and outs of fibronectin matrix assembly. *J. Cell Sci.* **116**, 3269-3276 (2003).

25. George,E.L., Georges-Labouesse,E.N., Patel-King,R.S., Rayburn,H., & Hynes,R.O. Defects in Mesoder, Neural Tube and Vascular Development in Mouse Embryos Lacking Fibronectin. *Development* **119**, 1079-1091 (1993).

26. Moursi,A.M., Damsky,C.H., Lull,J., Zimmerman,D., Doty,S.B., Aota,S.I., & Globus,R.K. Fibronectin regulates calvarial osteoblast differentiation. *J. Cell Sci.* **109**, 1369-1380 (1996).

27. Stephansson,S.N., Byers,B.A., & Garcia,A.J. Enhanced expression of the osteoblastic phenotype on substrates that modulate fibronectin conformation and integrin receptor binding. *Biomaterials* **23**, 2527-2534 (2002).

28. Garcia,A.J., Vega,M.D., & Boettiger,D. Modulation of cell proliferation and differentiation through substrate-dependent changes in fibronectin conformation. *Mol. Biol. Cell* **10**, 785-798 (1999).

29. Ingham,K.C., Brew,S.A., & Isaacs,B.S. Interaction of Fibronectin and Its Gelatin-Binding Domains with Fluorescent-Labeled Chains of Type-I Collagen. *J. Biol. Chem.* **263**, 4624-4628 (1988).

30. Sechler,J.L., Corbett,S.A., Wenk,M.B., & Schwarzbauer,J.E. Modulation of cell-extracellular matrix interactions. *Ann. N. Y. Acad. Sci.* **857**, 143-154 (1998).

31. Streuli,C.H. & Bissell,M.J. Expression of Extracellular-Matrix Components Is Regulated by Substratum. *J. Cell Biol.* **110**, 1405-1415 (1990).

32. Adams,J.C. & Watt,F.M. Regulation of Development and Differentiation by the Extracellular-Matrix. *Development* **117**, 1183-1198 (1993).

33. Mooney,D.J., Langer,R., & Ingber,D.E. Cytoskeletal Filament Assembly and the Control of Cell Spreading and Function by Extracellular-Matrix. *J. Cell Sci.* **108**, 2311-2320 (1995).

34. Fogerty,F.J., Akiyama,S.K., Yamada,K.M., & Mosher,D.F. Inhibition of Binding of Fibronectin to Matrix Assembly Sites by Anti-Integrin (Alpha-5-Beta-1) Antibodies. *J. Cell Biol.* **111**, 699-708 (1990).

35. Pankov,R., Cukierman,E., Katz,B.Z., Matsumoto,K., Lin,D.C., Lin,S., Hahn,C., & Yamada,K.M. Integrin dynamics and matrix assembly: Tensin-dependent translocation of alpha(5)beta(1) integrins promotes early fibronectin fibrillogenesis. *J. Cell Biol.* **148**, 1075-1090 (2000).

36. Wierzbicka-Patynowski,I. & Schwarzbauer,J.E. The ins and outs of fibronectin matrix assembly. *J. Cell Sci.* **116**, 3269-3276 (2003).

37. Mosher,D.F., Fogerty,F.J., Chernousov,M.A., & Barry,E.L.R. Assembly of Fibronectin Into Extracellular-Matrix. *Ann. N. Y. Acad. Sci.* **614**, 167-180 (1991).

38. Smilenov,L.B., Mikhailov,A., Pelham,R.J., Marcantonio,E.E., & Gundersen,G.G. Focal adhesion motility revealed in stationary fibroblasts. *Science* **286**, 1172-1174 (1999).

39. Baneyx,G., Baugh,L., & Vogel,V. Fibronectin extension and unfolding within cell matrix fibrils controlled by cytoskeletal tension. *Proc. Natl. Acad. Sci. USA* **99**, 5139-5143 (2002).

40. Ohashi,T., Kiehart,D.P., & Erickson,H.P. Dual labeling of the fibronectin matrix and actin cytoskeleton with green fluorescent protein variants. *J. Cell Sci* **115**, 1221-1229 (2002).

41. Ohashi,T., Kiehart,D.P., & Erickson,H.P. Dynamics and elasticity of the fibronectin matrix in living cell culture visualized by fibronectin-green fluorescent protein. *Proc. Natl. Acad. Sci. USA* **96**, 2153-2158 (1999).

42. Ilic,D., Kovacic,B., Johkura,K., Schlaepfer,D.D., Tomasevic,N., Han,Q., Kim,J.B., Howerton,K., Baumbusch,C., Ogiwara,N., Streblow,D.N., Nelson,J.A., Dazin,P., Shino,Y., Sasaki,K., & Damsky,C.H. FAK promotes organization of fibronectin matrix and fibrillar adhesions. *J. Cell Sci.* **117**, 177-187 (2004).

43. Zhong,C.L., Chrzanowska-Wodnicka,M., Brown,J., Shaub,A., Belkin,A.M., & Burridge,K. Rho-mediated contractility exposes a cryptic site in fibronectin and induces fibronectin matrix assembly. *J. Cell Biol.* **141**, 539-551 (1998).

44. Corbett,S.A., Lee,L., Wilson,C.L., & Schwarzbauer,J.E. Covalent cross-linking of fibronectin (FN) to fibrin is required for maximal cell adhesion to a FN-fibrin matrix. *Mol. Biol. Cell* **7**, 1418 (1996).

45. Schwarzbauer,J.E. & Sechler,J.L. Fibronectin fibrillogenesis: a paradigm for extracellular matrix assembly. *Curr. Opin. Cell Biol.* **11**, 622-627 (1999).

46. Sechler,J.L., Takada,Y., & Schwarzbauer,J.E. Altered rate of fibronectin matrix assembly by deletion of the first type III repeats. *J. Cell Biol.* **134**, 573-583 (1996).

47. Sechler,J.L., Corbett,S.A., & Schwarzbauer,J.E. Modulatory roles for integrin activation and the synergy site of fibronectin during matrix assembly. *Mol. Biol Cell* **8**, 2563-2573 (1997).

48. Sechler,J.L., Cumiskey,A.M., Gazzola,D.M., & Schwarzbauer,J.E. A novel RGD-independent fibronectin assembly pathway initiated by alpha4beta1 integrin binding to the alternatively spliced V region. *J. Cell Sci.* **113 (Pt 8)**, 1491-1498 (2000).

49. Bultmann,H., Santas,A.J., & Peters,D.M.P. Fibronectin fibrillogenesis involves the heparin II binding domain of fibronectin. *J. Biol. Chem.* **273**, 2601-2609 (1998).

50. Schwarzbauer,J.E. Identification of the fibronectin sequences required for assembly of a fibrillar matrix. *J. Cell Biol.* **113**, 1463-1473 (1991).

51. Morla,A. & Ruoslahti,E. A fibronectin self-assembly site involved in fibronectin matrix assembly: reconstruction in a synthetic peptide. *J. Cell Biol.* **118**, 421-429 (1992).

52. Sechler,J.L., Rao,H., Cumiskey,A.M., Vega-Colon,I., Smith,M.S., Murata,T., & Schwarzbauer,J.E. A novel fibronectin binding site required for fibronectin fibril growth during matrix assembly. *J. Cell Biol.* **154**, 1081-1088 (2001).

53. Colombi,M., Zoppi,N., De Petro,G., Marchina,E., Gardella,R., Tavian,D., Ferraboli,S., & Barlati,S. Matrix assembly induction and cell migration and invasion inhibition by a 13-amino acid fibronectin peptide. *J. Biol. Chem.* **278**, 14346-14355 (2003).

54. Sechler,J.L. & Schwarzbauer,J.E. Regulation of cell growth by assembly of a fibronectin matrix. *Mol. Biol. Cell* **8**, 1657 (1997).

55. Schense,J.C., Bloch,J., Aebischer,P., & Hubbell,J.A. Enzymatic incorporation of bioactive peptides into fibrin matrices enhances neurite extension. *Nat Biotech* **18**, 415-419 (2000).

56. Alsberg,E., Anderson,K.W., Albeiruti,A., Rowley,J.A., & Mooney,D.J. Engineering growing tissues. *Proc. Natl. Acad. Sci. USA* **99**, 12025-12030 (2002).

57. Zisch,A.H., Lutolf,M.P., & Hubbell,J.A. Biopolymeric delivery matrices for angiogenic growth factors. *Cardiovasc. Pathol.* **12**, 295-310 (2003).

58. West,J.L. & Hubbell,J.A. Polymeric biomaterials with degradation sites for proteases involved in cell migration. *Macromolecules* **32**, 241-244 (1999).

59. Ruoslahti,E. & Pierschbacher,M.D. New Perspectives in Cell-Adhesion - RGD and Integrins. *Science* **238**, 491-497 (1987).

60. Graf,J., Ogle,R.C., Robey,F.A., Sasaki,M., Martin,G.R., Yamada,Y., & Kleinman,H.K. A Pentapeptide from the Laminin-B1 Chain Mediates Cell-Adhesion and Binds the 67000-Laminin Receptor. *Biochemistry* **26**, 6896-6900 (1987).

61. Knight,C.G., Morton,L.F., Onley,D.J., Peachey,A.R., Messent,A.J., Smethurst,P.A., Tuckwell,D.S., Farndale,R.W., & Barnes,M.J. Identification in collagen type I of an integrin alpha(2)beta(1)-binding site containing an essential GER sequence. *J. Biol. Chem.* **273**, 33287-33294 (1998).

62. Knight,C.G., Morton,L.F., Peachey,A.R., Tuckwell,D.S., Farndale,R.W., & Barnes,M.J. The collagen-binding A-domains of integrins alpha(1)beta(1) and alpha(2)beta(1) recognize the same specific amino acid sequence, GFOGER, in native (triple-helical) collagens. *J. Biol. Chem.* **275**, 35-40 (2000).

63. Hubbell,J.A. Bioactive biomaterials. *Curr. Opin. Biotechnol.* **10**, 123-129 (1999).

64. Hersel,U., Dahmen,C., & Kessler,H. RGD modified polymers: biomaterials for stimulated cell adhesion and beyond. *Biomaterials* **24**, 4385-4415 (2003).

65. Yamada,K.M. Adhesive Recognition Sequences. *J. Biol.l Chem.* **266**, 12809-12812 (1991).

66. Dillow,A.K. & Tirrell,M. Targeted cellular adhesion at biomaterial interfaces. *Curr. Opin. Sol. St. & Mater. Sci.* **3**, 252-259 (1998).

67. Shin,H., Jo,S., & Mikos,A.G. Modulation of marrow stromal osteoblast adhesion on biomimetic oligo[poly(ethylene glycol) fumarate] hydrogels modified with Arg-Gly-Asp peptides and a poly(ethylene glycol) spacer. *J. Biomed. Mater. Res.* **61**, 169-179 (2002).

68. Sagnella,S.M., Kligman,F., Anderson,E.H., King,J.E., Murugesan,G., Marchant,R.E., & Kottke-Marchant,K. Human microvascular endothelial cell growth and migration on biomimetic surfactant polymers. *Biomaterials* **25**, 1249-1259 (2004).

69. Maheshwari,G., Brown,G., Lauffenburger,D.A., Wells,A., & Griffith,L.G. Cell adhesion and motility depend on nanoscale RGD clustering. *J. Cell Sci.* **113**, 1677-1686 (2000).

70. Rezania,A. & Healy,K.E. The effect of peptide surface density on mineralization of a matrix deposited by osteogenic cells. *J. Biomed. Mater. Res.* **52**, 595-600 (2000).

71. Barber,T.A., Golledge,S.L., Castner,D.G., & Healy,K.E. Peptide-modified p(AAm-co-EG/AAc) IPNs grafted to bulk titanium modulate osteoblast behavior in vitro. *J. Biomed. Mater. Res.* **64A**, 38-47 (2003).

72. Houseman,B.T. & Mrksich,M. The microenvironment of immobilized Arg-Gly-Asp peptides is an important determinant of cell adhesion. *Biomaterials* **22**, 943-955 (2001).

73. Massia,S.P. & Hubbell,J.A. An Rgd Spacing of 440Nm Is Sufficient for Integrin Alpha-V-Beta-3-Mediated Fibroblast Spreading and 140Nm for Focal Contact and Stress Fiber Formation. *J. Cell Biol.* **114**, 1089-1100 (1991).

74. VandeVondele,S., Voros,J., & Hubbell,J.A. RGD-Grafted poly-l-lysine-graft-(polyethylene glycol) copolymers block non-specific protein adsorption while promoting cell adhesion. *Biotechnol. Bioeng.* **82**, 784-790 (2003).

75. Hern,D.L. & Hubbell,J.A. Incorporation of adhesion peptides into nonadhesive hydrogels useful for tissue resurfacing. *J. Biomed. Mater. Res.* **39**, 266-276 (1998).

76. Rowley,J.A. & Mooney,D.J. Alginate type and RGD density control myoblast phenotype. *J. Biomed. Mater. Res.* **60**, 217-223 (2002).

77. Verrier,S., Pallu,S., Bareille,R., Jonczyk,A., Meyer,J., Dard,M., & Amedee,J. Function of linear and cyclic RGD-containing peptides in osteoprogenitor cells adhesion process. *Biomaterials* **23**, 585-596 (2002).

78. Garcia,A.J. & Keselowsky,B.G. Biomimetic surfaces for control of cell adhesion to facilitate bone formation. *Crit Rev. Eukaryot. Gene Expr.* **12**, 151-162 (2002).

79. Pierschbacher,M., Hayman,E.G., & Ruoslahti,E. Synthetic Peptide with Cell Attachment Activity of Fibronectin. *Proc. Natl. Acad. Sci. USA-Biol. Sci.* **80**, 1224-1227 (1983).

80. Akiyama,S.K., Olden,K., & Yamada,K.M. Fibronectin and Integrins in Invasion and Metastasis. *Canc.Metast. Rev.* **14**, 173-189 (1995).

81. Mann,B.K., Tsai,A.T., Scott-Burden,T., & West,J.L. Modification of surfaces with cell adhesion peptides alters extracellular matrix deposition. *Biomaterials* **20**, 2281-2286 (1999).

82. Reichardt,L.F. in Guidebook to Extracellular Matrices, Edn. sescond 335 (New York, NY; 1999).

83. Bentz,H., Schroeder,J.A., & Estridge,T.D. Improved local delivery of TGF-beta 2 by binding to injectable fibrillar collagen via difunctional polyethylene glycol. *J. Biomed. Mater. Res.* **39**, 539-548 (1998).

84. Kuhl,P.R. & GriffithCima,L.G. Tethered epidermal growth factor as a paradigm for growth factor-induced stimulation from the solid phase. *Nat. Med.* **2**, 1022-1027 (1996).

85. Sakiyama-Elbert,S.E., Panitch,A., & Hubbell,J.A. Development of growth factor fusion proteins for cell-triggered drug delivery. *Faseb J.* **15**, 1300-1302 (2001).

86. Edelman,E.R., Mathiowitz,E., Langer,R., & Klagsbrun,M. Controlled and Modulated Release of Basic Fibroblast Growth-Factor. *Biomaterials* **12**, 619-626 (1991).

87. SchroederTefft,J.A., Bentz,H., & Estridge,T.D. Collagen and heparin matrices for growth factor delivery. *J. Cont. Rel.* **48**, 29-33 (1997).

88. Wissink,M.J.B., Beernink,R., Pieper,J.S., Poot,A.A., Engbers,G.H.M., Beugeling,T., van Aken,W.G., & Feijen,J. Binding and release of basic fibroblast growth factor from heparinized collagen matrices. *Biomaterials* **22**, 2291-2299 (2001).

89. Sakiyama-Elbert,S.E. & Hubbell,J.A. Controlled release of nerve growth factor from a heparin-containing fibrin-based cell ingrowth matrix. *J. Cont. Rel.* **69**, 149-158 (2000).

90. Sakiyama-Elbert,S.E. & Hubbell,J.A. Development of fibrin derivatives for controlled release of heparin-binding growth factors. *J. Cont. Rel.* **65**, 389-402 (2000).

91. Seliktar,D., Zisch,A.H., Lutolf,M.P., Wrana,J.L., & Hubbell,J.A. MMP-2 sensitive, VEGF-bearing bioactive hydrogels for promotion of vascular healing. *J. Biomed. Mater. Res.* **68A**, 704-716 (2004).

92. Kopecek,J. Controlled Biodegradability of Polymers - A Key to Drug Delivery Systems. *Biomaterials* **5**, 19-25 (1984).

93. Taylor,S.J., McDonald,J.W., & Sakiyama-Elbert,S.E. Controlled release of neurotrophin-3 from fibrin gels for spinal cord injury. *J. Cont. Rel.* **98**, 281-294 (2004).

94. Delong,S.A., Mann,B.K., & West,J.L. Scaffolds modified with tethered growth factors to influence smooth muscle cell behavior. *Faseb J.* **16**, A36 (2002).

95. Werb,Z. ECM and cell surface proteolysis: Regulating cellular ecology. *Cell* **91**, 439-442 (1997).

96. Chang,C. & Werb,Z. The many faces of metalloproteases: cell growth, invasion, angiogenesis and metastasis. *Trends in Cell Biol.* **11**, S37-S43 (2001).

97. Hubbell,J.A. Synthetic biodegradable polymers for tissue engineering and drug delivery. *Curr. Opin. Sol. St. & Mater. Sci.* **3**, 246-251 (1998).

98. Kim,S. & Healy,K.E. Synthesis and characterization of injectable poly(N-isopropylacrylamide-co-acrylic acid) hydrogels with proteolytically degradable cross-links. *Biomacromolecules* **4**, 1214-1223 (2003).

99. Leach,J.B., Bivens,K.A., Patrick,C.W., & Schmidt,C.E. Photocrosslinked hyaluronic acid hydrogels: Natural, biodegradable tissue engineering scaffolds. *Biotechnol. Bioeng.* **82**, 578-589 (2003).

100. Bulpitt,P. & Aeschlimann,D. New strategy for chemical modification of hyaluronic acid: Preparation of functionalized derivatives and their use in the

formation of novel biocompatible hydrogels. *J. Biomed. Mater. Res.* **47**, 152-169 (1999).

101. Halstenberg,S., Panitch,A., Rizzi,S., Hall,H., & Hubbell,J.A. Biologically engineered protein-graft-poly(ethylene glycol) hydrogels: A cell adhesive and plasm in-degradable biosynthetic material for tissue repair. *Biomacromolecules* **3**, 710-723 (2002).

102. Schense,J.C. & Hubbell,J.A. Cross-linking exogenous bifunctional peptides into fibrin gels with factor XIIIa. *Bioconj. Chem.* **10**, 75-81 (1999).

103. Lutolf,M.P., Lauer-Fields,J.L., Schmoekel,H.G., Metters,A.T., Weber,F.E., Fields,G.B., & Hubbell,J.A. Synthetic matrix metalloproteinase-sensitive hydrogels for the conduction of tissue regeneration: Engineering cell-invasion characteristics. *Proc. Natl. Acad. Sci. USA* **100**, 5413-5418 (2003).

104. Pernodet,N., Rafailovich,M., Sokolov,J., Xu,D., Yang,N.L., & McLeod,K. Fibronectin fibrillogenesis on sulfonated polystyrene surfaces. *J Biomed Mater Res* **64A**, 684-692 (2003).

105. Sharma,S.K. & Mahendroo,P.P. Affinity chromatography of cells and cell membranes. *J. Chromatogr.* **184**, 471-499 (1980).

106. Langer,R. & Vacanti,J.P. Tissue Engineering. *Science* **260**, 920-926 (1993).

107. Baier,R.E. & Dutton,R.C. Initial events in interactions of blood with a foreign surface. *J. Biomed. Mater. Res.* **3**, 191-206 (1969).

108. Andrade,J.D. & Hlady,V. Protein Adsorption and Materials Biocompatibility - A Tutorial Review and Suggested Hypotheses. *Adv. Poly. Sci.* **79**, 1-63 (1986).

109. Brash,J.L. Protein Adsorption at the Solid-Solution Interface in Relation to Blood Material Interactions. *ACS Sym. Ser.* **343**, 490-506 (1987).

110. Anderson,J.M., Bonfield,T.L., & Ziats,N.P. Protein adsorption and cellular adhesion and activation on biomedical polymers. *Int. J. Artif. Organs* **13**, 375-382 (1990).

111. Shen,M. & Horbett,T.A. The effects of surface chemistry and adsorbed proteins on monocyte/macrophage adhesion to chemically modified polystyrene surfaces. *J. Biomed. Mater. Res.* **57**, 336-345 (2001).

112. Tsai,W.B., Grunkemeier,J.M., & Horbett,T.A. Human plasma fibrinogen adsorption and platelet adhesion to polystyrene. *J. Biomed. Mater. Res.* **44**, 130-139 (1999).

113. Grinnell,F. & Feld,M.K. Adsorption characteristics of plasma fibronectin in relationship to biological activity. *J. Biomed. Mater. Res.* **15**, 363-381 (1981).

114. Prime,K.L. & Whitesides,G.M. Self-Assembled Organic Monolayers - Model Systems for Studying Adsorption of Proteins at Surfaces. *Science* **252**, 1164-1167 (1991).

115. Lewandowska,K., Pergament,E., Sukenik,C.N., & Culp,L.A. Cell-type-specific adhesion mechanisms mediated by fibronectin adsorbed to chemically derivatized substrata. *J. Biomed. Mater. Res.* **26**, 1343-1363 (1992).

116. Garcia,A.J. & Boettiger,D. Integrin-fibronectin interactions at the cell-material interface: initial integrin binding and signaling. *Biomaterials* **20**, 2427-2433 (1999).

117. Tegoulia,V.A. & Cooper,S.L. Leukocyte adhesion on model surfaces under flow: effects of surface chemistry, protein adsorption, and shear rate. *J. Biomed. Mater. Res.* **50**, 291-301 (2000).

118. Keselowsky,B.G., Collard,D.M., & Garcia,A.J. Surface chemistry modulates fibronectin conformation and directs integrin binding and specificity to control cell adhesion. *J. Biomed. Mater. Res.* **66A**, 247-259 (2003).

119. Mrksich,M. & Whitesides,G.M. Using self-assembled monolayers to understand the interactions of man-made surfaces with proteins and cells. *Ann. Rev. Biophys. Biomol. Struct.* **25**, 55-78 (1996).

120. Garcia,A.J., Ducheyne,P., & Boettiger,D. Effect of surface reaction stage on fibronectin-mediated adhesion of osteoblast-like cells to bioactive glass. *J. Biomed. Mater. Res.* **40**, 48-56 (1998).

121. Lan,M.A., Gersbach,C.A., Michael,K.E., Keselowski,B.G., & Garcia,A.J. Myoblast proliferation and differentiation on fibronectin-coated self assembled monolayers presenting different surface chemistries. *Biomaterials* **In Press**, (2005).

122. Lee,J.H., Kopecek,J., & Andrade,J.D. Protein-resistant surfaces prepared by PEO-containing block copolymer surfactants. *J. Biomed. Mater. Res.* **23**, 351-368 (1989).

123. Fujimoto,K., Inoue,H., & Ikada,Y. Protein adsorption and platelet adhesion onto polyurethane grafted with methoxy-poly(ethylene glycol) methacrylate by plasma technique. *J. Biomed. Mater. Res.* **27**, 1559-1567 (1993).

124. Kidane,A., Lantz,G.C., Jo,S., & Park,K. Surface modification with PEO-containing triblock copolymer for improved biocompatibility: in vitro and ex vivo studies. *J. Biomater. Sci. Polym. Ed.* **10**, 1089-1105 (1999).

125. Morra,M. On the molecular basis of fouling resistance. *J. Biomater. Sci. Polym. Ed.* **11**, 547-569 (2000).

126. Zhu,B., Eurell,T., Gunawan,R., & Leckband,D. Chain-length dependence of the protein and cell resistance of oligo(ethylene glycol)-terminated self-assembled monolayers on gold. *J. Biomed. Mater. Res.* **56**, 406-416 (2001).

127. Leckband,D., Sheth,S., & Halperin,A. Grafted poly(ethylene oxide) brushes as nonfouling surface coatings. *J. Biomater. Sci. Polym. Ed* **10**, 1125-1147 (1999).

128. Mrksich,M., Dike,L.E., Tien,J., Ingber,D.E., & Whitesides,G.M. Using microcontact printing to pattern the attachment of mammalian cells to self-assembled monolayers of alkanethiolates on transparent films of gold and silver. *Exp. Cell Res.* **235**, 305-313 (1997).

129. Roberts,C., Chen,C.S., Mrksich,M., Martichonok,V., Ingber,D.E., & Whitesides,G.M. Using mixed self-assembled monolayers presenting RGD and (EG)(3)OH groups to characterize long-term attachment of bovine capillary endothelial cells to surfaces. *J Am. Chem. Soc.* **120**, 6548-6555 (1998).

130. Ostuni,E., Chapman,R.G., Holmlin,R.E., Takayama,S., & Whitesides,G.M. A survey of structure-property relationships of surfaces that resist the adsorption of protein. *Langmuir* **17**, 5605-5620 (2001).

131. Nelson,C.M., Raghavan,S., Tan,J.L., & Chen,C.S. Degradation of micropatterned surfaces by cell-dependent and -independent processes. *Langmuir* **19**, 1493-1499 (2003).

132. Luk,Y.Y., Kato,M., & Mrksich,M. Self-assembled monolayers of alkanethiolates presenting mannitol groups are inert to protein adsorption and cell attachment. *Langmuir* **16**, 9604-9608 (2000).

133. Ostuni,E., Kane,R., Chen,C.S., Ingber,D.E., & Whitesides,G.M. Patterning mammalian cells using elastomeric membranes. *Langmuir* **16**, 7811-7819 (2000).

134. Chen,C.S., Mrksich,M., Huang,S., Whitesides,G.M., & Ingber,D.E. Geometric control of cell life and death. *Science* **276**, 1425-1428 (1997).

135. Thomas,C.H., Lhoest,J.B., Castner,D.G., McFarland,C.D., & Healy,K.E. Surfaces designed to control the projected area and shape of individual cells. *J. Biomech. Eng. Trans. Asme* **121**, 40-48 (1999).

136. Flynn,N.T., Tran,T.N.T., Cima,M.J., & Langer,R. Long-term stability of self-assembled monolayers in biological media. *Langmuir* **19**, 10909-10915 (2003).

137. Branch,D.W., Wheeler,B.C., Brewer,G.J., & Leckband,D.E. Long-term stability of grafted polyethylene glycol surfaces for use with micro stamped substrates in neuronal cell culture. *Biomaterials* **22**, 1035-1047 (2001).

138. Park,K., Shim,H.S., Dewanjee,M.K., & Eigler,N.L. In vitro and in vivo studies of PEO-grafted blood-contacting cardiovascular prostheses. *J. Biomater. Sci. Polym. Ed* **11**, 1121-1134 (2000).

139. Biomaterials Science: An Introduction to Materials in Medicine. (Elsevier Academic Press,2004).

140. Chapman,R.G., Ostuni,E., Yan,L., & Whitesides,G.M. Preparation of mixed self-assembled monolayers (SAMs) that resist adsorption of proteins using the reaction of amines with a SAM that presents interchain carboxylic anhydride groups. *Langmuir* **16**, 6927-6936 (2000).

141. Prime,K.L. & Whitesides,G.M. Self-assembled organic monolayers: model systems for studying adsorption of proteins at surfaces. *Science* **252**, 1164-1167 (1991).

142. Mrksich,M., Dike,L.E., Tien,J., Ingber,D.E., & Whitesides,G.M. Using microcontact printing to pattern the attachment of mammalian cells to self-assembled monolayers of alkanethiolates on transparent films of gold and silver. *Exp. Cell Res.* **235**, 305-313 (1997).

143. Bain,C.D., Troughton,E.B., Tao,Y.T., Evall,J., Whitesides,G.M., & Nuzzo,R.G. Formation of Monolayer Films by the Spontaneous Assembly of Organic Thiols from Solution Onto Gold. *J. Am. Chem. Soc.* **111**, 321-335 (1989).

144. Bain,C.D., Evall,J., & Whitesides,G.M. Formation of Monolayers by the Co adsorption of Thiols on Gold - Variation in the Head Group, Tail Group, and Solvent. *J. Am. Chem. Soc.* **111**, 7155-7164 (1989).

145. Bain,C.D. & Whitesides,G.M. Formation of Monolayers by the Co adsorption of Thiols on Gold - Variation in the Length of the Alkyl Chain. *J. Am. Chem. Soc.* **111**, 7164-7175 (1989).

146. Prime,K.L. & Whitesides,G.M. Adsorption of Proteins Onto Surfaces Containing End-Attached Oligo(Ethylene Oxide) - A Model System Using Self-Assembled Monolayers. *J. Am. Chem. Soc.* **115**, 10714-10721 (1993).

147. Martins,M.C.L., Ratner,B.D., & Barbosa,M.A. Protein adsorption on mixtures of hydroxyl- and methyl terminated alkanethiols self-assembled monolayers. *J. Biomed. Mater. Res.* **67A**, 158-171 (2003).

148. Bain,C.D., Troughton,E.B., Tao,Y.T., Evall,J., Whitesides,G.M., & Nuzzo,R.G. Formation of Monolayer Films by the Spontaneous Assembly of

Organic Thiols from Solution Onto Gold. *J. Am. Chem. Soc.* **111**, 321-335 (1989).

149. Porter,M.D., Bright,T.B., Allara,D.L., & Chidsey,C.E.D. Spontaneously Organized Molecular Assemblies .4. Structural Characterization of Normal-Alkyl Thiol Monolayers on Gold by Optical Ellipsometry, Infrared-Spectroscopy, and Electrochemistry. *J. Am. Chem. Soc.* **109**, 3559-3568 (1987).

150. Poirier,G.E. & Pylant,E.D. The self-assembly mechanism of alkanethiols on Au(111). *Science* **272**, 1145-1148 (1996).

151. Nuzzo,R.G., Zegarski,B.R., & Dubois,L.H. Fundamental-Studies of the Chemisorption of Organosulfur Compounds on Au(111) - Implications for Molecular Self-Assembly on Gold Surfaces. *J. Am. Chem. Soc.* **109**, 733-740 (1987).

152. Ulman,A. Formation and Structure of Self-Assembled Monolayers. *Chem. Rev.* **96**, 1533-1554 (1996).

153. Dubois,L.H. & Nuzzo,R.G. Synthesis, Structure, and Properties of Model Organic-Surfaces. *Ann. Rev. Phys. Chem.* **43**, 437-463 (1992).

154. Ulman,A., Kang,J.F., Shnidman,Y., Liao,S., Jordan,R., Choi,G.Y., Zaccaro,J., Myerson,A.S., Rafailovich,M., Sokolov,J., & Fleischer,C. Self-assembled monolayers of rigid thiols. *J. Biotechnol.* **74**, 175-188 (2000).

155. Laibinis,P.E., Whitesides,G.M., Allara,D.L., Tao,Y.T., Parikh,A.N., & Nuzzo,R.G. Comparison of the Structures and Wetting Properties of Self-Assembled Monolayers of Normal-Alkanethiols on the Coinage Metal-Surfaces, Cu, Ag, Au. *J. Am. Chem. Soc.* **113**, 7152-7167 (1991).

156. Pardo,L. & Boland,T. A quantitative approach to studying structures and orientation at self-assembled monolayer/fluid interfaces. *J. Coll. Inter. Sci.* **257**, 116-120 (2003).

157. Jiang,Y., Wang,Z., Yu,X., Shi,F., Yu,H., & Zhang,X. Self-Assembled Monolayers of Dendron Thiols for Electrodeposition of Gold Nanostructures: Toward Fabrication of Superhydrophobic/Superhydrophilic Surface and pH-Responsive Surfaces. *Langmuir* **ASAP**, (2005).

158. Zhou,Y.F., Bruening,M.L., Bergbreiter,D.E., Crooks,R.M., & Wells,M. Preparation of hyperbranched polymer films grafted on self-assembled monolayers. *J. Am. Chem. Soc.* **118**, 3773-3774 (1996).

159. Kim,T.S., Crooks,R.M., Tsen,M., & Sun,L. Polymeric Self-Assembled Monolayers .2. Synthesis and Characterization of Self-Assembled

Polydiacetylene Monolayers and Multilayers. *J. Am. Chem. Soc.* **117**, 3963-3967 (1995).

160. Sigal,G.B., Mrksich,M., & Whitesides,G.M. Effect of surface wettability on the adsorption of proteins and detergents. *J. Am. Chem. Soc.* **120**, 3464-3473 (1998).

161. Ostuni,E., Chapman,R.G., Liang,M.N., Meluleni,G., Pier,G., Ingber,D.E., & Whitesides,G.M. Self-assembled monolayers that resist the adsorption of proteins and the adhesion of bacterial and mammalian cells. *Langmuir* **17**, 6336-6343 (2001).

162. Deng,L., Mrksich,M., & Whitesides,G.M. Self-assembled monolayers of alkanethiolates presenting tri(propylene sulfoxide) groups resist the adsorption of protein. *J. Am. Chem. Soc.* **118**, 5136-5137 (1996).

163. Capadona,J.R., Collard,D.M., & Garcia,A.J. Fibronectin adsorption and cell adhesion to mixed monolayers of tri(ethylene glycol)- and methyl-terminated alkanethiols. *Langmuir* **19**, 1847-1852 (2003).

164. Evens-Nguyen,K.M. & Schoenfish,M.H. Fibrin Proliferation at Model Surfaces: Influence of Surface Properties. *Langmuir* **ASAP**, (2005).

165. Chen,C.S., Mrksich,M., Huang,S., Whitesides,G.M., & Ingber,D.E. Micropatterned surfaces for control of cell shape, position, and function. *Biotechnol. Prog.* **14**, 356-363 (1998).

166. Lahiri,J., Ostuni,E., & Whitesides,G.M. Patterning ligands on reactive SAMs by microcontact printing. *Langmuir* **15**, 2055-2060 (1999).

167. Love,J.C., Wolfe,D.B., Paul,K.E., Chabinyc,M.L., Nuzzo,R.G., & Whitesides,G.M. Self-assembled monolayers on palladium improve the quality of features generated by microcontact printing. *Abs. Papers Am. Chem. Soc.* **224**, U431 (2002).

168. Gallant,N.D., Capadona,J.R., Frazier,A.B., Collard,D.M., & Garcia,A.J. Micropatterned surfaces to engineer focal adhesions for analysis of cell adhesion strengthening. *Langmuir* **18**, 5579-5584 (2002).

169. Mrksich,M., Grunwell,J.R., & Whitesides,G.M. Biospecific Adsorption of Carbonic-Anhydrase to Self-Assembled Monolayers of Alkanethiolates That Present Benzenesulfonamide Groups on Gold. *J. Am. Chem. Soc.* **117**, 12009-12010 (1995).

170. Hodneland,C.D., Lee,Y.S., Min,D.H., & Mrksich,M. Selective immobilization of proteins to self-assembled monolayers presenting active site-directed capture ligands. *Proc. Natl. Acad. Sci. USA* **99**, 5048-5052 (2002).

171. Nelson,K.E., Gamble,L., Jung,L.S., Boeckl,M.S., Naeemi,E., Golledge,S.L., Sasaki,T., Castner,D.G., Campbell,C.T., & Stayton,P.S. Surface characterization of mixed self-assembled monolayers designed for streptavidin immobilization. *Langmuir* **17**, 2807-2816 (2001).

172. Lahiri,J., Isaacs,L., Grzybowski,B., Carbeck,J.D., & Whitesides,G.M. Biospecific binding of carbonic anhydrase to mixed SAMs presenting benzenesulfonamide ligands: A model system for studying lateral steric effects. *Langmuir* **15**, 7186-7198 (1999).

173. Lahann,J., Mitragotri,S., Tran,T.N., Kaido,H., Sundaram,J., Choi,I.S., Hoffer,S., Somorjai,G.A., & Langer,R. A reversibly switching surface. *Science* **299**, 371-374 (2003).

174. Kato,M. & Mrksich,M. Rewiring cell adhesion. *J. Am. Chem. Soc.* **126**, 6504-6505 (2004).

175. Hodneland,C.D. & Mrksich,M. Biomolecular surfaces that release ligands under electrochemical control. *J. Am. Chem. Soc.* **122**, 4235-4236 (2000).

176. Arwin,H. Spectroscopic ellipsometry and biology: recent developments and challenges. *Thin Solid Films* **313**, 764-774 (1998).

177. Lahiri,J., Isaacs,L., Tien,J., & Whitesides,G.M. A strategy for the generation of surfaces presenting ligands for studies of binding based on an active ester as a common reactive intermediate: a surface plasmon resonance study. *Anal. Chem.* **71**, 777-790 (1999).

178. Garcia,A.J., Huber,F., & Boettiger,D. Force required to break alpha5beta1 integrin-fibronectin bonds in intact adherent cells is sensitive to integrin activation state. *J. Biol. Chem.* **273**, 10988-10993 (1998).

179. Garcia,A.J., Schwarzbauer,J.E., & Boettiger,D. Distinct activation states of alpha5beta1 integrin show differential binding to RGD and synergy domains of fibronectin. *Biochemistry* **41**, 9063-9069 (2002).

180. Bolton,A.E. & Hunter,W.M. Labeling of Proteins to High Specific Radioactivities by Conjugation to A I-125-Containing Acylating Agent - Application to Radioimmunoassay. *Biochem. J.* **133**, 529-538 (1973).

181. Kane,R.S., Deschatelets,P., & Whitesides,G.M. Kosomotropes Form the Basis of Protein-Resistan Surfaces. *J. Am. Chem. Soc.* **19**, 2388-2391 (2003).

182. Jeon,S.I. & Andrade,J.D. Protein-Surface Interactions in the Presence of olyethylene Oxide: Effect of Protein Size. *J. Coll. Inter. Sci.* **142**, 159-166 (1991).

183. Jeon,S.I., Lee,J.H., & Andrade,J.D. Protein-Surface Interactions in the Presence of Polyethylene Oxide: Simplified Theory. *J. Coll. Inter. Sci.* **142**, 149-158 (1991).

184. Wang,R.L.C., Kreuzer,H.J., & Grunze,M. Molecular Conformation and Solvation of Oligo(ethylene glycol)-Terminated Self-Assembled Monolayers and Their Resistance to Protein Adsorption. *J. Phys. Chem.* **101B**, 9767-9773 (1997).

185. Herrwerth,S., Eck,W., Reinhardt,S., & Grunze,M. Factors that determine the protein resistance of oligoether self-assembled monolayers - Internal hydrophilicity, terminal hydrophilicity, and lateral packing density. *J. Am. Chem. Soc.* **125**, 9359-9366 (2003).

186. Harder,P., Grunze,M., Dahint,R., Whitesides,G.M., & Laibinis,P.E. Molecular conformation in oligo(ethylene glycol)-terminated self-assembled monolayers on gold and silver surfaces determines their ability to resist protein adsorption. *J. Phys. Chem.* **102B**, 426-436 (1998).

CHAPTER 3

FIBRONECTIN ADSORPTION AND CELL ADHESION TO MIXED MONOLAYERS OF TRI(ETHYLENE GLYCOL)- AND METHYL-TERMINATED ALKANETHIOLS*

SUMMARY

Surface chemistries that prevent protein adsorption and render surfaces non-adhesive have emerged as promising biomaterial modifications for minimizing host-implant inflammatory responses and providing a non-specific background for the presentation of bioactive motifs to elicit directed cellular responses. Oligo(ethylene glycol) moieties [$-(CH_2CH_2O)_n-$, abbreviated as EG_n] have proven to be the most protein-resistant functionality and remain the standard for comparison. In the present study, we analyzed fibronectin (FN) adsorption and cell adhesion to CH_3/EG_3 mixed self-assembled monolayers. In contrast to previous studies with ellipsometry and surface plasmon resonance spectroscopy, we demonstrate significant radiolabeled FN adsorption onto EG_3-containing surfaces, including pure EG_3 monolayers. These FN-coated surfaces supported FN density-dependent increases in fibroblast adhesion strength. However, while FN adsorbed irreversibly to CH_3-terminated surfaces, adsorbed FN was removed from EG_3 monolayers and the corresponding cell adhesion eliminated by long-term (16 h) incubation in either protein-free or serum-containing solutions. Once the adsorbed FN was eluted, EG_3 monolayers remained non-adhesive, even in the presence of serum-containing media. These

*Capadona, J.R., Collard, D.M. and García, A.J. *Langmuir*. 19(5):1847-1852. (2003).

results provide new insights into the interactions between cells and synthetic, non-adhesive surfaces.

INTRODUCTION

Cell adhesion to synthetic surfaces is critical to numerous biomedical and biotechnological applications, including biomaterials, tissue engineering, and in vitro culture substrates.[1-3] In most instances, cell-material interactions are mediated by specific binding of cellular receptors to proteins adsorbed onto material surfaces. For example, many proteins, including immunoglobulins, fibrinogen, and fibronectin (FN), adsorb onto implant surfaces upon contact with physiological fluids.[4-6] These adsorbed proteins mediate the adhesion and activation of platelets, neutrophils, and macrophages which in turn modulate subsequent inflammatory responses.[7-9] Because of the central role of protein adsorption in cell adhesion, inflammation, and tissue formation, extensive research efforts have focused on the analysis of protein adsorption to synthetic surfaces. Numerous studies have shown that the type, quantity, and structure of adsorbed proteins are dynamically influenced by the underlying substrate.[10-14] Of particular importance, surface chemistries that prevent protein adsorption and render surfaces non-adhesive have emerged as promising biomaterial modifications for minimizing host-implant inflammatory responses and providing a non-specific background for the presentation of bioactive motifs to elicit specific cellular responses.[15-20]

Model substrates with well-controlled surface properties represent useful tools for the analysis of surface-protein-cell interactions. In particular, self-assembled monolayers (SAMs) of alkanethiols on gold have provided a robust system to systematically investigate the effects of surface chemistry on protein adsorption without altering other surface properties such as roughness.[11,21] ω-functionalized, long-chain alkanethiolates [$HS-(CH_2)_n-X$, $n \geq 10$] spontaneously assemble from solution onto gold surfaces to form stable, well-packed and ordered monolayers.[22] The physicochemical properties of these monolayers are controlled by the tail group, X. Early work demonstrated the general trend that hydrophobic tail groups enhance protein adsorption while neutral hydrophilic groups exhibit reduced protein adsorption.[11,23] Oligo(ethylene glycol) moieties [$-(CH_2CH_2O)_n-$, abbreviated as EG_n] have proven to be the most protein-resistant functionality and remain the standard for comparison.[11,24,25] Using mixed monolayers of methyl- and EG_n-terminated alkanethiols, Prime and Whitesides demonstrated that, above a critical surface density of EG_n, surfaces effectively resist protein adsorption as determined by ellipsometry and longer EG repeats prevent protein adsorption at lower mole fractions in the monolayer.[24] Leckband and colleagues showed that although EG_n-SAMs with $n \geq 3$ resisted protein adsorption from serum-containing media as measured by surface plasmon resonance (SPR), these monolayers supported significant levels of fibroblast adhesion which decreased with increasing EG chain length.[26] This study indicated that EG_n moieties can support cell adhesion, presumably by adsorbing adhesive proteins from serum, and contrasts with a large body of literature

documenting the effectiveness of short EG_n (n=3-6) groups in preventing protein adsorption and cell adhesion in micropatterning applications.[21,27,28] It is important to point out that the protein measurement techniques used in most of these studies (ellipsometry, SPR) have limited sensitivity and protein densities below the detection limit of these methods (~2 ng/cm^2 reported for SPR[26]) have been shown to support robust cell adhesion.[29,30] In the present study, we used radiolabeled FN to analyze protein adsorption onto mixed monolayers of methyl- and EG_3-terminated alkanethiols. We demonstrate that EG_3-terminated SAMs support FN adsorption at levels that mediate cell adhesion. Unlike CH_3 SAMs, the adsorbed FN can be eluted from the EG_3 monolayers and the corresponding cell adhesion eliminated by long term (16 h) incubation in protein-free or serum-containing solutions. These results provide new insights into our understanding of mechanisms controlling surface-protein-cell interactions.

EXPERIMENTAL SECTION

Materials

Murine NIH3T3 fibroblasts (CRL-1658) were obtained from ATCC (Manassas, VA) and maintained in Dulbecco's modified Eagle's medium (DMEM) supplemented with 10% newborn calf serum (NCS), penicillin (100 units/mL), and streptomycin (100 mg/mL). Cell culture reagents, including human plasma FN and Dulbecco's phosphate buffered saline (PBS), were purchased from Life Technologies (Rockville, MD). Newborn calf serum was obtained from HyClone (Logan, UT). Calcein-AM fluorescent dye was obtained from Molecular Probes

(Eugene, OR). All starting materials for synthesis, 1-dodecanethiol (HS-$(CH_2)_{11}$-CH_3), and all other chemical reagents were used as received from Aldrich Chemical Company (St. Louis, MO). Bolton Hunter Reagent was purchased from NEN Life Sciences (Boston, MA).

Methods

Synthesis of HS-$(CH_2)_{11}$-EG_3-OH

Tri(ethylene glycol)-terminated alkanethiol (HS-$(CH_2)_{11}$-$(EG)_3$OH) was synthesized (**Scheme 3.1**) as previously described[31] and characterized by ^{1}H- and ^{13}C-NMR, Fourier transformed infrared spectroscopy, and mass spectroscopy.

Undec-1-en-11-yltriethlene glycol (1)

A mixture of tri(ethylene glycol) (35.20 g, 234.7 mmol) and 3.75 mL of 50% NaOH was refluxed for 0.5 h at 100 ^{o}C under an atmosphere of nitrogen and 11- bromoundec-1-ene (10.40 ml, 47.4 mmol) was added. The mixture was refluxed for 24 h, cooled and extracted with hexane (6 x 50 mL). The hexane extracts were combined and the solvent was evaporated under reduced pressure to afford a yellow oil. The oil was purified using chromatography (silica gel; gel 1 of ethyl acetate, followed by gel 2 of 19:1 $CHCl_3$/MeOH) to give 5.71 g (79%) of monoether (**1**): ^{1}H NMR (300 MHz, $CDCl_3$) δ1.2 (br m, 12 H, alkane), 1.55 (qui, 2H, *J* = 7 Hz, C-10), 1.95 (q, 2H, *J* = 7 Hz, C-3), 2.85 (br s, 1H, C-OH), 3.35 (t, 2H, *J* = 7 Hz, C-11), 3.6 (m, 12 H, OCH_2CH_2O), 4.85 (qq, 2H, *J* = 3.3, 1.65, C-1),

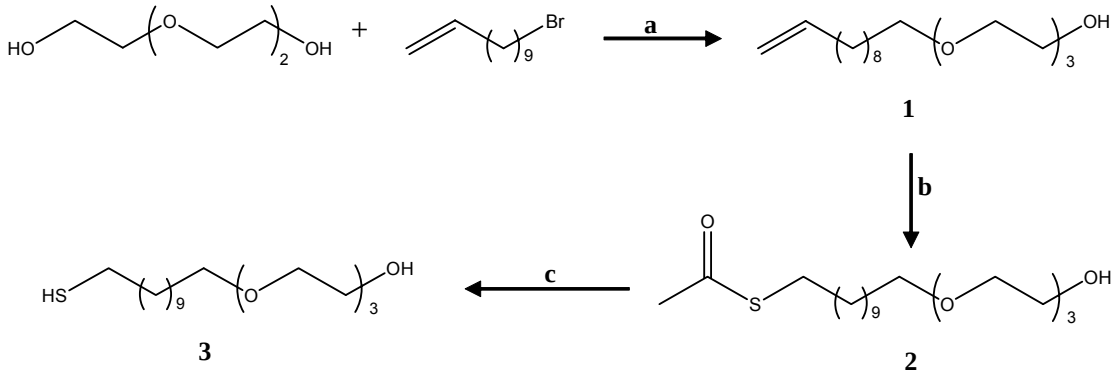

SCHEME 3.1. Conditions; a) Tri(ethylene glycol), 50% NaOH, 100 ^{o}C, 0.5 h; 11-bromoundec-1-ene, 100 ^{o}C, N_2, 24 h. b) AIBN, Thiolacetic acid, dry THF, over night, N_2, hv. c) 0.4 M HCl in MeOH, r.t. 4-5 d, N_2.

5.75 (qt, 1H, J = 7, 3.3, C-2); ^{13}C NMR (75 MHz, $CDCl_3$) δ139.02, 113.98, 72.42, 71.40, 70.46, 70.20, 69.87, 61.52, 33.65, 29.43, 29.38, 29.28, 28.96, 28.76, 25.91; MS (CI, ammonia), M+1 303.2, M+18 320.3; IR (neat, cm^{-1}) v_{max} 3459.78 (C-OH), 3070.83 (C=C H-stretching), 2854.74 (CH_2 symmetric), 1463.15 (CH_2 scissoring) , 1126.05 (C-O stretch).

[1-[(Methylcarbonyl)thio]undec-11-yl]-tri(ethylene glycol) (2)

Undec-1-en-11-yltriethlene glycol (1) (1.0g, 3.3 mmol) was added to a solution of thiolacetic acid (0.94 mL, 13.2mmol) and AIBN 0.15 g, 0.91 mmol) in dry THF (8.25 mL) and the mixture was irradiated overnight under an atmosphere of nitrogen with a 450-W medium pressure mercury submersion lamp. The solvent was removed on a rotorary evaporator to give crude product. The oil was purified using chromatography (silica gel; 30:1 CH_2Cl_2/ MeOH) to give thioacetate **2** at 79%: was used without further purification; ^{1}H NMR (300 MHz, $CDCl_3$) δ1.2 (br s, 12 H, alkane), 1.6 (m, 4 H, C-9, C-10), 2.33 (s, 3 H, -CH_3), 2.85 (t, 2 H, *J* = 7 Hz, C-1), 3.45 (t, 2 H, *J* = 7 Hz, C-11), 3.6-3.8 (m, 12 H, OCH_2CH_2O); ^{13}C NMR (75 MHz, $CDCl_3$) δ 72.42, 71.40, 70.46, 70.20, 69.87, 61.52, 33.65, 29.43, 29.38, 29.28, 28.96, 28.76, 25.91; MS (CI, ammonia), M+1 379.2; IR (neat, cm^{-1}) v_{max} 3455.46 (C-OH stretch), 2928.21 (CH_2 asymmetric stretch), 2850.42 (CH_2 symmetric stretch), 2245.38 (S-C=0-CH_3), 1467.47 (CH_2 scissoring), 1350.78 (CH_2 wagging), 1247.06 (out of plane bending), 1108.76 (C-O), 732.77 (C-S-C).

(1-Mercaptoundec-11-yl)tri(ethylene glycol) (HS-11-(EG)$_3$OH, 3)

Thioacetate **2** was dissolved in 0.4 M HCl in MeOH, and the mixture was stirred at room temperature for 4-5 d under nitrogen. Solvent was removed and the crude product was purified using chromatography (silica gel; 8:8:1 EtAc/ CH_2Cl_2/ MeOH) 86% yield; 1H NMR (300 MHz, $CDCl_3$) δ 1.1 (br s, 14 H, alkane), 1.2 (t, 1 H, *J*= 7 Hz, C-SH), 1.5 (m, 4 H, C-9, C-10), 2.5 (q, 2 H, *J* = 7, C-1), 3.0 (br s, 1 H, C-OH), 3.4 (t, 2 H, *J* = 7, C-11), 3.5-3.75 (m, 12 H, OCH_2CH_2O); 13C NMR (75 MHz, $CDCl_3$) δ 72.51, 71.54, 70.53, 70.28, 69.96, 61.67, 33.98, 29.51, 29.45, 29.00, 28.31, 26.00, 24.59; MS (EI) M+1 337, IR (neat, cm-1) v max 3451.14 (C-OH stretch), 2923.89 (CH_2 asymmetric stretch), 2850.42 (CH_2 symmetric stretch), 2560.86 (S-H stretch), 1467.47 (CH_2 scissoring), 1350.78 (CH_2 wagging), 1294.60 (CH_2 twisting), 1130.37 (C-O stretch), 724.13 (CH_2 rocking).

Preparation of Substrates and Monolayer Formation.

Glass coverslips (9 mm^2) were cleaned in 70% H_2SO_4/30% H_2O_2 for 1 h at 90^{o}C, rinsed with diH_2O, then EtOH, and dried under a stream of N_2. Lab-Tek 16-well chamber slides (Nalge Nunc, Naperville, IL) were cleaned by oxygen plasma etching for 3 min in a barrel etcher (LFE Plasma Systems, Clinton, MA). All substrates were coated with 50 Å Ti, then 150 Å Au using a Thermionics VE-100 electron beam evaporator (Modesto, CA). To assemble CH_3/EG_3 mixed monolayers, Au-coated samples were immersed in ethanolic solutions containing mixtures of the two alkanethiols. The mole fractions of the two thiols were varied

while the total alkanethiol solution concentration was maintained constant at 2 mM. For contact angle and X-ray photoelectron spectroscopy (XPS) characterization, SAMs were immersed in alkanethiol solutions for 10 h. For all other experiments unless noted, monolayers were assembled for 4 h. After immersion in alkanethiol solutions, samples were rinsed in EtOH and dried under a stream of N_2 prior to use.

Contact Angle Measurements.

Ambient air-water-surface contact angles for SAMs comprising varying EG_3 mole fractions were measured as described previously.[32,33] Briefly, a 5 μL drop of diH_2O was placed on the surface and advancing contact angles were measured from opposite edges of the drop using a Ramé-Hart model #100-00 goniometer (Mountain Lakes, NJ) fitted with a digital camera and analyzed using in-house image analysis software.

X-ray Photoelectron Spectroscopy (XPS).

XPS analysis was carried out with a Surface Science Model SSX-100 with small spot ESCA spectrometer. SAMs were prepared as described above using solution mole fractions ranging from 0 to 1.0 in increments of 0.1. Survey scans for S, C, and O were first obtained for elemental analysis of the surface. Detailed scans for O1s and C1s were obtained for each surface composion. Surface mole fractions for EG_3 (χ_{EG3}) were calculated as the ratio of the intensity of the O1s peak for the sample to the intensity of the O1s peak for pure EG_3 SAM.

FN Adsorption Measurements.

FN adsorption to SAMs was quantified using ^{125}I-labeled FN. FN was iodinated using the Bolton-Hunter Reagent as described previously.[13,30] Briefly, the Bolton-Hunter Reagent was concentrated in the reaction vessel by evaporating the benzene solvent under a stream of N_2. FN (100 μg, 10 μg/mL in 0.1 M sodium borate, pH = 8.5) was added and incubated overnight at 4°C. The coupling reaction was quenched with 50 μL of 0.2 M glycine in 0.1 M sodium borate. Labeled FN (^{125}I-FN) was purified by size exclusion chromatography using a Sephadex G-25 column. The column was blocked overnight with 1% bovine serum albumin (BSA) prior to use. ^{125}I-FN fractions were pooled and stored at 4°C. Specific activity (1.9 x 10^6 cpm/μg) was determined with the NanoOrange Protein Quantification Kit (Molecular Probes) along with measurements of radioactivity using a COBRA II Auto Gamma Counter (Packard Bioscience, Meridien, CT). To demonstrate that the iodination procedure did not alter the activity of the protein, control adsorption experiments with different ratios of labeled and unlabeled protein were performed.

For this and all subsequent experiments, mole fractions reported for SAMs were surface composition as determined from XPS analysis. SAMs were assembled on Au-coated 9 mm^2 glass cover slips and pre-soaked in diH_2O for 30 min. Samples were then immersed in ^{125}I-FN solutions (mixed with unlabeled FN in PBS) for 1 h. After removing FN solutions, samples were immersed in 1% BSA for 1 h. Samples were transferred to clean tubes and radioactivity was measured using a gamma counter. Adsorbed ^{125}I-FN was quantified as

radioactive counts (cpm) and converted to adsorbed FN surface densities (ng/cm^2). For FN elution studies, samples were coated with FN and BSA as described above, then incubated in PBS or 10% NCS in DMEM for 1 h or 16 h, and the remaining FN adsorbed on the sample was quantified.

Cell Adhesion Assay.

Cell adhesion to SAMs was measured using a centrifugation assay that applies well-controlled detachment forces.[32,34] SAMs were assembled in Au-coated Lab-Tek chamber slides and incubated in different FN concentrations for 1 h and then blocked in 1% BSA for 1 h to prevent non-specific adhesion. NIH3T3 fibroblasts were labeled with 2 μg/mL calcein-AM and seeded at 200 cells/mm^2 in 10% NCS in DMEM onto chamber slides for 1 h at room temperature. Initial fluorescence intensity was measured to quantify the number of adherent cells prior to the application of force. After filling the wells with media and sealing with transparent adhesive tape, substrates were spun at a fixed speed in a centrifuge (Beckman Allegra 6, GH 3.8 rotor) to apply a centrifugal force corresponding to 46g. After centrifugation, media was exchanged and fluorescence intensity was read to measure remaining adherent cells. For each well, adherent cell fraction was calculated as the ratio of post-spin to pre-spin fluorescence readings.

Statistical Analysis.

Results were analyzed by ANOVA using SYSTAT 8.0 (SPSS, Chicago, IL). If treatments were determined to be significant, pair-wise comparisons were performed using Tukey post-hoc test. A 95% confidence level was considered significant.

RESULTS AND DISCUSSION

Surface Characterization.

Mixed CH_3/EG_3-terminated SAMs were assembled by varying the ratio of the two alkanethiols in solution but keeping a constant total thiol solution concentration. Ambient air-water-surface contact angles decreased with increasing EG_3-thiol concentration (**Figure 3.1**) and values are consistent with published results.[24,31] EG_3 mole fractions in the monolayer (χ_{EG3}) were lower than the corresponding solution EG_3 mole fraction (**Figure 3.1**) indicating that the CH_3-terminated thiol assembled preferentially. The observed surface-solution EG_3 mole fraction relationship agrees well with other reports of coadsorption of alkanethiols.[31,33] This empirical relationship was then used to adjust the solution concentrations of the two thiols in order to assemble monolayers with surface mole fractions ranging from 0 to 1.0 at 0.1 increments.

FN Adsorption to Mixed SAMs.

FN was selected as the protein model for our study because of its critical importance in mediating cell adhesion to surfaces and widespread use in

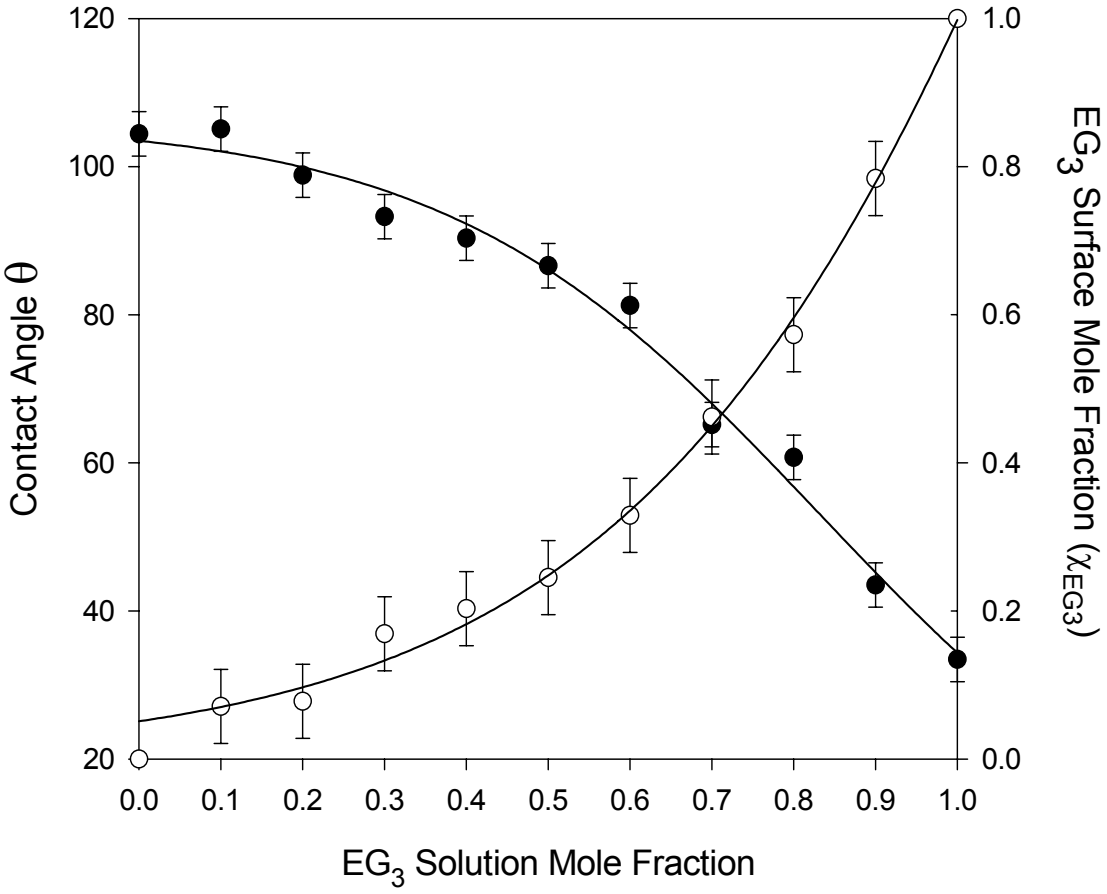

FIGURE 3.1 Characterization of mixed SAMs of CH3/EG3-terminated alkanethiols by contact angle (●, left axis) and XPS (○, right axis). Monolayers were assembled by immersion in 2 mM ethanolic solutions containing mixtures of the two alkanethiols for 10 h. Ambient air-water-surface advancing contact angle measurements represent mean (3-4 drops) + standard error. Surface mole fractions determined by XPS are reported values determined from the ratio of the intensity of O1s peak for the sample divided by the O1s peak intensity for pure EG3 monolayer.

biomedical and biotechnological applications, including SAM micropatterning. FN adsorption onto SAMs was quantified as a function of coating concentration using radiolabeled FN. We have previously demonstrated that this technique provides direct measurements of protein adsorption with high sensitivity (0.01 ng/cm^2).[29,30] **Figure 3.2a** shows adsorption profiles for different SAMs exhibiting a linear adsorption regime at low coating concentrations and approaching a saturation plateau at higher concentrations, as expected for single component adsorption.[6] Our adsorption measurements for CH_3-SAMs and glass (control, not shown) are in excellent agreement with previous studies.[30,32] **Figure 3.2b** shows adsorbed FN density as a function of EG_3 surface mole fraction for different FN coating concentrations. For all EG_3 mole fractions, FN adsorption increased with increasing coating concentration ($p < 0.000003$). For a given coating concentration, FN adsorption exhibited sigmoidal decreases with increasing EG_3 surface composition ($p < 0.0007$) with a sharp drop-off around 0.5 EG_3 mole fraction. This trend in adsorption is qualitatively similar to that observed with ellipsometry and SPR.[24,35] However, at high FN coating concentrations, significant amounts of FN adsorbed to the higher EG_3 composition SAMs, including the pure EG_3 SAM (**Figure 3.2b**). This result contradicts previous reports documenting the ability of EG_3 moieties to prevent protein adsorption.[11,24,26] While this behavior may be unique to FN, we attribute this observation to the enhanced sensitivity of our measurement method. It is important to note that adsorption studies with SPR have reported detection of a layer of surface-associated protein which is quickly (in a manner of seconds)

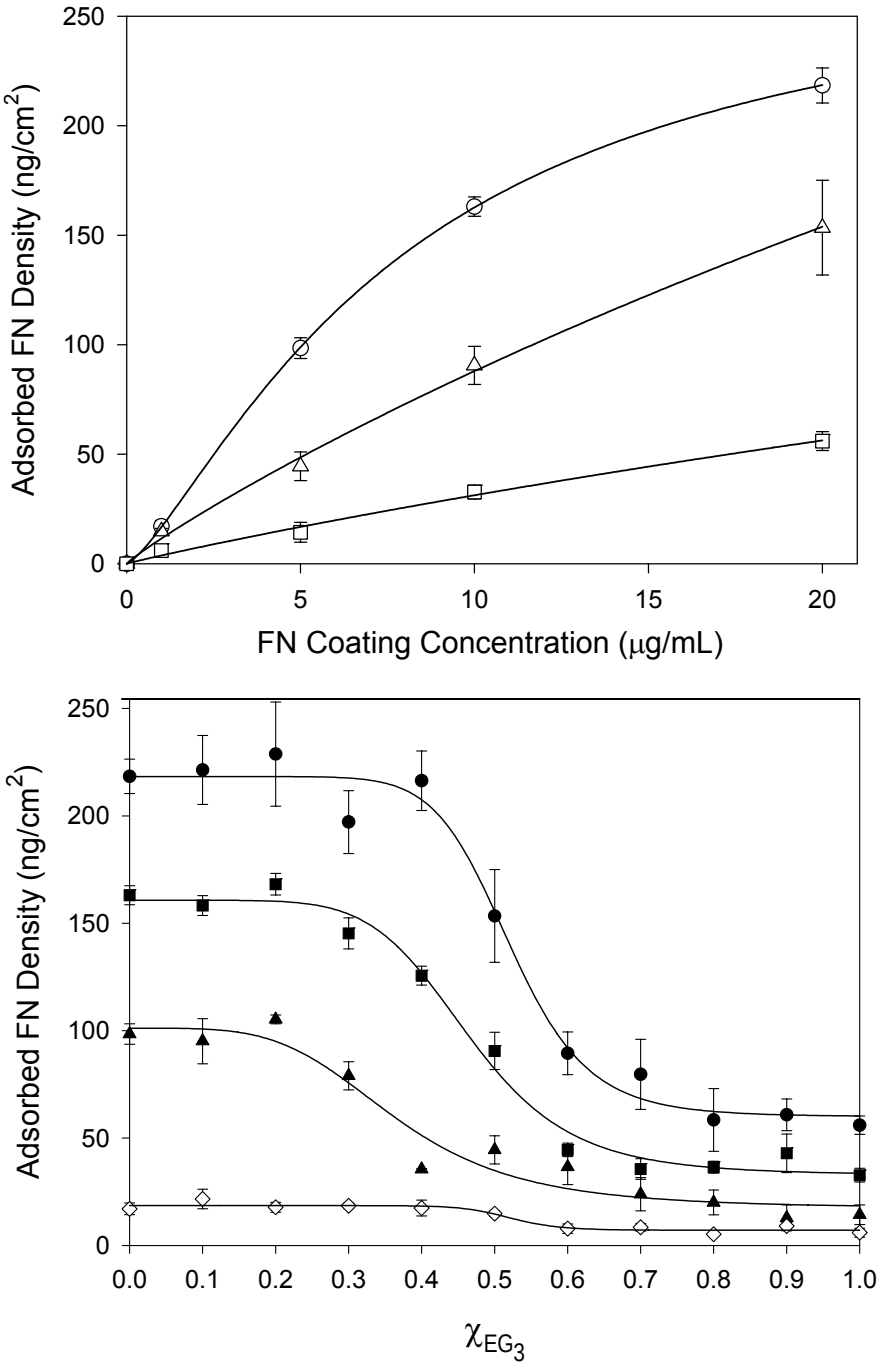

FIGURE 3.2 (a) FN adsorption onto SAMs as a function of FN coating concentration showing characteristic adsorption isotherms and differences among EG_3 surface composition; χEG_3 ○ = 0.0, △ = 0.5, □ = 1.0. (b) FN adsorption to mixed SAMs as a function of surface composition (χEG_3) showing sigmoidal decreases with EG_3 surface mole fraction (two separate runs in duplicate, mean + standard error); FN coating concentration ● = 20 μg/mL, ■ = 10 μg/mL, ▲ = 5 μg/mL, ◇ = 1 μg/mL.

lost upon removal of the protein coating solution.[23,26] This "loosely" associated protein layer is not responsible for the FN adsorption observed in this study as the SAMs are incubated in BSA solutions for 1 h after FN coating. In addition, we have observed no differences in FN adsorption when the samples are rinsed in PBS after FN coating.

Cell Adhesion to FN-Coated SAMs.

Our adsorption measurements revealed significant FN adsorption onto CH_3/EG_3 mixed SAMs, including pure EG_3 monolayers. In order to determine whether the amounts of adsorbed FN were sufficient to mediate specific cellular responses, we quantified cell adhesion at 1 h to mixed SAMs as a function of FN density using a centrifugation assay. We previously demonstrated that this assay applies controlled and reproducible detachment forces to adherent cells and provides relative measurements of adhesion strength.[32,34] For a constant centrifugal force, the fraction of adherent cells increases sigmoidally with adsorbed FN density (**Figure 3.3**). Left-right shifts in the adhesion profile (adherent cell fraction vs. adsorbed FN density) reflect differences in adhesion strength with a left-ward shift indicating higher adhesion at lower FN densities and corresponding to higher adhesion strength. For all EG_3 mole fractions, adherent cell fraction increased with adsorbed FN density ($p < 0.001$), demonstrating that the adsorbed FN is present at levels sufficient to mediate cell adhesion (**Figure 3.3**). Interestingly, increasing the EG_3 surface composition increased the efficiency of the adsorbed FN to support cell adhesion as indicated

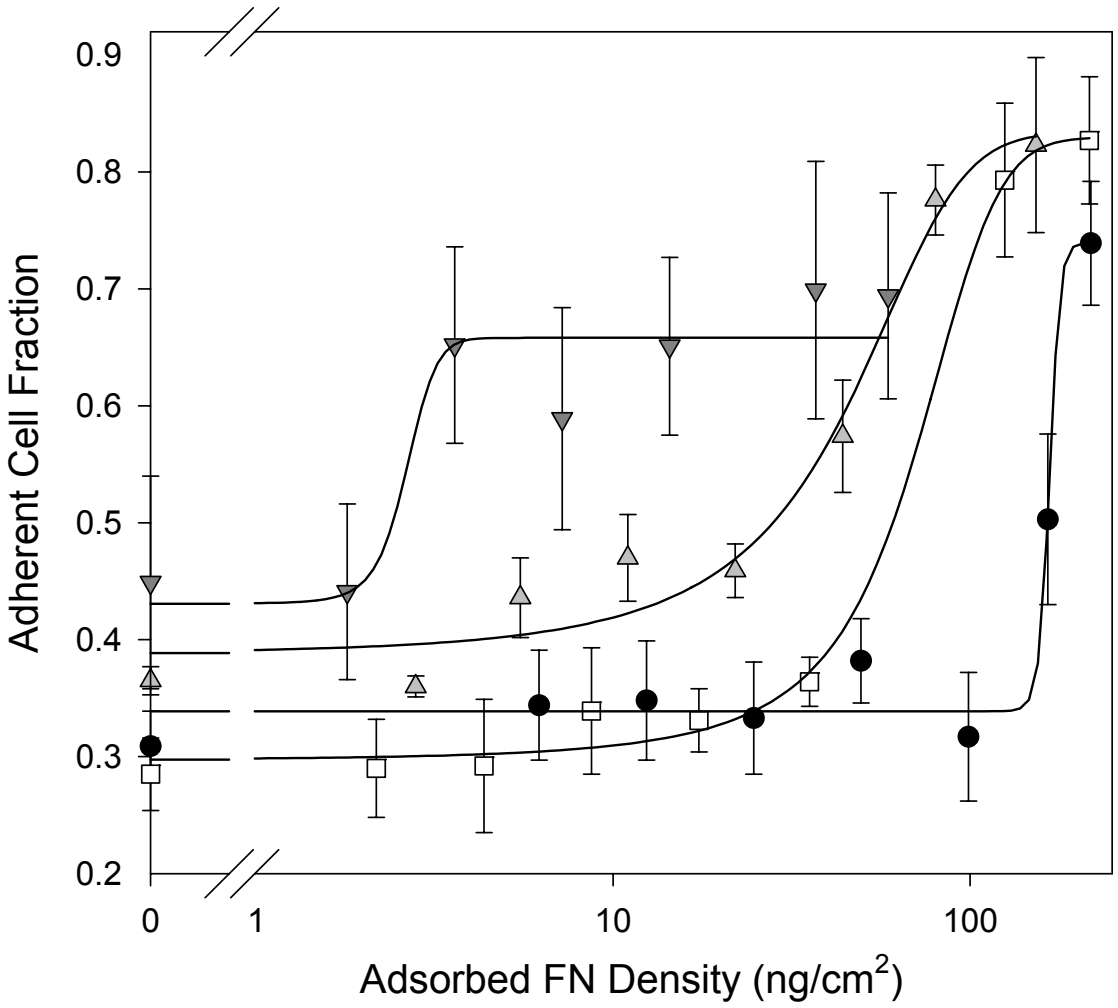

FIGURE 3.3 NIH cell adhesion to FN-coated SAMs depends on EG_3 surface composition. Adhesion profile shows adherent cell fraction as a function of adsorbed FN density and sigmoidal curve fits. Shifts in adhesion profiles demonstrate differences in cell adhesion strength with χEG_3 (three separate runs in duplicate, mean + standard error), χEG3 ● = 0.0, □ = 0.4, △ = 0.5, ▽ = 1.0.

by left-ward shifts in the adhesion profiles. We attribute this increased efficiency to substrate-dependent differences in the structure of adsorbed FN. Consistent with previous work,[10,13,35-37] we have recently demonstrated, using alkanethiol SAMs presenting different functional tail groups, that surface chemistry alters FN structure and modulates cell adhesion to adsorbed FN.[32] In particular, the hydrophobic CH_3 group exhibited signficant loses in FN adhesion activity while the hydrophilic OH moieity supported enhanced cell adhesion. The present findings for the CH_3-SAM and the neutral hydrophilic EG_3 group are in excellent agreement with these observations.

The results that FN adsorbs onto EG_3 SAMs and supports cell adhesion indicate that this functional group is not as protein-resistant as previously thought. This finding is consistent with the observations of Leckband and co-workers[26] but appears to conflict with several studies demonstrating that cells do not adhere to EG_3-functionalized surfaces in the presence of serum-containing solutions.[21,27,38,39] Leckband et al. noted that cells adhering to EG_3-terminated SAMs in the presence of serum-containing solutions could be detached by incubating in serum-free solutions. These investigators postulated that the adsorbed serum proteins mediating cell adhesion were removed from the surface in the absence of serum proteins.

Elution of Adsorbed FN from Mixed SAMs.

To establish whether adsorbed FN is removed from EG_3 SAMs in serum-free solutions, we measured retention of adsorbed FN on SAMs after incubation

in either protein-free (PBS) or serum-containing (10% NCS) solutions for 1 h and 16 h. As shown in **Figure 3.4**, the ability to remove adsorbed FN is dependent on the surface and the presence of serum proteins. For the CH_3-terminated SAM (χ_{EG3} = 0), there were no differences in adsorbed FN among control and incubation treatments ($p < 0.27$), indicating no removal or displacement of adsorbed FN after incubation for up to 16 h in either protein-free or serum-containing solutions. This result is consistent with previous studies demonstrating irreversible adsorption of FN onto hydrophobic surfaces.[10,40] For monolayers with 50% EG_3, slightly lower densities of FN were measured after incubation for 16 h in both protein-free and serum-containing solutions but these were not statistically significant from the control (no incubation) group. In constrast, incubation of FN-coated pure EG_3 SAM in either protein-free or serum-containing solutions resulted in significant removal of pre-adsorbed FN ($p < 0.00002$). Long-term (16 h) incubation in PBS was particularly effective in removing adsorbed FN down to undetectable levels. Interestingly, removal of adsorbed FN from EG_3 surfaces behaved differently from FN removal from glass (**Figure 3.4**). Incubation in either protein-free or serum-containing solutions removed adsorbed FN from glass, but the serum-containing solution was significantly more effective at removing FN at longer time points. This result is consistent with a model in which serum proteins displace adsorbed FN on glass.[6] On the other hand, incubating in PBS was more effective than 10% serum in removing FN adsorbed on the EG_3 monolayer ($p < 0.002$), suggesting elution of the adsorbed FN by concentration gradients rather than displacement by other

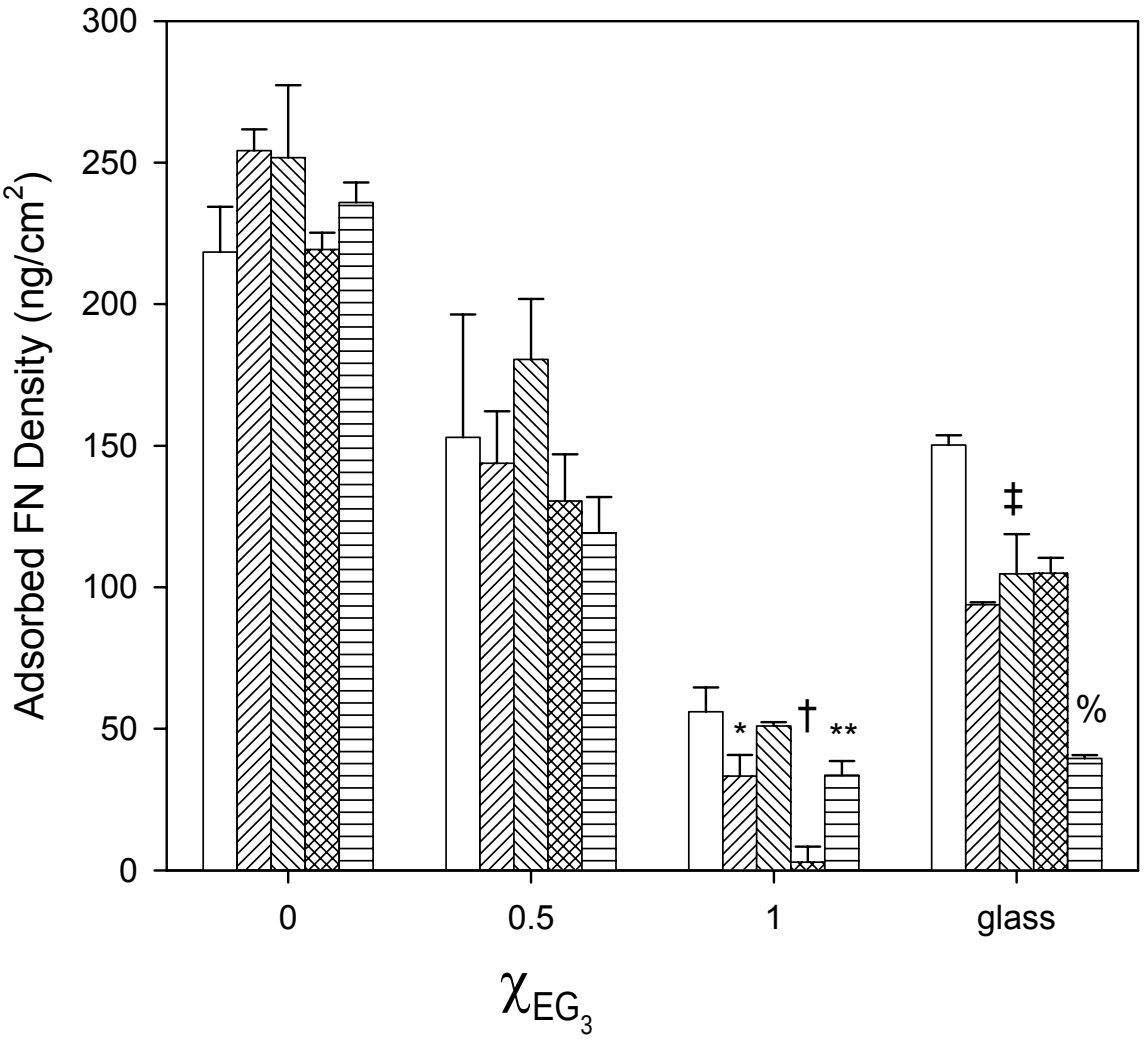

FIGURE 3.4 Retention of adsorbed FN to CH_3/EG_3 mixed SAMs after incubation in protein-free (PBS) and serum-containing (10% NCS) solutions demonstrating surface composition- and solution-dependent elution of adsorbed FN. SAMs were coated with 125I-FN (20 μg/mL), blocked with BSA, and retained radioactivity was measured after various elution treatments; no incubation control (▭), incubation in PBS for 1 h (▨) or 16 h (▩), incubation in 10% NCS for 1 h (▧) or 16 h (▤). $\chi EG_3 = 1.0$, ANOVA $p < 0.00002$, * control > PBS 1 h ($p < 0.02$), † control > PBS 16 h ($p < 0.00002$), ** control > 10% NCS 16 h ($p < 0.02$); glass, ANOVA $p < 0.0001$, ‡ control > PBS 1 h, PBS 16 h, 10% NCS 1 h ($p < 0.01$), % control > 10% NCS 16 h ($p < 0.00002$).

proteins. Nonetheless, the exact mechanism(s) for the removal of adsorbed FN from these surfaces remains to be elucidated.

Cell Adhesion to FN-Eluted Mixed SAMs.

We next compared cell adhesion (1 h) to FN-coated SAMs that were either pre-incubated in PBS or 10% serum for 16 h or used immediately after FN and BSA coating. Consistent with the FN measurements, there were no differences in cell adhesion to CH_3-terminated SAMs (**Figure 3.5**). Incubation in 10% serum reduced cell adhesion to the 50% EG_3 monolayer ($p < 0.05$), while incubation in PBS had no effect on cell adhesion. For the pure EG_3 monolayer, incubation in either PBS or 10% serum reduced adhesion values to background levels, whereas control surfaces (no incubation in PBS or 10% serum) again supported cell adhesion ($p < 0.02$) (**Figure 3.5**). Furthermore, there were no differences in cell adhesion between EG_3 monolayers incubated in PBS and 10% serum, indicating that once FN is eluted the surface remains non-adhesive even in the presence of serum-containing solutions. A possible explanation for this non-adhesive behavior is the adsorption of inert serum proteins that compete out adsorption sites on the surface. This phenomenon also explains our unpublished observations that cells adhering to FN-coated EG_3 monolayers adhere and spread but eventually detach after 6-12 h in culture. These results reconcile observations of FN adsorption and cell adhesion to EG_3-functionalized surfaces with the body of literature documenting the protein-resistant and non-adhesive nature of these substrates.

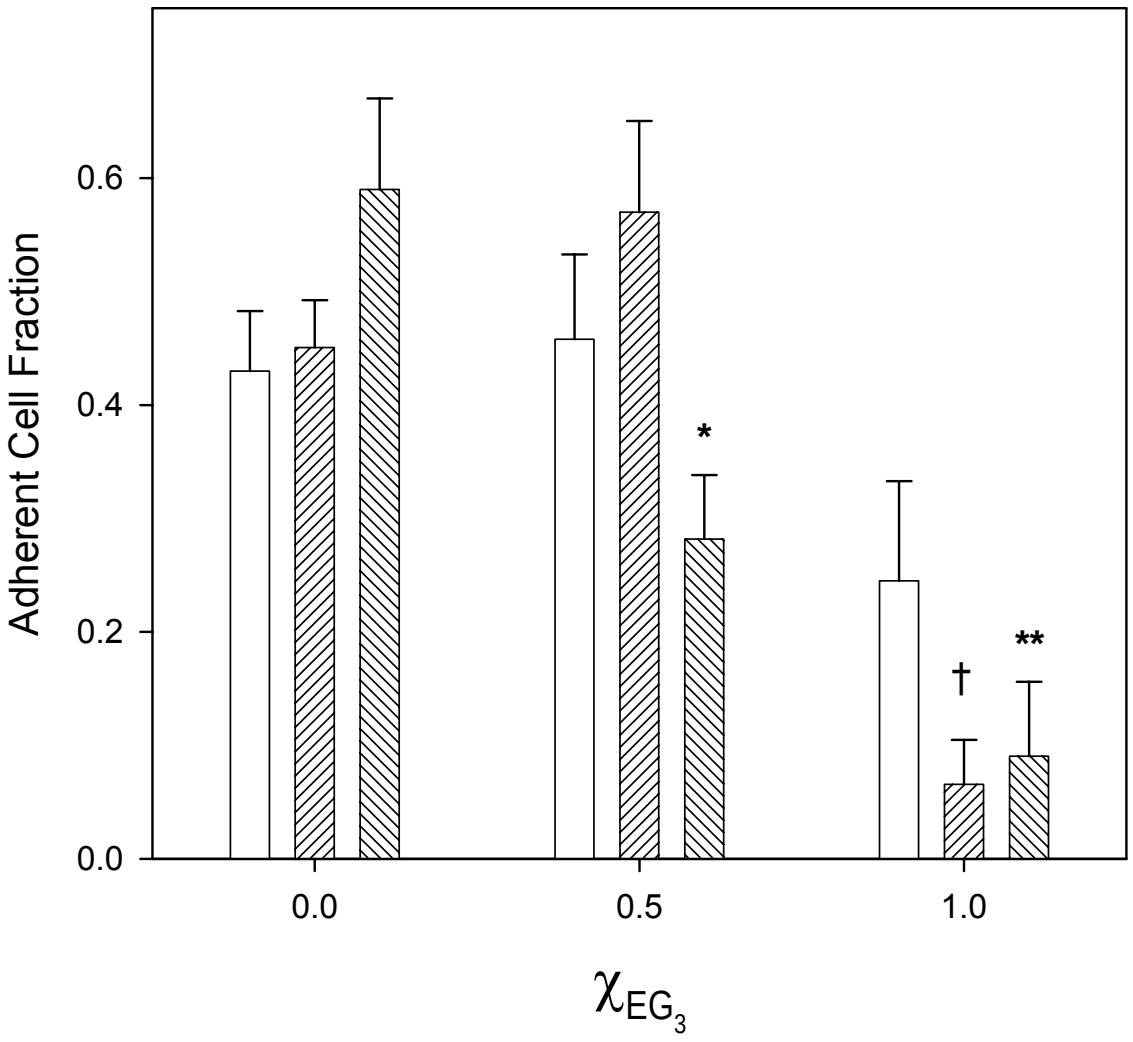

FIGURE 3.5 Effects of pre-incubation in protein-free (PBS) and serum-containing (10% NCS) solutions on cell adhesion to FN-coated SAMs showing surface composition-dependent differences. Cells were seeded on FN-coated SAMs that were either pre-incubated in PBS or 10% serum for 16 h or used immediately after FN coating (20 μg/mL); no incubation (▭), incubated in PBS for 16 h (▨), incubated in 10% NCS for 16 h (▨). χEG_3 = 0.5, ANOVA $p < 0.05$, * control, PBS > 10% NCS ($p < 0.05$); χEG_3 = 1.0, ANOVA $p < 0.02$, † control > PBS ($p < 0.02$), ** control > 10% NCS ($p < 0.04$).

Effects of Monolayer Assembly Time on FN Adsorption.

Lastly, we examined the effects of EG_3 monolayer assembly time on FN adsorption to rule out that our results for FN adsorption and cell adhesion were due to longer assembly times (4 h) compared to other studies (typically 1-2 h). Although EG_3 monolayers assemble within 1 h,[41] Mrksich et al. recommended using assembly times of less than 12 h for micropatterning applications as they observed protein adsorption on EG_3 monolayers assembled for longer time periods.[21] Monolayers assembled for 1, 4, and 16 h were coated with ^{125}I-FN (20 μg/mL), blocked with BSA, and retained radioactivity was measured immediately or after incubation in PBS for 16 h (**Figure 3.6**). Significant amounts of FN adsorbed onto EG_3 SAMs ($p < 0.0003$) and monolayer assembly time had no effect on FN adsorption ($p < 0.6$). For all assembly times, incubation in PBS for 16 h reduced FN adsorption close to background levels.

CONCLUSIONS

Using highly sensitive protein adsorption and cell adhesion assays, we demonstrate significant FN adsorption and cell adhesion to CH_3/EG_3 mixed SAMs, including pure EG_3 monolayers. While FN adsorbed irreversibly to CH_3-terminated surfaces, adsorbed FN was removed from EG_3 monolayers and the corresponding cell adhesion eliminated by long-term (16 h) incubation in protein-free or serum-containing solutions. Once the adsorbed FN was eluted, EG_3 monolayers remained non-adhesive, even in the presence of serum-containing

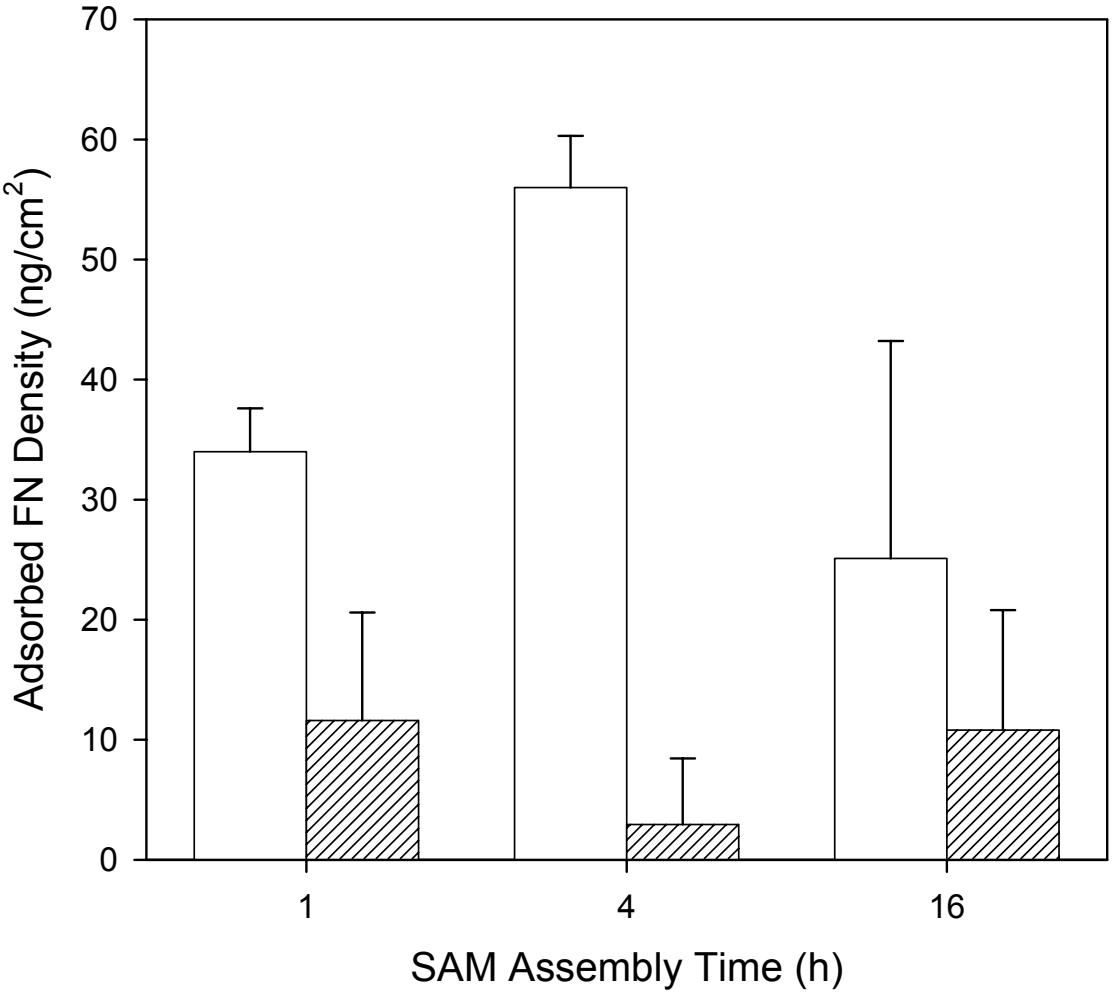

FIGURE 3.6 Effects of monolayer assembly time on retention of adsorbed FN for pure EG_3 SAMs. Monolayers were coated with 125I-FN (20 μg/mL), blocked with BSA, and retained radioactivity was measured immediately (▭) or after incubation in PBS for 16 h (▨). Adsorbed FN measurements revealed no dependence on SAM assembly time.

media. These results provide new insights into the interactions between cells and synthetic, non-adhesive surfaces.

REFERENCES

1. Ziats,N.P., Miller,K.M., & Anderson,J.M. In vitro and in vivo interactions of cells with biomaterials. *Biomaterials* **9**, 5-13 (1988).

2. Sharma,S.K. & Mahendroo,P.P. Affinity chromatography of cells and cell membranes. *J. Chromatogr.* **184**, 471-499 (1980).

3. Langer,R. & Vacanti,J.P. Tissue engineering. *Science* **260**, 920-926 (1993).

4. Baier,R.E. & Dutton,R.C. Initial events in interactions of blood with a foreign surface. *J. Biomed. Mater. Res.* **3**, 191-206 (1969).

5. Brash,J.L. Protein Adsorption at the Solid-Solution Interface in Relation to Blood Material Interactions. *ACS Symposium Series* **343**, 490-506 (1987).

6. Andrade,J.D. & Hlady,V. Protein Adsorption and Materials Biocompatibility - A Tutorial Review and Suggested Hypotheses. *Adv. Poly. Sci.* **79**, 1-63 (1986).

7. Anderson,J.M., Bonfield,T.L., & Ziats,N.P. Protein adsorption and cellular adhesion and activation on biomedical polymers. *Int. J. Artif. Organs* **13**, 375-382 (1990).

8. Shen,M. & Horbett,T.A. The effects of surface chemistry and adsorbed proteins on monocyte/macrophage adhesion to chemically modified polystyrene surfaces. *J. Biomed. Mater. Res.* **57**, 336-345 (2001).

9. Tsai,W.B., Grunkemeier,J.M., & Horbett,T.A. Human plasma fibrinogen adsorption and platelet adhesion to polystyrene. *J. Biomed. Mater. Res.* **44**, 130-139 (1999).

10. Grinnell,F. & Feld,M.K. Adsorption characteristics of plasma fibronectin in relationship to biological activity. *J. Biomed. Mater. Res.* **15**, 363-381 (1981).

11. Prime,K.L. & Whitesides,G.M. Self-assembled organic monolayers: model systems for studying adsorption of proteins at surfaces. *Science* **252**, 1164-1167 (1991).

12. Lewandowska,K., Pergament,E., Sukenik,C.N., & Culp,L.A. Cell-type-specific adhesion mechanisms mediated by fibronectin adsorbed to chemically derivatized substrata. *J. Biomed. Mater. Res.* **26**, 1343-1363 (1992).

13. Garcia,A.J., Vega,M.D., & Boettiger,D. Modulation of cell proliferation and differentiation through substrate-dependent changes in fibronectin conformation. *Mol. Biol. Cell* **10**, 785-798 (1999).

14. Tegoulia,V.A. & Cooper,S.L. Leukocyte adhesion on model surfaces under flow: effects of surface chemistry, protein adsorption, and shear rate. *J. Biomed. Mater. Res.* **50**, 291-301 (2000).

15. Lee,J.H., Kopecek,J., & Andrade,J.D. Protein-resistant surfaces prepared by PEO-containing block copolymer surfactants. *J. Biomed. Mater. Res.* **23**, 351-368 (1989).

16. Fujimoto,K., Inoue,H., & Ikada,Y. Protein adsorption and platelet adhesion onto polyurethane grafted with methoxy-poly(ethylene glycol) methacrylate by plasma technique. *J. Biomed. Mater. Res.* **27**, 1559-1567 (1993).

17. Kidane,A., Lantz,G.C., Jo,S., & Park,K. Surface modification with PEO-containing triblock copolymer for improved biocompatibility: in vitro and ex vivo studies. *J. Biomater. Sci. Polym. Ed* **10**, 1089-1105 (1999).

18. Hern,D.L. & Hubbell,J.A. Incorporation of adhesion peptides into nonadhesive hydrogels useful for tissue resurfacing. *J. Biomed. Mater. Res.* **39**, 266-276 (1998).

19. Leckband,D., Sheth,S., & Halperin,A. Grafted poly(ethylene oxide) brushes as nonfouling surface coatings. *J. Biomater. Sci. Polym. Ed.* **10**, 1125-1147 (1999).

20. Morra,M. On the molecular basis of fouling resistance. *J. Biomater. Sci. Polym. Ed.* **11**, 547-569 (2000).

21. Mrksich,M., Dike,L.E., Tien,J., Ingber,D.E., & Whitesides,G.M. Using microcontact printing to pattern the attachment of mammalian cells to self-assembled monolayers of alkanethiolates on transparent films of gold and silver. *Exp. Cell Res.* **235**, 305-313 (1997).

22. Bain,C.D., Troughton,E.B., Tao,Y.T., Evall,J., Whitesides,G.M., & Nuzzo,R.G. Formation of Monolayer Films by the Spontaneous Assembly of Organic Thiols from Solution Onto Gold. *J. Am. Chem. Soc.* **111**, 321-335 (1989).

23. Sigal,G.B., Mrksich,M., & Whitesides,G.M. Effect of surface wettability on the adsorption of proteins and detergents. *J. Am. Chem. Soc.* **120**, 3464-3473 (1998).

24. Prime,K.L. & Whitesides,G.M. Adsorption of Proteins Onto Surfaces Containing End-Attached Oligo(Ethylene Oxide) - A Model System Using Self-Assembled Monolayers. *J. Am. Chem. Soc.* **115**, 10714-10721 (1993).

25. Luk,Y.Y., Kato,M., & Mrksich,M. Self-assembled monolayers of alkanethiolates presenting mannitol groups are inert to protein adsorption and cell attachment. *Langmuir* **16**, 9604-9608 (2000).

26. Zhu,B., Eurell,T., Gunawan,R., & Leckband,D. Chain-length dependence of the protein and cell resistance of oligo(ethylene glycol)-terminated self-assembled monolayers on gold. *J. Biomed. Mat. Res.* **56**, 406-416 (2001).

27. Singhvi,R., Kumar,A., Lopez,G.P., Stephanopoulos,G.N., Wang,D.I.C., Whitesides,G.M., & Ingber,D.E. Engineering Cell-Shape and Function. *Science* **264**, 696-698 (1994).

28. Chen,C.S., Mrksich,M., Huang,S., Whitesides,G.M., & Ingber,D.E. Micropatterned surfaces for control of cell shape, position, and function. *Biotechnol. Prog.* **14**, 356-363 (1998).

29. Garcia,A.J., Ducheyne,P., & Boettiger,D. Effect of surface reaction stage on fibronectin-mediated adhesion of osteoblast-like cells to bioactive glass. *J. Biomed. Mater. Res.* **40**, 48-56 (1998).

30. Garcia,A.J., Huber,F., & Boettiger,D. Force required to break alpha5beta1 integrin-fibronectin bonds in intact adherent cells is sensitive to integrin activation state. *J. Biol. Chem.* **273**, 10988-10993 (1998).

31. Palegrosdemange,C., Simon,E.S., Prime,K.L., & Whitesides,G.M. Formation of Self-Assembled Monolayers by Chemisorption of Derivatives of Oligo(Ethylene Glycol) of Structure $HS(CH_2)_{11}(OCH_2CH_2)$Meta-OH on Gold. *J. Am. Chem. Soc.* **113**, 12-20 (1991).

32. Keselowsky,B.G., Collard,D.M., & Garcia,A.J. Surface chemistry modulates fibronectin conformation and directs integrin binding and specificity to control cell adhesion. *J. Biomed. Mater. Res.* **66A**, 247-259 (2003).

33. Bain,C.D., Evall,J., & Whitesides,G.M. Formation of Monolayers by the Coadsorption of Thiols on Gold - Variation in the Head Group, Tail Group, and Solvent. *J. Am. Chem. Soc.* **111**, 7155-7164 (1989).

34. Reyes,C.D. & Garcia,A.J. A centrifugation cell adhesion assay for high-throughput screening of biomaterial surfaces. *J. Biomed. Mat. Res.* **67A**, 328-333 (2003).

35. Pettit,D.K., Horbett,T.A., & Hoffman,A.S. Influence of the Substrate Binding Characteristics of Fibronectin on Corneal Epithelial-Cell Outgrowth. *J. Biomed. Mat. Res.* **26**, 1259-1275 (1992).

36. Steele,J.G., Dalton,B.A., Johnson,G., & Underwood,P.A. Adsorption of Fibronectin and Vitronectin Onto Primaria(Tm) and Tissue-Culture Polystyrene and Relationship to the Mechanism of Initial Attachment of Human Vein Endothelial-Cells and Bhk-21 Fibroblasts. *Biomaterials* **16**, 1057-1067 (1995).

37. McClary,K.B., Ugarova,T., & Grainger,D.W. Modulating fibroblast adhesion, spreading, and proliferation using self-assembled monolayer films of alkylthiolates on gold. *J. Biomed. Mat. Res.* **50**, 428-439 (2000).

38. Chen,C.S., Mrksich,M., Huang,S., Whitesides,G.M., & Ingber,D.E. Geometric control of cell life and death. *Science* **276**, 1425-1428 (1997).

39. Dike,L.E., Chen,C.S., Mrksich,M., Tien,J., Whitesides,G.M., & Ingber,D.E. Geometric control of switching between growth, apoptosis, and differentiation during angiogenesis using micropatterned substrates. *In Vitro Cell. & Develop. Biol.-Animal* **35**, 441-448 (1999).

40. Pettit,D.K., Hoffman,A.S., & Horbett,T.A. Correlation Between Corneal Epithelial-Cell Outgrowth and Monoclonal-Antibody Binding to the Cell-Binding Domain of Adsorbed Fibronectin. *J. Biomed. Mat. Res.* **28**, 685-691 (1994).

41. Harder,P., Grunze,M., Dahint,R., Whitesides,G.M., & Laibinis,P.E. Molecular conformation in oligo(ethylene glycol)-terminated self-assembled monolayers on gold and silver surfaces determines their ability to resist protein adsorption. *J. Phys. Chem.* **102B**, 426-436 (1998).

CHAPTER 4

SURFACES THAT DIRECT ASSEMBLY OF FIBRILLAR EXTRACELLULAR MATRICES

SUMMARY

Biomimetic engineering focuses on integrating recognition/structural motifs from biological macromolecules with synthetic or natural substrates to generate biofunctional materials. However, current biomimetic approaches do not reconstitute spatial or temporal organization associated with natural extracellular matrices (ECMs). In the present study, we engineered model surfaces that promote cell-mediated assembly of robust ECMs. By tethering a short peptide from the self-assembly domain of the ECM protein fibronectin (FN) onto non-fouling supports, we generated surfaces which promote cell-mediated assembly of robust FN matrices compared to control and bioadhesive RGD-functionalized supports. Furthermore, these ECM-mimetic surfaces direct the co-assembly of type I collagen (COL) fibrils within the FN architecture, and increases the proliferation rates of adherent cells nearly two-fold compared to conventional supports. Given the critical roles of fibrillar matrices on cell migration, proliferation, and differentiation, this approach provides a promising strategy for enhanced surface-induced control of cellular activities.

INTRODUCTION

Biologically-inspired materials have emerged as promising substrates for enhanced repair in various therapeutic and regenerative medicine applications, including nervous and vascular tissues, bone, and cartilage.[1-4] The extracellular matrix (ECM) plays a central role in tissue morphogenesis, homeostasis, and repair,[5] and characteristics of the ECM are therefore worthy of mimicking to provide control of cellular activities on synthetic substrates. The ECM is a dynamic-insoluble network of proteins and polysaccharides secreted and assembled locally by cells.[6] Cells are constantly remodeling the ECM to maintain the structure and presentation of protein ligands and growth factors. The complex organization of matrix-assembled proteins provides structural support to cells within tissues while also providing signaling cues vital for cellular regulation, development, migration, proliferation, shape and function.[6-12]

Biomimetic materials incorporating recognition and structural motifs from biological macromolecules provide innovative targets for the engineering of substrates with tailored biofunctionality and novel properties.[1,13] These strategies primarily focus on the development of materials which incorporate well-characterized domains from biomacromolecules to mimic individual functions of the ECM, including cell adhesive motifs,[13,14] growth factor binding sites,[15] and protease sensitivity.[16] While current biomimetic materials imitate selected ECM attributes, they exhibit reduced activity compared to natural matrices and often do not encompass the full spectrum of functions necessary for robust control of cell activities associated with natural ECMs.[17]

These current materials displaying ECM characteristics also fail to reconstitute the vital fibrillar supramolecular structure of the natural ECM. The fibrillar structure of fibronectin (FN) matrices modulates cell cycle progression, migration, gene expression, cell differentiation, and the assembly of other matrix proteins.[5,7,10,18] However, recent efforts have focused on mimicking the fibrillar nature of native ECM by electrospinning of proteins[19] and synthetic polymers[20] into nanofibers. Stupp and coworkers have made advancements in self-assembly of amphiphilic nanofibers which incorporate biomolecules,[21] while McLeod and colleagues have developed sulfonated polystyrene surfaces which mediate FN fibrillogenesis.[22] Ma and coworkers have developed nano-fibrous polymer scaffold that enhance serum protein adsorption leading to increased cell attachment.[23] Even though these methods produce fibrillar scaffolds, there is little control over the spatial or temporal distribution of bioactive domains, or the non-specific adsorption of serum proteins. Current biomaterials do not actively promote cellular deposition and assembly of ECM. In the present study, we describe biomimetic surfaces that direct cell-mediated co-assembly of robust fibrillar FN and type I COL matrices through the use of an oligopeptide sequence (FN13) from the self-assembly domain of FN which enhances matrix assembly when added in soluble form.[24] Furthermore, tethering of this oligopeptide to non-fouling substrates significantly enhanced cell-mediated ECM assembly. Cells cultured on FN13-functionalized surfaces also exhibit increases in proliferation rates. Given the critical roles of fibrillar matrices on regulating numerous cell

functions, these results offer new insights for enhanced design of ECM mimetic materials.

EXPERIMENTAL SECTION

Materials

MC3T3-E1 osteoblast-like cells were obtained from the RIKEN Cell Bank (Tokyo, Japan). Cells were maintained in α-Modified Eagle's Medium supplemented with 10% fetal bovine serum (FBS, HyClone, Logan, UT), penicillin (100 units/mL), and streptomycin (100 mg/mL). Cell culture reagents, including human plasma FN and Dulbecco's phosphate buffered saline (DPBS) were purchased from Invitrogen (Carlsband, CA). Tri(ethylene glycol)-terminated alkanethiol ($HS\text{-}(CH_2)_{11}\text{-}(EG)_3OH$, EG_3)[25] was synthesized as previously described (previous chapter) and characterized by ^1H and ^{13}C NMR, FTIR, and mass spectrometry. All starting materials for synthesis, cell culture and chemical reagents as well as rabbit anti-FITC alkaline phosphatase-conjugated antibodies were used as received from Sigma Aldrich (St. Louis, MO). Texas Red®-conjugated goat anti-rabbit IgG, ethidium homodimer-2, AlexaFluor488-conjugated anti-mouse IgG, and Hoechst dye were purchased from Molecular Probes (Eugene, OR). Mouse anti-BrdU antibody was purchased from Becton Dickinson (Franklin Lakes, NJ).

Methods

Synthesis of HS-$(CH_2)_{11}$-EG_6-OCH_2-COOH

Carboxylic acid functionalized hexa(ethylene glycol)-terminated alkanethiol (HS-$(CH_2)_{11}$-$(EG)_6$-OCH_2-COOH) was synthesized (**Scheme 4.1**) as previously described[26] and characterized by ^{1}H- and ^{13}C-NMR, Fourier transformed infrared spectroscopy, and mass spectrometry.

Undec-1-en-11-ylhexaethlene glycol (4)

A mixture of hexa(ethylene glycol) (234.7 mmol) and 3.75 ml of 50% NaOH was refluxed for 0.5 h at 100 ^{o}C under an atmosphere of nitrogen and 11-bromoundec-1-ene (10.40 ml, 47.4 mmol) was added. The mixture was refluxed for 24 h, cooled and extracted with hexane (6 x 50 ml). The hexane extracts were combined and the solvent was evaporated under reduced pressure to afford a yellow oil. The oil was purified using chromatography (silica gel; gel 1 of ethyl acetate, followed by gel 2 of 19:1 $CHCl_3$/MeOH) to give of monoether (75%, **4**): ^{1}H NMR (300 MHz, $CDCl_3$) δ1.25 (br m, 12 H, alkane), 1.55 (qui, 2H, *J* = 7 Hz, C-10), 1.7 (br s, 1H, C-OH), 2.05 (q, 2H, *J* = 7 Hz, C-3), 3.45 (t, 2H, *J* = 7 Hz, C-11), 3.55-3.75 (m, 24H, OCH_2CH_2O), 4.90-5.05 (qq, 2H, *J* = 6.7, 3.4, 1.65, C-1), 5.75 (qt, 1H, *J* = 6.7, 3.4, C-2); ^{13}C NMR (75 MHz, $CDCl_3$) δ139.13, 114.02, 72.45, 71.43, 70.46, 70.20, 69.27, 61.58, 33.69, 29.51, 29.43, 29.37, 28.82, 25.97; MS (CI, ammonia), M+1 435.2, M+18 454.3; IR (neat, cm^{-1}) v_{max} 3468.43 (C-OH), 3079.47 (C=C H-stretching), 2919.57 (CH_2 symmetric), 1121.73 (C-O stretch).

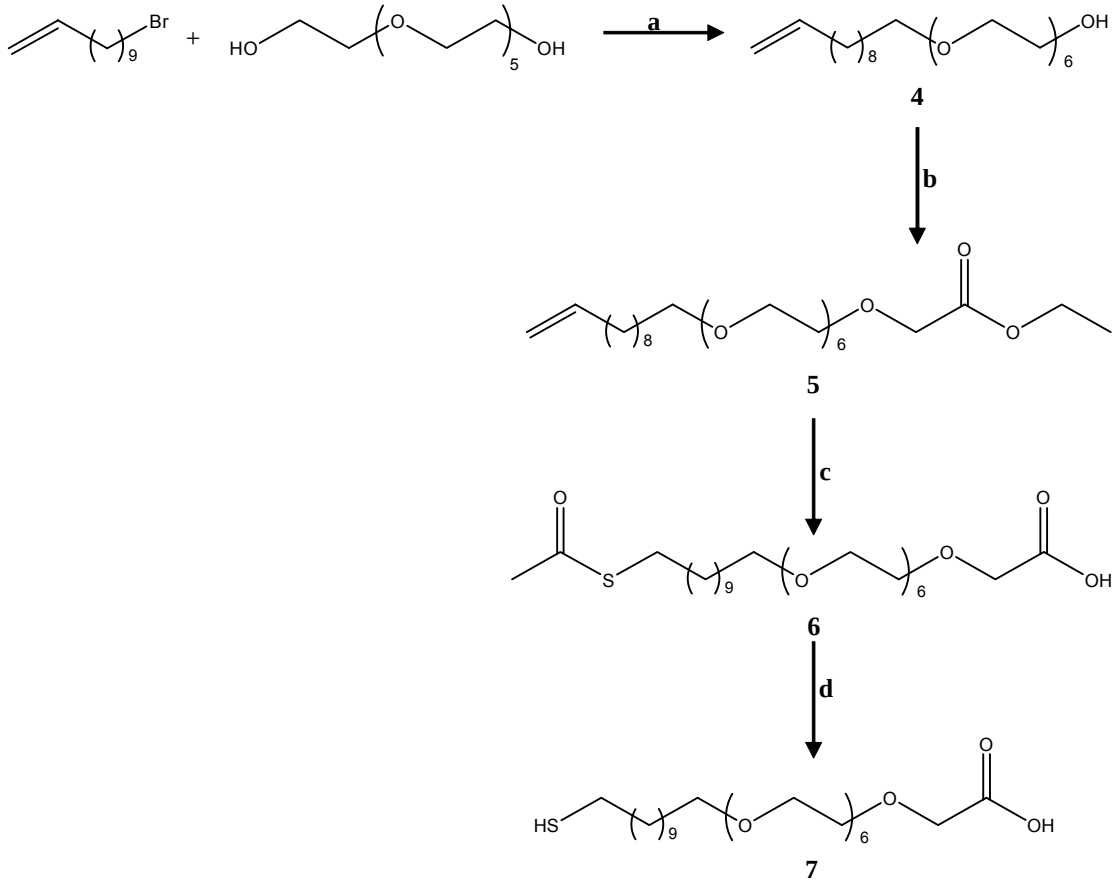

SCHEME 4.1. Conditions; a) Hexa(ethylene glycol), 50% NaOH, 100 ^{o}C, 0.5 h; 11-bromoundec-1-ene, 100 ^{o}C, N_2, 24 h. b) Ethyl diazoacetate, $BF_3{\cdot}Et_2O$, dry CH_2Cl_2, 0 ^{o}C 0.5 h, 2 h r.t. c) AIBN, Thiolacetic acid, dry THF, over night, N_2, *hv*. d) 0.8 M HCl in CH_2Cl_2, r.t. 16 h, N_2.

Undec-1-en-11-yl hexa(ethylene glycol) ethyl ester (5)

All starting materials were cooled to 0 ^{o}C before combined. **4** (10.06 g, 23.18 mmol), ethyl diazoacetate (3.28 mL, 25.92 mmol), and $BF_3{\cdot}Et_2O$ (0.23 ml, 2.31 mmol) were dissolved in 50 ml of dry CH_2Cl_2. The reaction mixture was stirred at 0 ^{o}C for 0.5 h, then allowed to warm to room temperature for 2 h. Saturated aqueous ammonium chloride (25 ml) was added and the reaction was placed into a separatory funnel. The organic phase was collected and the aqueous phase was washed with CH_2Cl_2 (5 X 20 ml). The combined organic phases were dried with magnesium sulfate and the solvent was removed to give a yellow oil. Flash column chromatography (eluant: 1:1 ethyl acetate/hexanes → methanol) gave **5** a clear oil (30%); ^{1}H NMR (300 MHz, $CDCl_3$) δ 1.25-1.35 (br s, 16 H, alkane, C-27), 1.55-1.60 (qui, 2 H, *J* = 6.6, 6.9 Hz, C-10), 2.0-2.09 (dd, 2 H, *J* = 6.9 Hz, C-3), 3.43-3.48 (t, 2 H, *J* = 6.6 Hz, C-11), 3.55-3.75 (m, 24 H, OCH_2CH_2O), 4.15 (s, 2 H, C-24), 4.18-4.25 (q, 2 H, *J* = 7.2 Hz, C-26), 4.9-5.05 (qq, 2 H, *J* = 3.3, 6.6 Hz, C-1), 5.75-5.85 (qt, 1 H, *J* = 3.3, 6.6, C-2); ^{13}C NMR (75 MHz, $CDCl_3$) δ 170.426, 139.188, 114.067, 71.490, 70.837, 70.534, 70.003, 68.682, 60.743, 33.755, 29.581, 29.475, 29.414, 29.065, 28.868, 26.029, 14.144; MS (EI, molecule shows self CI) M+1 521.36886; IR (neat, cm^{-1}) ν_{max} 3080.0 (CH sp^2), 2926.17 (CH asymmetric sp^3), 2857.49 (CH_2 symmetric), 1754.58 (C=O), 1120.62 (C-O stretch).

[1-[(Methylcarbonyl)thio]undec-11-yl]-hexa(ethylene glycol) ethyl ester (6)

Compound **5** (4.0 mmol) was added to a solution of thiolacetic acid (16.0 mmol) and AIBN (1 mmol) in dry THF (20 ml) and the mixture was irradiated overnight under an atmosphere of nitrogen with a 450-W medium pressure mercury submersion lamp. The solvent was evaporated under reduced pressure, and the crude product (**6**) was purified with flash column chromatography (eluant: 30:1 CH_2Cl_2/MeOH) to yield a yellow oil (80%); ^{1}H NMR (300 MHz, $CDCl_3$) δ 1.25 (m, 17H, alkanes), 1.52 (m, 4H, C-9, C-10), 2.32 (s, 3H, -C$\underline{H}_3$), 2.85 (t, *J* = 7.2, 2H, S-C$\underline{H}_2$), 3.44 (t, *J* = 6.9, 2H, O-C$\underline{H}_2$, C11), 3.56-3.74 (m, 24H, OC$\underline{H}_2$C$\underline{H}_2$O), 4.15 (s, 2H, OC$\underline{H}_2$C=O), 4.22 (q, *J* = 7.2, 2H, OC$\underline{H}_2$CH$_3$): ^{13}C NMR (75 MHz, $CDCl_3$) δ 14.18, 26.03, 28.76, 29.05, 29.42, 29.57, 60.76, 68.65, 69.99, 70.52, 70.82, 71.49, 170.44, 195.96; FAB M+1 597.3672; IR (neat, cm^{-1}) ν_{max} 3323.32, 2926.14 (CH_2 asymmetric stretch), 2856.99 (CH_2 symmetric stretch), 2368.74 (S-C), 2340.53 (S-C), 1754.19 (C=O), 1121.34 (C-O).

11-[19-Carboxymethylhexa(ethylene glycol)]undec-1-yl-thiol (7)

Thioacetate **6** was dissolved in 0.8 M HCl in CH_2Cl, and the mixture was stirred at room temperature for 16 h under nitrogen. Solvent was removed and the crude product was purified using chromatography (silica gel; 88:5:5:2 $CHCl_3$/MeOH/Hexanes/AcOH, if needed) 86% yield; 1H NMR (300 MHz, $CDCl_3$) δ 1.3 (br s, 18 H, alkane), 1.67 (t, 1 H, *J*= 7 Hz, C-SH), 2.5 (dt, 2 H, C$\underline{H}_2$-S), 3.4 (t, 2 H, *J* = 7, C-11), 3.5-3.75 (m, 24 H, OC$\underline{H}_2$C$\underline{H}_2$O), 4.1 (br s, 1 H, C-OH); 13C NMR (75 MHz, $CDCl_3$) δ 24.52, 26.62, 28.73, 28.80, 29.06, 29.56, 29.80, 29.91,

29,97, 30.03, 30.79, 30.24, 30.33, 34.56, 70.92, 171.50; MS (EI) M+1 527.4, IR (neat, cm-1) ν_{max} 3498.34 (-OH, COOH stretch), 2925.45 (CH_2 asymmetric stretch), 2855.92 (CH_2 symmetric stretch), 1754.2 (C=O), 1461.72 (CH_2 scissoring), 1350.13 (CH_2 wagging), 1247.64 (CH_2 twisting), 1116.11 (C-O stretch), 732.75 (CH_2 rocking).

SAM Assembly.

Glass cover slips and chamber slides were cleaned by O_2 etching for 3 min in a plasma etcher (Plasmatic Systems, Inc., North Brunswick, NJ). Substrates were sequentially coated with 100 Å Ti and 150 Å Au (2.0 X 10^{-6} torr, 2.0 Å/sec) using a Thermionics VE-100 electron beam evaporator (Modesto, CA). Mixed SAMs were prepared by immersing Au substrates in a 1 mM solution (total thiol concentration) containing a 19:1 ratio of EG_3 and EG_6-COOH for 4 or 16 h. The composition of monolayers was assumed to be the same as the ratio in solution.[27] SAMs containing carboxylic acids were incubated for 30 min in 2 mM EDC (1-ethyl-3-(3-dimethyl-aminopropyl)carbodiimide hydrochloride) and 5 mM NHS (N-hydroxysuccinimide) in 0.1 M 2-(N-morpholino)-ethanesulfonic acid and 0.5 M NaCl, pH 6.0, and then immersed in a 20 mM solution of 2-mercaptoethanol in deionized water for 5 min. FN13 peptide (synthesized by the BioScience Center, Georgia Institute of Technology, Atlanta, GA), scrFN13 (synthesized by the Emory University Microchemical Facility, Atlanta, GA), or RGD peptide (GRGDSPC, BACHEM, San Diego, CA) was then tethered to activated SAMs (FN13 & scrFN13 = 23 μM (40 μg/ml) , RGD = 72 μM (50 μg/ml),

unless noted). Unreacted active NHS esters were quenched in 20 mM glycine for 10 min, followed by treatment with 1% heat-denatured bovine serum albumin (BSA) for 30 min. Peptide tethering steps were monitored by PIERS for signature infrared carbonyl peaks. Detection was performed using a Nexus 470 FT-IR spectrometer with a SMART SAGA accessory and a DTGS KBr detector (Thermo Nicolet, Madison, WI). Spectra were obtained from 1024 scans at 2 cm^{-1} resolution and reported as relative intensities measured in absorbance. Peak assignments were based on Frey and Corn.[28]

Quantification of Surface Peptide Density.

ENZYME LINKED IMMUNOSORBENT ASSAY (ELISA)

Peptides were biotinylated at the cysteine residue to quantify immobilized density. Each peptide was reconstituted at 1 mg/ml in 100 mM sodium phosphate and 5 mM EDTA, pH 6.0. EZ-Link™ PEO-maleimide activated biotin (10 mM) was added to the peptide solution and incubated in the dark at room temperature for 16 h. After blocking in 1% BSA, SAMs were incubated in alkaline phosphatase-conjugated anti-biotin antibodies in 5% FBS blocking buffer for 1h at 37 ^{o}C. After rinsing, substrates were incubated in 5-methylumbelliferyl phosphate (100 μM) for 1h at 37 ^{o}C. Reaction supernatants were transferred to black 96-well plates and the resulting fluorescence (360 nm excitation/ 465 nm emission) was recorded using a HTS 7000 Plus BioAssay microwell plate reader (Perkin Elmer, Norwalk, CT). Relative fluorescence intensity, which is proportional to the amount of peptide tethered, was determined as a function of

peptide coating concentration. Control immobilization experiments at various ratios of labeled and unlabeled peptide demonstrated no adverse effects of biotinylation on peptide tethering.

ELLIPSOMETRY

SAM surface thickness was characterized using null ellipsometry at λ = 6328 Å, and a 75^{o} angle of incidence (Sopra GES 5). Ellipsometry readings were taken on the SAM coated gold cover slips prior to peptide tethering to establish the bulk optical constants, and after peptide immobilization to calculate the thickness of the peptide layer using a three-phase ambient / film / SAM substrate model (Winell: Version 4.07 Sopra, Inc. Westford, MA) in which the film was assumed to be isotropic and assigned a scalar refractive index value of 1.40. Elliptical constants used were confirmed experimentally with those previously reported.[27,29] Four separate points were measured on each sample and the readings were averaged. Film thickness was converted to absolute peptide density using the de Feijter's formula.[30]

FN Matrix Assembly.

FN matrix assembly was visualized by immunofluorescence staining. SAMs functionalized with saturating levels of peptides (~35 pmol/cm^2) were seeded with MC3T3-E1 cells (200 cells/mm^2) in culture media. After 48 h, the media was aspirated and substrates were rinsed twice with DPBS. Samples were fixed with 3.6% formaldehyde for 10 min, rinsed and blocked in 1% BSA for

10 min. Samples were then incubated in rabbit polyclonal antibody against FN, followed by Texas Red®-conjugated goat anti-rabbit IgG and Hoechst. Digital images at equal exposures were obtained and analyzed for FN staining area. FN quantification was normalized by cell number and reported as FN matrix/ cell on images taken with a 100 X objective.

Biochemical Analysis of Assembled FN Matrix.

Isolation and detection of DOC–insoluble material was performed as described by Sechler et al.[31] After 48 h in culture, cells were rinsed with DPBS and lysed in deoxycholate (DOC) lysis buffer (2% DOC, 0.02 M Tris-HCl, pH 8.8, 2 mM phenylmethylsulfonylfluoride, 2 mM EDTA, 2 mM iodoacetic acid, and 2 mM N-ethylmaleimide). DOC-insoluble fraction was isolated by centrifugation and solubilized in 1% SDS, 25 mM Tris-HCl (pH 8.0), 2 mM phenylmethylsulfonylfluoride, 2 mM EDTA, 2 mM iodoacetic acid, and 2 mM N-ethylmaleimide. After normalizing by cell number, samples were separated by electrophoresis on 5% polyacrylamide gels under reducing conditions. Following transfer to nitrocellulose membranes, immunodetection was performed with rabbit polyclonal antibodies against FN followed by anti-rabbit alkaline phosphatase conjugated antibody (or with anti-FITC alkaline phosphatase conjugated antibody to detect FITC labeled FN). Nitrocellulose membranes were then incubated in ECF substrate, imaged on a Fuji FLA-3000 phosphoimager, and quantified by image analysis.

FN was fluorescently labeled with FITC-maleimide (Pierce Biotechnology) at the cysteine residue to quantify soluble FN incorporation within the assembled matrix. FN was reconstituted at 1 mg/ml in 100 mM sodium phosphate and 5 mM EDTA, pH 6.0. FITC-maleimide (10 mM in DMSO) was added to the FN solution, and incubated in the dark at room temperature (16 h). Unreacted FITC was removed by centrifugation with a 30 kDa filter (Micon Bioseparations). Final concentration of FITC-FN were determined using optical constants. FITC-FN was supplemented in FN-depleted serum (20 nM), and used to culture cells.

Collagen Fibril Assembly.

Following 24 h of culture, media was replaced with equal volumes of fresh culture media (37 ^{o}C) and culture media supplemented with FITC-labeled type I collagen (25 ^{o}C, Chondrex, Inc., Redmond, WA) to give a final concentration of 1 μg/ml. Following additional 24 h incubation with FITC-collagen, substrates were fixed and stained for FN as described above.

Cell Proliferation.

MC3T3-E1 cells were synchronized by culturing under serum-free conditions (α-MEM + 0.1% albumin) for 3 days. Cells were then seeded at a low density (50 cells/mm^2) to ensure logarithmic growth in αMEM supplemented with 10% FBS onto ligand-functionalized substrates. After 24 h in culture, cells were pulsed for 4 h with BrdU (10 mg/ml final concentration). Substrates were then washed with DPBS, fixed with 95% ethanol for 10 min, and denatured in HCl for

20 min. Following neutralization in 50 mM NaCl (in 100 mM Tris-HCl, pH 7.4) and blocking in 5 % FBS + 1 % BSA, cultures were sequentially incubated in mouse anti-BrdU antibody (25 ng/ml) and Alexa-Fluor488-conjugated anti-mouse IgG (10 μg/ml). Cell nuclei were counter-stained with ethidium homo-dimer 2 (1 μM). Substrates were then scored by fluorescence microscopy for proliferation as the percentage of cells positive for BrdU incorporation relative to the total number of cell nuclei. At least twenty representative images were analyzed per sample.

Micropatterned Surfaces.

Microcontact printing was used to pattern self-assembled monolayers (SAMs) of alkanethiols on Au into adhesive and nonadhesive domains.[32] Using standard photolithograpy methods, we manufactured master templates of microarrays of linear patterns (10 μm wide with 50 μm line-line spacing), on Si wafers as previously described.[33] Briefly, photoresist (5 μm thick) was spun onto a Si wafer and exposed to UV light through an optical mask containing the desired pattern to degrade the photoresist. The exposed areas were then etched away, leaving a template mold of recessed wells (5 μm deep) with the desired patterns. The template was exposed to (tridecafluoro-1,1,2,2-tetrahydrooctyl)-1-trichlorosilane under vacuum to prevent adhesion of the elastomer to the exposed Si. The PDMS precursors (Sylgard 184/186, 10:1) and curing agents were mixed (10:1), poured over the template in a dish (forming an approximately 10-mm-thick layer), evacuated under vacuum to remove air bubbles from the

elastomer, and cured at 65 °C for 12 h. The cured PDMS stamp containing the desired array of circular posts was then peeled from the template.

Stamps were cleaned by sonicating in 50% EtOH for 15 min and the flat back of the stamp was allowed to self-seal to a glass slide to provide a rigid backing. Au-coated cover slips were rinsed with 95% EtOH and dried under a stream of N_2. The face of the stamp was inked with 1 mM ethanolic solution 19:1 EG_3:EG_6-Acid and then quickly blown dry with N_2. The stamp was brought into conformal contact with the Au-coated substrate for 2 min to produce an array of linear islands of the desired thiol mixture. Subsequently, the cover slips were incubated in a 1 mM ethanolic solution of tri(ethylene glycol)-terminated alkanethiols for 4 h to create a nonfouling and nonadhesive background around the islands. Finally, micropatterned substrates were rinsed in 95% EtOH and dried with N_2. Micropatterned substrates were treated as above to tether saturating densities of FN13 peptide, followed by MC3T3-E1 seeding at 200 cells/cm^2. After 48 h, cells were fixed and stained to visualize FN matrix.

Statistical Analysis.

Results were analyzed by analysis of variance using SYSTAT 8.0 (SPSS). If treatments were determined to be significant, pair-wise comparisons were performed using Fisher's least-significant-difference test. A 95% confidence level was considered significant.

RESULTS AND DISCUSSION

Surface Characterization.

To create non-fouling substrates that can selectively immobilize ligands with controlled densities, we used mixed self-assembled monolayers (SAMs) of alkanethiols on Au (19:1 EG_3: EG_6-COOH, **Figure 4.1a**). SAMs have been used to immobilize biomolecules to inert surfaces for several applications.[34-36] This surface composition was selected for its ability to resist non-specific protein adsorption from solution while retaining the ability to support cell adhesion to tethered ligands. The carboxylic acids present in the SAM were converted to N-hydroxysuccinimide (NHS) esters which underwent reaction with oligopeptides to immobilize the ligands by amine groups (**Figure 4.1b**).[27,37,38] The chemical conversion of this reaction was monitored step-by-step by polarized infrared external reflectance spectrometry (PIERS, **Figure 4.1c**). Pure EG_3 SAMs display no peaks in the carbonyl region of the spectrum, while SAMs consisting of 19:1 EG_3: EG_6-COOH show a sharp peak at 1621 cm^{-1} corresponding to the carbon-oxygen double bond stretch of the carboxylic acid. The intensity of this peak was reduced after treatment with EDC and NHS, indicating conversion of the acid to the NHS ester. New peaks at 1741 cm^{-1}, 1780 cm^{-1}, and 1819 cm^{-1} indicate asymmetric stretch of the NHS carbonyl bonds, symmetric stretch of the NHS carbonyl bonds, and activated ester carbonyl bonds, respectively. Subsequent tethering of peptide ligand is indicated by the appearance of an amide carbonyl stretching vibration (1659 cm^{-1}) from both the peptide backbone and the peptide-

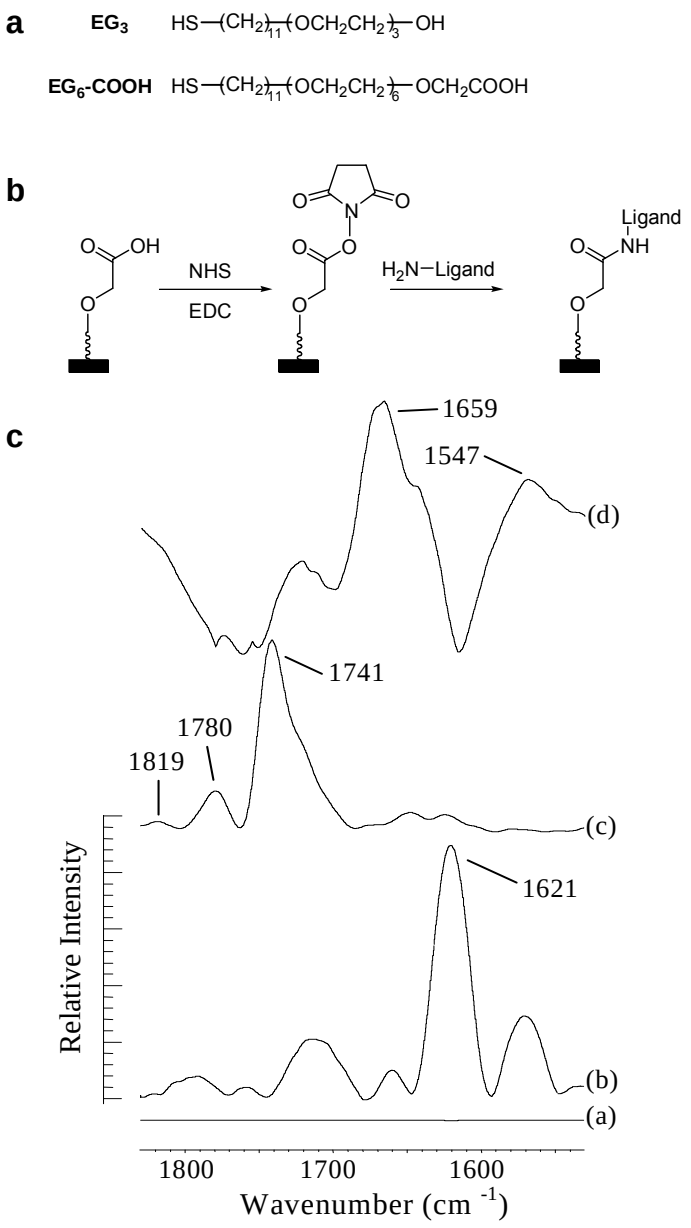

FIGURE 4.1 Surface composition and characterization of the model non-fouling surfaces used to create ligand-tethered surfaces. (a) Structures of functionalized alkanethiols used to create nonfouling SAMs with COOH groups for ligand tethering. (b) Scheme for reaction of surface-bound carboxylic acids. (c) PIERS spectra acquired for **a** pure EG_3 SAM, **b** mixed unmodified SAM of 19:1 EG_3: EG_6-COOH, **c** a mixed SAM of 19:1 EG_3: EG_6-COOH following activation with NHS, and **d** peptide-tethered surface.

SAM tether. The peak corresponding to N-H bending at 1547 cm^{-1} gives further indication of peptide immobilization.

Peptide Immobilization.

Schwarzbauer at colleagues have used recombinant FN molecules to identify domains within FN that play a role in FN matrix assembly.[39] These truncated FN molecules readily incorporate into the FN matrices of numerous cell types. Ruoslahti and coworkers have identified a 14 kDa fragment located between the first two type III repeats of FN which specifically binds FN.[40] A 31-amino acid sequence from this peptide retained activity, and is believed to play a role in the secondary mechanisms of FN matrix assembly. More recently, Barlati has discovered a 13-amino acid sequence (FN13) from the COL binding domain of FN that has been shown to increase FN matrix assembly when added to the culture media of several cell types.[24] This peptide also promoted the co-assembly of COL matrices. Since this 13-amino acid sequence is currently to smallest sequence isolated that promotes FN matrix assembly, it represented an excellent strategy for surface-induced FN matrix assembly to non-fouling supports.

Three oligopeptides were immobilized using this strategy: FN13 (KGGGAHEEICTTNEGVM), a control scrambled sequence (scrFN13, KGGGITCETNEGEVAMH), and bioadhesive RGD (GRGDSPC).[14,35] The FN13 and scrFN13 peptides were extended with an additional KGGG spacer on the N-terminus to tether these sequences to the SAM. Each peptide was biotinylated

at the cysteine residue to quantify relative tethered density by ELISA using alkaline phosphatase-conjugated anti-biotin antibodies. All of the peptides exhibited similar immobilization profiles (**Figure 4.2**). There was an initial linear increase in tethered peptide density upon increasing the concentration of the peptide in solution, followed by a saturation plateau at high solution concentration. SAM surfaces that were not transformed with NHS esters prior to peptide exposure displayed consistently low levels of tethered peptide, regardless of the coating concentration. Together, these results indicate that the amount of peptide tethered to the surface can be tightly controlled by varying the coating concentration (**Figure 4.2**). Aside from only obtaining relative immobilized peptide levels, an additional limitation of this technique is that steric interactions between antibody molecules could underestimate peptide densities at high concentrations.

To overcome this limitation, ellipsometry was used to obtained absolute surface densities of the immobilized peptides by measuring changes in the peptide film thickness. This analytical technique was utilized for its convenient (no vacuum or labeling of peptide required) and non-destructive ability to directly measure changes in film thickness with precision at low resolution (0.01 nm or better).[30] By using the de Feijter's formula, changes in film thickness were converted to absolute peptide surface density (**Figure 4.3**):[41]

$$\Gamma = \frac{t(n - n_0)}{d_n/d_c}$$

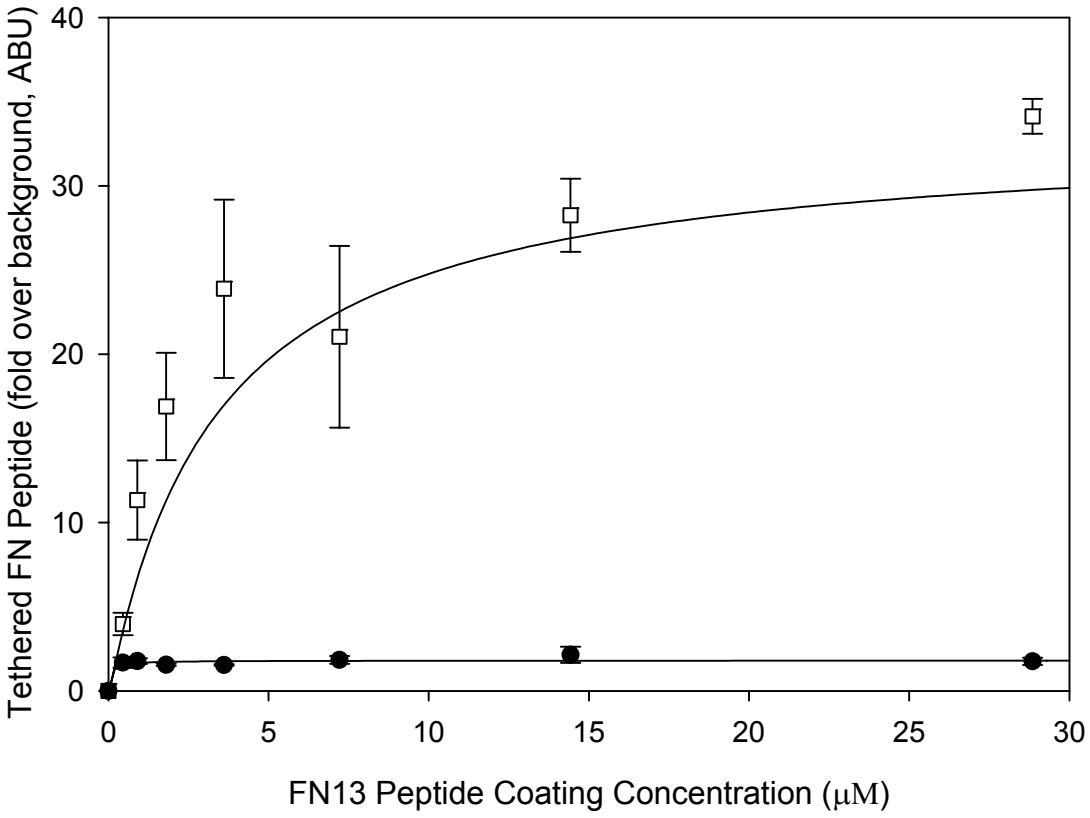

FIGURE 4.2 FN13 tethering profile by ELISA. Relative surface density of biotinylated-FN13 peptide on both NHS activated (□), and Unmodified (●) SAMs.

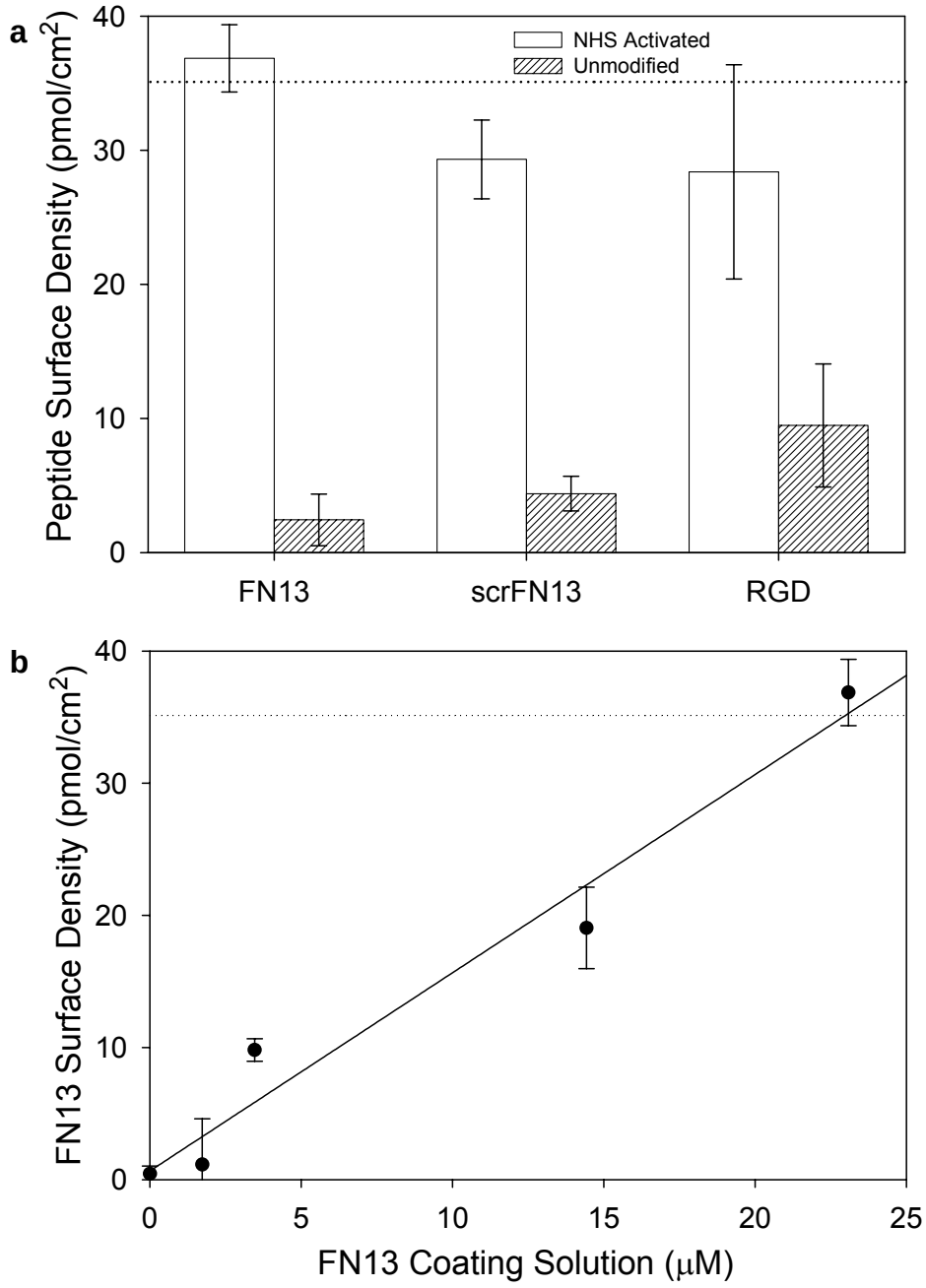

FIGURE 4.3 Peptide tethering densities measured by Ellipsometry. Dotted line represents theoretical maximum surface density for complete conversion of available binding sites. (a) NHS Activated (▭), and Unmodified (▨) SAMs. There were no significant differences between activated surfaces exposed to peptides, or between unmodified surfaces that were exposed to peptides. Significant differences in peptide densities were determined between NHS activated and unmodified surfaces exposed to peptides. ($p < 0.0002$). (b) FN13 immobilization profile. Curve fit to linear model and used to determine densities over full range of coating conditions. $y = 1.54x$ $R^2 = 0.96$.

Here, Γ is defined as surface concentration (g/cm^2), t is the film thickness (cm), n is the refractive index of the peptide (assumed 1.40),[30] n_0 is the ambient refractive index, and d_n/d_c is the refractive index formula (cm^3/g). **Figure 4.3a** shows the surface density of each peptide obtained for both NHS activated and unmodified surface treatments. The peptide coating solutions used for this measurement are the same used in all subsequent experiments, unless noted. By varying the coating concentration of FN13 peptide in solution we were able to obtain an immobilization profile for the peptide as a function of peptide coating concentration (**Figure 4.3b**). This data is in excellent agreement with ELISA in that a linear relationship between solution concentration and surface density was obtained at low densities. By simply varying the peptide solution concentration, we are able to control the surface density of FN13 peptide.

FN Matrix Assembly.

To investigate the ability of these surfaces to direct FN matrix assembly, MC3T3-E1 osteoblast-like cells were seeded on substrates presenting molar equivalent peptide densities. Matrix assembly was analyzed after 48 h in culture by immunofluorescence staining. Robust fibrillar FN matrices were assembled on surfaces presenting FN13 (**Figure 4.4a**). Remarkably, FN13-tethered surfaces promoted higher levels of FN matrix assembly than RGD-functionalized substrates. Cells do not assemble matrices on the scrFN13 modified surfaces, or unmodified (19:1 EG_3:EG_6-COOH SAM) control surfaces. The low levels of FN matrices detected on RGD-functionalized surfaces are consistent with previous

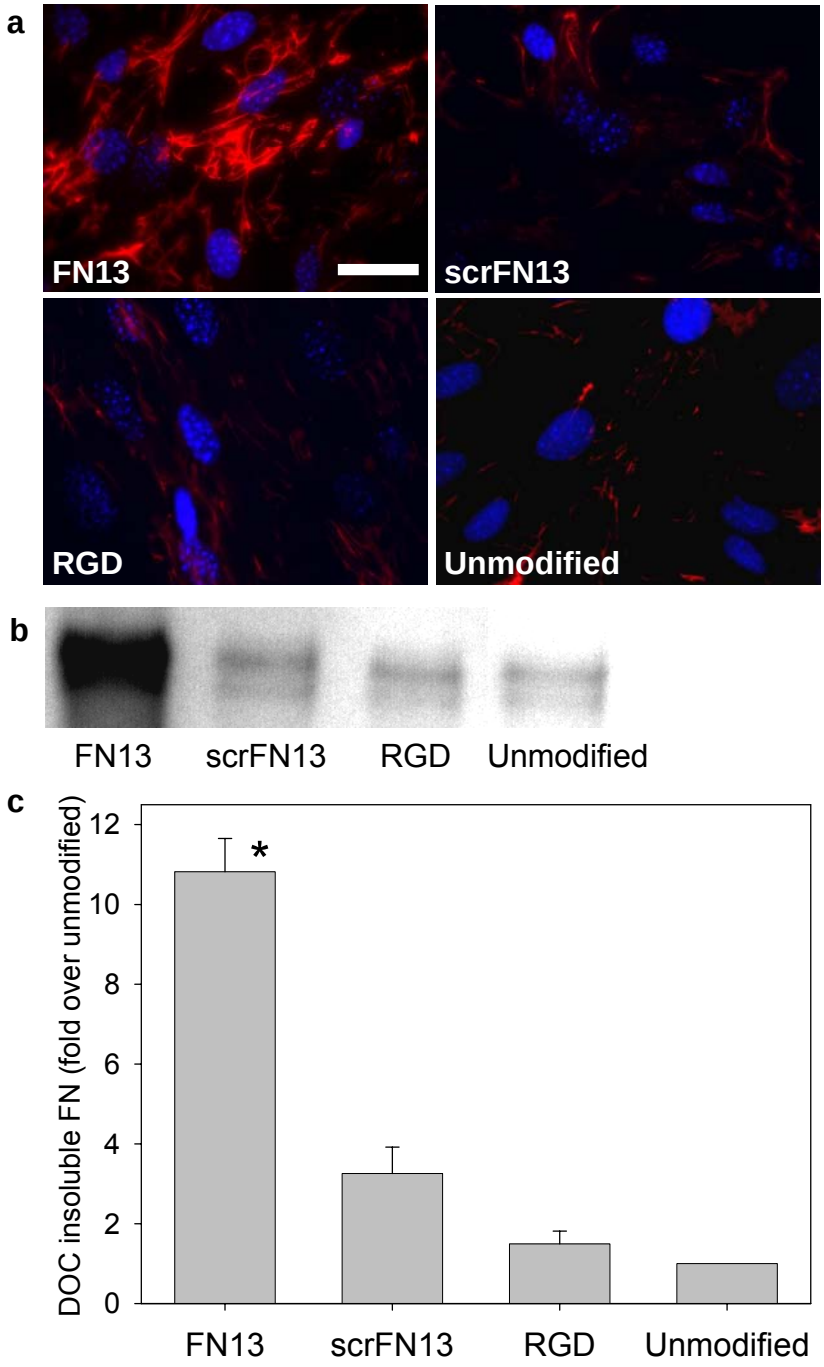

FIGURE 4.4 FN matrix assembly on peptide-functionalized surfaces. (a) Assembled FN matrix architecture for functionalized surfaces (FN = red, DNA = blue, scale bar 10 μm). (b) Western blot for DOC detergent insoluble FN (250 kD) under reduced conditions. (c) Quantification of FN matrix assembly, values reported as fold over Unmodified surface. * vs. Unmodified ($p < 0.00006$).

studies illustrating decreased levels of assembled ECM on substrates functionalized with increasing densities of RGD containing peptides.[42]

During cell-mediated matrix assembly, FN at the surface of the cell is cross-linked into high molecular weight multimers through disulfide bond formation and assembled into supramolecular structures through cytoskeleton-induced tension.[43,44] Matrix-assembled FN is characterized by deoxycholate (DOC)-insoluble fibrils stabilized through disulfide cross-linking.[39] Further characterization of our FN13 oligopeptide-induced matrix assembly by Western blot analyses of DOC-insoluble matrices was in excellent agreement with immunostaining observations (**Figure 4.4b**). Our results indicated differences in FN matrix assembly on ligand-functionalized substrates (FN13 > scrFN13 > RGD = Unmodified) as detected via both immunofluorescent staining and isolation of DOC detergent-insoluble FN matrix. FN13-tethered surfaces promoted nearly ten-fold higher levels of DOC-insoluble FN matrix compared to RGD-functionalized substrates and control surfaces presenting no oligopeptides (**Figure 4.4c**). This data reports the *first* biomimetic surface that actively promotes cell-mediated assembly of FN matrices.[1,45]

Critical FN13 Surface Density.

To examine the dependency of cell-mediated FN matrix assembly on the surface density of FN13 peptides, we functionalized the surfaces with a range of FN13 densities. Interestingly, we saw no density-dependent response in assembled FN matrices over a wide range of FN13 coating concentrations.

DOC-insoluble FN matrices were detected in equal amounts on FN13-functionalized surface that were functionalized with FN13 peptide ranging from 8.9 fmol/cm^2 to saturation at 35 pmol/cm^2 (**Figure 4.5**). This high level of FN13 induced FN matrix was followed by a sharp decrease in FN matrix to background levels at lower surface densities (6.2 fmol/cm^2 and below); indicating that the amount of FN13 above a critical density had no effect on the extent of assembled FN matrices.

For a better understanding of the significance of this critical FN13 surface density, we calculated the distribution of peptides on the surface. We determined the spacing of FN13 peptides at the critical density to be ~105 nm. The extended length of a FN molecule is between 90-120 nm. This spacing of peptides supports Erickson's model for FN elasticity described by the extension of FN dimmers.[46,47] These FN13-functionalized surfaces may provide an additional means to studying the controversial mechanism surrounding FN elasticity within FN matrices.[46,48]

FN Incorporation into Matrices.

FN matrices are commonly assembled from FN that is either secreted by the cell, or from soluble FN within the surrounding environment.[18] To investigate the source of FN within assembled matrices, MC3T3-E1 cells were seeded on FN13-tethered surfaces in FN-depleted media. The culture media for half of the samples were supplemented with FITC-labeled FN (20 nM). The composition of FN matrices was examined via both Western blot analyses of DOC-insoluble FN

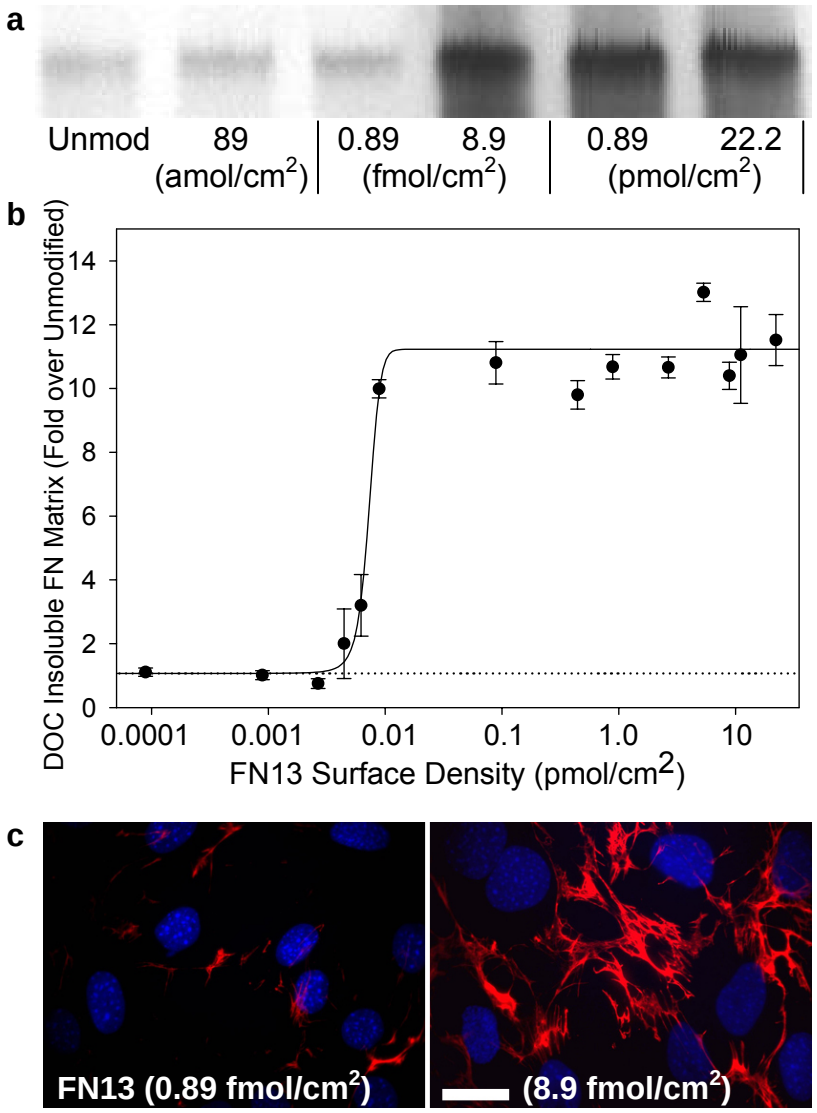

FIGURE 4.5 Critical FN13 density required to assembly FN matrices. (a) Western blot for DOC detergent insoluble FN (250 kD) under reduced conditions. Values represent the surface density of FN13. (b) Quantification of FN matrix assembly, values reported as fold over Unmodified surface ($n \geq 3$, +/- stder, ···· represents values for Unmodified surface). Curve fit to nonlinear regression ($R^2 = 0.97$). (c) Assembled FN matrix architecture for FN13-functionalized surfaces (FN = red, DNA = blue, scale bar 10 μm).

and immunofluorescence staining. Western blots with anti-FN antibodies, for total FN, showed equal amounts of FN assembled with or without addition of soluble FN to the culture media (**Figure 4.6a**). Furthermore, no FITC-labeled FN was detected in DOC-insoluble fractions indicating that soluble FN from media was not incorporated into the FN matrices. The lack of detectable staining for FN matrix on FN13-presenting surfaces cultured in the absence of cells determined that the matrix assembly on these substrates is entirely cell mediated. Interestingly, addition of soluble FN13 (40 μg/mL) to cells on surfaces which lack the immobilized ligand did not result in FN matrix assembly (**Figure 4.6b**). Additional evidence of the surface directed FN13-induced FN matrices was explored using micropatterning techniques.[32,33] By pattering the 19:1 EG_3:EG_6-Acid thiol mixture into 10 μm lanes, FN13 peptides were selectively immobilized into linear patterns surrounded by a non-adhesive background. Cells were only able to adhere and assemble FN matrices within those domains (**Figure 4.7**). Together, these results highlight the necessity of surface-immobilization of FN13 to promote the cell-mediated assembly of secreted FN matrices.

Peptide Induced ECM Co-assembly.

The FN13 peptide was originally isolated from a 13-amino acid sequence of the $FNII_1$-FNI_7 domains.[24] This region of FN poses the main collagen (COL) binding domain in assembled FN matrices. Native FN matrices display a distinct region for binding type I COL molecules, and FN matrices have been shown to regulate the deposition of COL.[24,49] The bioactivity of these surfaces were

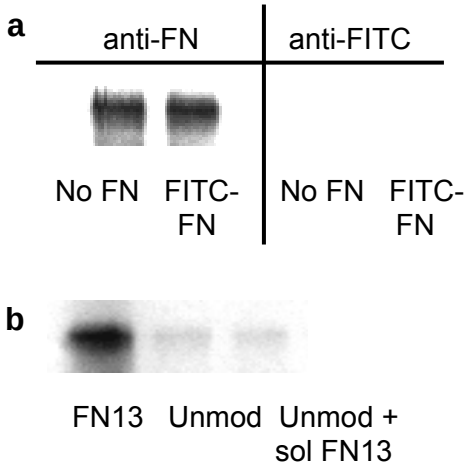

FIGURE 4.6 Investigation of FN13-induced FN matrices. (a) Western blot for DOC detergent insoluble FN for cells cultured in FN-depleted serum either without (No FN) or with (FITC-FN) supplemented FITC-labeled FN (20 nM). Total FN matrix assembled as detected with either anti-FN antibodies, or anti-FITC antibodies. (b) Effect of soluble FN13 (40 μg/ml) added to cells on unmodified SAM surfaces compared to FN13-tethered and unmodified SAMs.

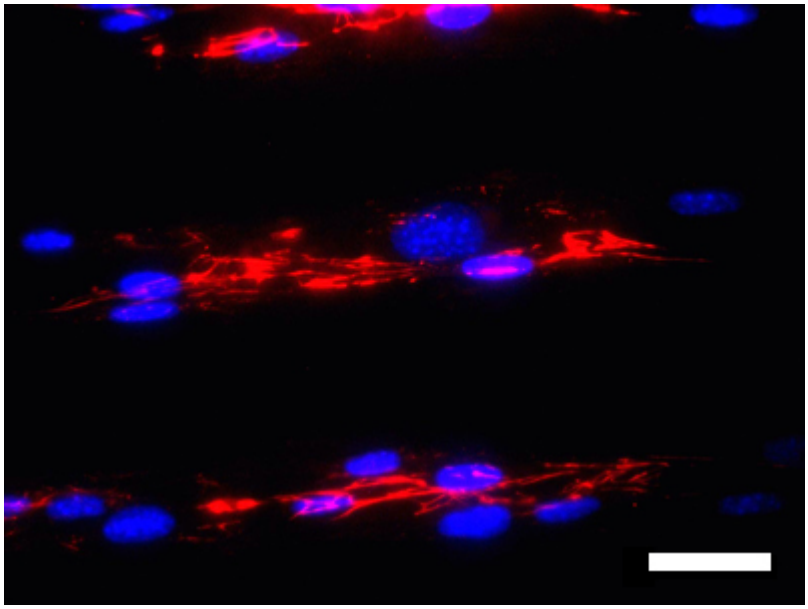

FIGURE 4.7 Micropatterned substrates functionalized with FN13 peptide. Lanes composed of 19:1 EG_3:EG_6-Acid with a EG_3 non-adhesive background. FN13 functionalized lanes (10 μm wide with a 50 μm spacing) induce localized FN matrix assembly (Scale bar = 20 μm, FN = red, DNA = blue).

examined by detection of assembled type I COL fibrils within the FN architectures. FITC-labeled type I COL added to the culture media (1μg/mL) was visualized within FN matrices by immunofluorescent staining. In excellent agreement with results indicating that FN13-functionalized surfaces directed FN matrix assembly, these surfaces assembled robust matrices with co-assembled FN and type I COL (**Figure 4.8a**). In contrast, control surfaces presenting no oligopeptides assembled minimal levels of FITC-COL, and cells seeded on scrFN13 and RGD-functionalized surfaces did not incorporate COL into their matrix. The co-assembly of type I COL and FN matrices demonstrates the ability of the FN13-tethered surface to direct assembly of ECMs (**Figure 4.8b**).

Peptide Dependent Bioactivity: Proliferation.

To further investigate the peptide-dependent control over cell activities, cell proliferation rates were examined for ligand-functionalized surfaces. Assembled FN matrices have been shown to regulate cell cycle progression by modulating cell proliferation rates.[10] Cells cultured for 24 hours on ligand-functionalized substrates demonstrated peptide-dependent proliferation rates (**Fig. 4.9**). FN13-functionalized surfaces showed nearly a two-fold increase in the number of proliferating cells (as determined by BrdU incorporation) compared to control scrambled peptide sequences, RGD functionalized substrates, and unmodified supports. Taken together, these results demonstrate that FN13-functionalized surfaces promote the assembly of robust FN matrices mimicking the fibrillar structure and biochemical characteristics of native ECMs. These FN

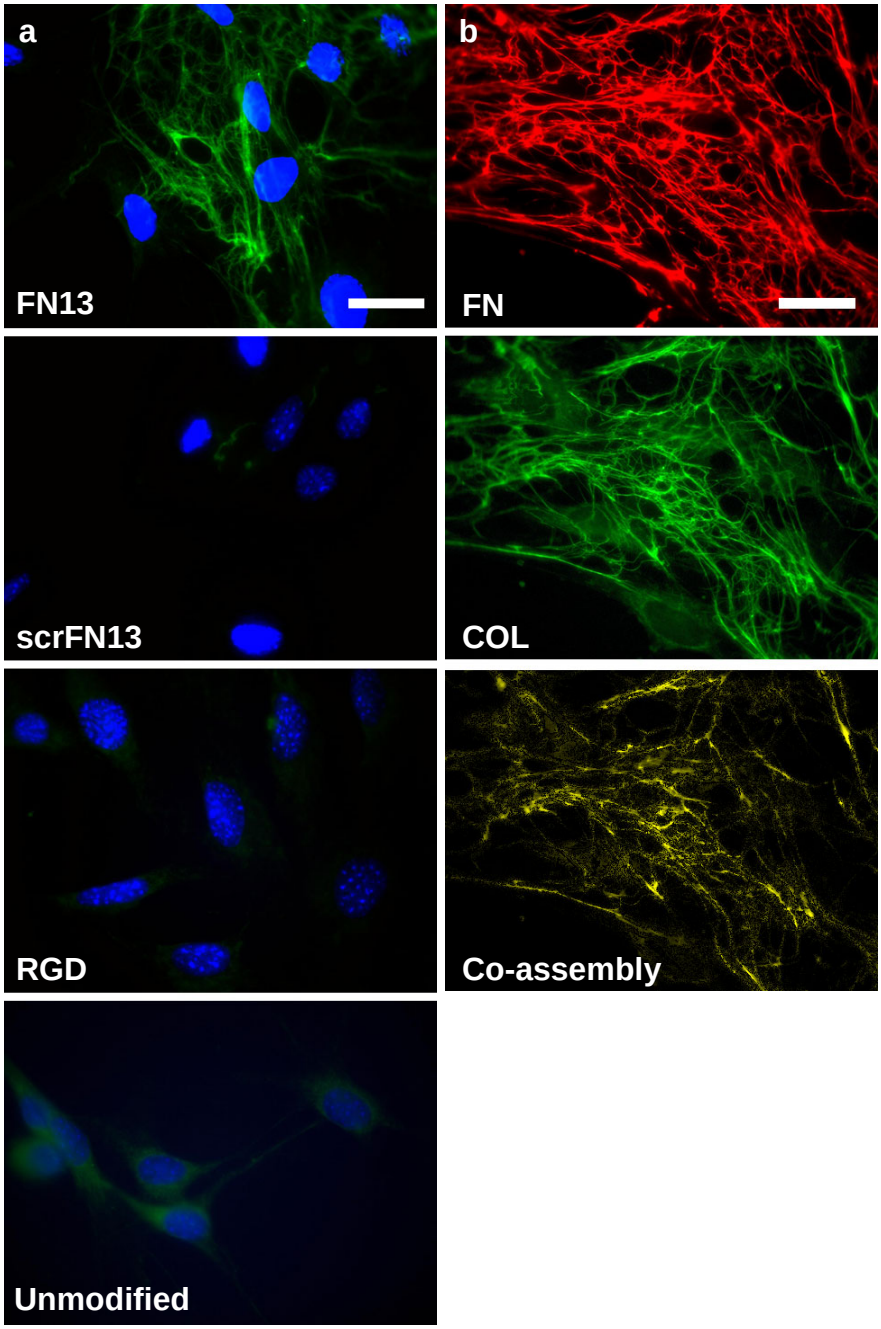

FIGURE 4.8 Co-assembly of type I collagen fibrils within the FN matrices. Column (a) Type I COL matrix assembly on ligand-functionalized surfaces (COL = green, DNA = blue; scale bar 10 μm). Column (b) Assembled matrix architecture for FN13-functionalized surfaces displaying co-assembly (FN = red, Col = green, co-assembled matrix = yellow; scale bar 10 μm).

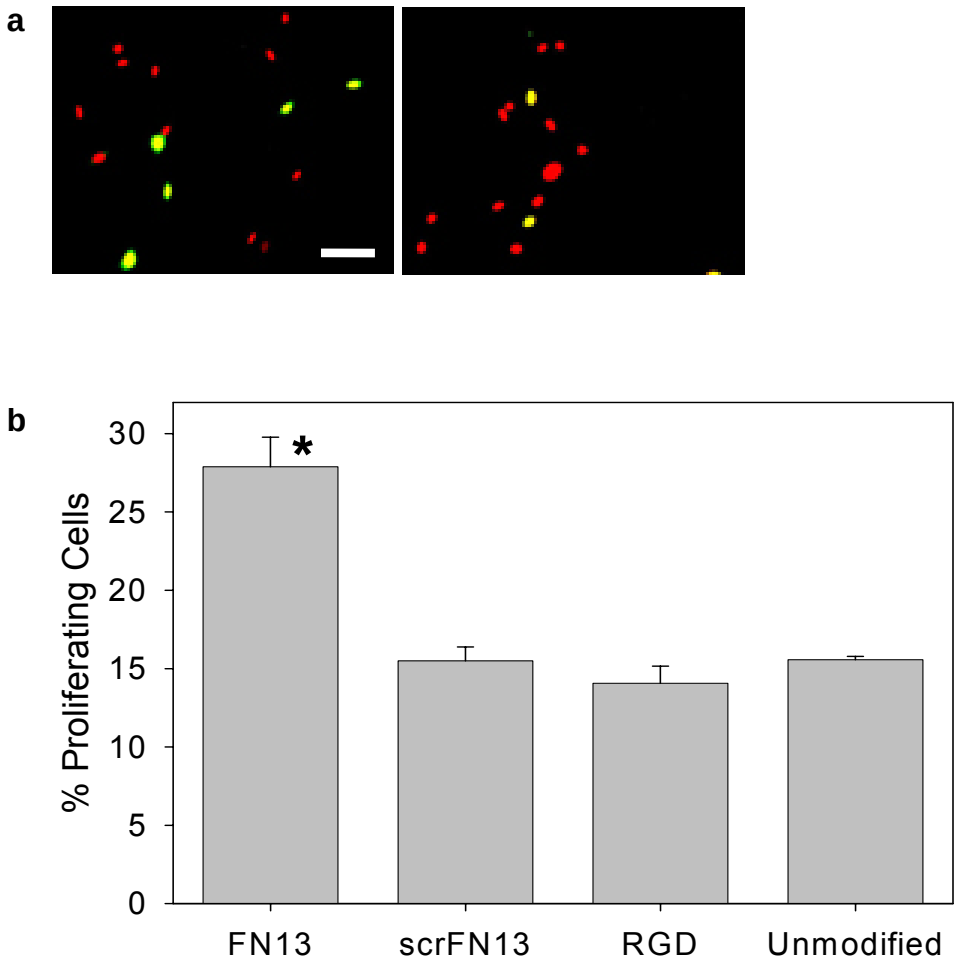

FIGURE 4.9 Cell proliferation rates on ligand-functionalized surfaces. a, Cells actively synthesizing DNA are stained green while all cellular DNA is counter stained red for total cell counts (scale bar = 200 μm). b, Quantification of proliferating cells after 24 hrs in culture on ligand-functionalized surfaces. * vs. Unmodified ($p < 0.0006$).

matrices also regulate distinct cell functions associated with native ECMs.

CONCLUSIONS

We have demonstrated that surface tethering of an oligopeptide sequence from the FN self-assembly domain promotes the assembly of fibrillar FN matrices compared to bioadhesive RGD-functionalized and control substrates. This surface advances the field of biomaterials as the first biomimetic surface that actively promotes cell mediated ECM assembly. Identification of a critical surface density of FN13 peptide provides substantial information for the rational design of next generation FN13-functionalized materials. Cell-mediated FN matrices assembled on FN13 immobilized surfaces also direct the co-assembly of type I collagen matrices, and increases cell proliferation rates. Given the critical importance of fibrillar FN structures in cell cycle and function, the development of such biomimetic surfaces provides a promising strategy for the engineering of bioactive ECM-mimetic supports for enhanced molecular control of cellular activities.

REFERENCES

1. Lutolf,M.P. & Hubbell,J.A. Synthetic biomaterials as instructive microenvironments for morphogenesis in tissue engineering. *Nat. Biotech.* **23**, 47-55 (2005).

2. Schense,J.C., Bloch,J., Aebischer,P., & Hubbell,J.A. Enzymatic incorporation of bioactive peptides into fibrin matrices enhances neurite extension. *Nat. Biotech.* **18**, 415-419 (2000).

3. Alsberg,E., Anderson,K.W., Albeiruti,A., Rowley,J.A., & Mooney,D.J. Engineering growing tissues. *Proc. Natl. Acad. Sci. USA* **99**, 12025-12030 (2002).

4. Ehrbar,M., Djonov,V.G., Schnell,C., Tschanz,S.A., Martiny-Baron,G., Schenk,U., Wood,J., Burri,P.H., Hubbell,J.A., & Zisch,A.H. Cell-demanded liberation of VEGF(121) from fibrin implants induces local and controlled blood vessel growth. *Circ. Res.* **94**, 1124-1132 (2004).

5. Adams,J.C. & Watt,F.M. Regulation of Development and Differentiation by the Extracellular-Matrix. *Development* **117**, 1183-1198 (1993).

6. Staffan Johansson in Molecular Components and Interactions, Edn. 2 68-94 (Harwood Academic Publishers GmbH, Netherlands; 1996).

7. Sakai,T., Larsen,M., & Yamada,K.M. Fibronectin requirement in branching morphogenesis. *Nature* **423**, 876-881 (2003).

8. Zhu,X.Y., Ohtsubo,M., Bohmer,R.M., Roberts,J.M., & Assoian,R.K. Adhesion-dependent cell cycle progression linked to the expression of cyclin D1, activation of cyclin E-cdk2, and phosphorylation of the retinoblastoma protein. *J Cell Biol.* **133**, 391-403 (1996).

9. Boudreau,N., Myers,C., & Bissell,M.J. From Laminin to Lamin - Regulation of Tissue-Specific Gene-Expression by the Ecm. *Trends in Cell Biol.* **5**, 1-4 (1995).

10. Sechler,J.L. & Schwarzbauer,J.E. Control of cell cycle progression by fibronectin matrix architecture. *J. Biol. Chem.* **273**, 25533-25536 (1998).

11. Bourdoulous,S., Orend,G., MacKenna,D.A., Pasqualini,R., & Ruoslahti,E. Fibronectin matrix regulates activation of Rho and Cdc42 GTPases and cell cycle progression. *J. Cell Biol.* **143**, 267-276 (1998).

12. Corbett,S.A., Wilson,C.L., & Schwarzbauer,J.E. Changes in cell spreading and cytoskeletal organization are induced by adhesion to a fibronectin-fibrin matrix. *Blood* **88**, 158-166 (1996).

13. Langer,R. & Tirrell,D.A. Designing materials for biology and medicine. *Nature* **428**, 487-492 (2004).

14. Hersel,U., Dahmen,C., & Kessler,H. RGD modified polymers: biomaterials for stimulated cell adhesion and beyond. *Biomaterials* **24**, 4385-4415 (2003).

15. Zisch,A.H., Lutolf,M.P., & Hubbell,J.A. Biopolymeric delivery matrices for angiogenic growth factors. *Cardiovasc. Pathol.* **12**, 295-310 (2003).

16. West,J.L. & Hubbell,J.A. Polymeric biomaterials with degradation sites for proteases involved in cell migration. *Macromolecules* **32**, 241-244 (1999).

17. Cutler,S.M. & Garcia,A.J. Engineering cell adhesive surfaces that direct integrin alpha(5)beta(1) binding using a recombinant fragment of fibronectin. *Biomaterials* **24**, 1759-1770 (2003).

18. Wierzbicka-Patynowski,I. & Schwarzbauer,J.E. The ins and outs of fibronectin matrix assembly. *J. Cell Sci.* **116**, 3269-3276 (2003).

19. Wnek,G.E., Carr,M.E., Simpson,D.G., & Bowlin,G.L. Electrospinning of nanofiber fibrinogen structures. *Nano Letters* **3**, 213-216 (2003).

20. Kenawy,E.R., Layman,J.M., Watkins,J.R., Bowlin,G.L., Matthews,J.A., Simpson,D.G., & Wnek,G.E. Electrospinning of poly(ethylene-co-vinyl alcohol) fibers. *Biomaterials* **24**, 907-913 (2003).

21. Niece,K.L., Hartgerink,J.D., Donners,J.J.J.M., & Stupp,S.I. Self-assembly combining two bioactive peptide-amphiphile molecules into nanofibers by electrostatic attraction. *J. Am. Chem. Soc.* **125**, 7146-7147 (2003).

22. Pernodet,N., Rafailovich,M., Sokolov,J., Xu,D., Yang,N.L., & McLeod,K. Fibronectin fibrillogenesis on sulfonated polystyrene surfaces. *J. Biomed. Mater. Res.* **64A**, 684-692 (2003).

23. Woo,K.M., Chen,V.J., & Ma,P.X. Nano-fibrous scaffolding architecture selectively enhances protein adsorption contributing to cell attachment. *J. Biomed. Mat. Res.* **67A**, 531-537 (2003).

24. Colombi,M., Zoppi,N., De Petro,G., Marchina,E., Gardella,R., Tavian,D., Ferraboli,S., & Barlati,S. Matrix assembly induction and cell migration and invasion inhibition by a 13-amino acid fibronectin peptide. *J. Biol. Chem.* **278**, 14346-14355 (2003).

25. Palegrosdemange,C., Simon,E.S., Prime,K.L., & Whitesides,G.M. Formation of Self-Assembled Monolayers by Chemisorption of Derivatives of Oligo(Ethylene Glycol) of Structure $HS(CH_2)_{11}(OCH_2CH_2)$Meta-OH on Gold. *J. Am. Chem. Soc.* **113**, 12-20 (1991).

26. Roberts,C., Chen,C.S., Mrksich,M., Martichonok,V., Ingber,D.E., & Whitesides,G.M. Using mixed self-assembled monolayers presenting RGD and (EG)(3)OH groups to characterize long-term attachment of bovine capillary endothelial cells to surfaces. *J. Am. Chem. Soc.* **120**, 6548-6555 (1998).

27. Lahiri,J., Isaacs,L., Tien,J., & Whitesides,G.M. A strategy for the generation of surfaces presenting ligands for studies of binding based on an active ester as a common reactive intermediate: a surface plasmon resonance study. *Anal. Chem.* **71**, 777-790 (1999).

28. Frey,B.L. & Corn,R.M. Covalent Attachment and Derivatization of Poly(L-lysine) Monolayers on Gold Surfaces As Charcacterized by Polarization-Modulation FT-IR Spectroscopy. *Anal. Chem.* **68**, 3187-3193 (1996).

29. Prime,K.L. & Whitesides,G.M. Adsorption of Proteins Onto Surfaces Containing End-Attached Oligo(Ethylene Oxide) - A Model System Using Self-Assembled Monolayers. *J. Am. Chem. Soc.* **115**, 10714-10721 (1993).

30. Arwin,H. Spectroscopic ellipsometry and biology: recent developments and challenges. *Thin Solid Films* **313**, 764-774 (1998).

31. Sechler,J.L., Corbett,S.A., & Schwarzbauer,J.E. Modulatory roles for integrin activation and the synergy site of fibronectin during matrix assembly. *Mol. Biol. Cell* **8**, 2563-2573 (1997).

32. Mrksich,M. & Whitesides,G.M. Patterning Self-Assembled Monolayers Using Microcontact Printing - A New Technology for Biosensors. *Trends in Biotechnol.* **13**, 228-235 (1995).

33. Gallant,N.D., Capadona,J.R., Frazier,A.B., Collard,D.M., & Garcia,A.J. Micropatterned surfaces to engineer focal adhesions for analysis of cell adhesion strengthening. *Langmuir* **18**, 5579-5584 (2002).

34. Mrksich,M., Grunwell,J.R., & Whitesides,G.M. Biospecific Adsorption of Carbonic-Anhydrase to Self-Assembled Monolayers of Alkanethiolates That Present Benzenesulfonamide Groups on Gold. *J. Am. Chem. Soc.* **117**, 12009-12010 (1995).

35. Roberts,C., Chen,C.S., Mrksich,M., Martichonok,V., Ingber,D.E., & Whitesides,G.M. Using mixed self-assembled monolayers presenting RGD and (EG)(3)OH groups to characterize long-term attachment of bovine capillary endothelial cells to surfaces. *J. Am. Chem. Soc.* **120**, 6548-6555 (1998).

36. Jiang,X., Ferrigno,R., Mrksich,M., & Whitesides,G.M. Electrochemical desorption of self-assembled monolayers noninvasively releases patterned

cells from geometrical confinements. *J. Am. Chem. Soc.* **125**, 2366-2367 (2003).

37. Prime,K.L. & Whitesides,G.M. Self-Assembled Organic Monolayers - Model Systems for Studying Adsorption of Proteins at Surfaces. *Science* **252**, 1164-1167 (1991).

38. Herrwerth,S., Eck,W., Reinhardt,S., & Grunze,M. Factors that determine the protein resistance of oligoether self-assembled monolayers - Internal hydrophilicity, terminal hydrophilicity, and lateral packing density. *J. Am. Chem. Soc.***125**, 9359-9366 (2003).

39. Wierzbicka-Patynowski,I. & Schwarzbauer,J.E. The ins and outs of fibronectin matrix assembly. *J. Cell Sci.* **116**, 3269-3276 (2003).

40. Morla,A. & Ruoslahti,E. A Fibronectin Self-Assembly Site Involved in Fibronectin Matrix Assembly: Reconstruction in a Synthetic Peptide. *J. Cell Biol.* **118**, 421-429 (1992).

41. Feijter,J.A., Benjamins,J., & Veer F.A. Ellipsometry as a Tool to Study the Adsorption Behavior of Synthetic and Biopolymers. *Biopolymers* **17**, 1759-1772 (1978).

42. Mann,B.K., Tsai,A.T., Scott-Burden,T., & West,J.L. Modification of surfaces with cell adhesion peptides alters extracellular matrix deposition. *Biomaterials* **20**, 2281-2286 (1999).

43. Ohashi,T., Kiehart,D.P., & Erickson,H.P. Dual labeling of the fibronectin matrix and actin cytoskeleton with green fluorescent protein variants. *J. Cell Sci.* **115**, 1221-1229 (2002).

44. Pankov,R., Cukierman,E., Katz,B.Z., Matsumoto,K., Lin,D.C., Lin,S., Hahn,C., & Yamada,K.M. Integrin dynamics and matrix assembly: Tensin-dependent translocation of alpha(5)beta(1) integrins promotes early fibronectin fibrillogenesis. *J. Cell Biol.* **148**, 1075-1090 (2000).

45. Langer,R. & Tirrell,D.A. Designing materials for biology and medicine. *Nature* **428**, 487-492 (2004).

46. Ohashi,T., Kiehart,D.P., & Erickson,H.P. Dynamics and elasticity of the fibronectin matrix in living cell culture visualized by fibronectin-green fluorescent protein. *Proc. Natl. Acad. Sci. USA* **96**, 2153-2158 (1999).

47. Erickson,H.P. Stretching fibronectin. *J. Muscle Res. Cell Mot.* **23**, 575-580 (2002).

48. Baneyx,G., Baugh,L., & Vogel,V. Fibronectin extension and unfolding within cell matrix fibrils controlled by cytoskeletal tension. *Proc. Natl. Acad. Sci. USA* **99**, 5139-5143 (2002).

49. Sottile,J. & Hocking,D.C. Fibronectin Polymerization Regulates the Composition and Stability of Extrcellular Matrix Fibrils and Cell-Matrix Adhesion. *Mol. Biol. Cell* **13**, 3546-3559 (2002).

CHAPTER 5

CONCLUSIONS AND RECOMMENDATIONS FOR FUTURE WORK

The goal of this research was to engineer biomaterial surfaces that modulate cell-mediated assembly of extracellular matrices (ECM) in order to direct cell function. The ECM plays a central role in tissue morphogenesis, homeostasis, and repair, and ECM characteristics are therefore worthy of mimicking to provide control of cellular activities on synthetic substrates. The approach of controlling the cell-material interaction through the immobilization of bioactive peptides on a non-fouling support represents a versatile method to control cellular responses for biomaterial and tissue engineering applications. By focusing on osteoblasts, the cells responsible for bone matrix production and mineralization, this research is relevant to the engineering of surfaces that may lead to improvements in biomaterials for orthopedic implants, bone grafting substrates and tissue engineering scaffolds. By utilizing biochemical analysis of cellular assembled fibrillar matrices, we have contributed towards establishing a fundamental framework for the rational design of biomimetic surfaces to control cell function.

A significant advantage of our experimental system over previous studies is the use of model surfaces consisting of SAMs of alkanethiols on gold presenting well-defined chemistries. Using highly sensitive protein adsorption and cell adhesion assays, we demonstrate significant FN adsorption and cell adhesion to CH_3/EG_3 mixed SAMs, including pure EG_3 monolayers. We

developed a protocol for the removal of non-specifically adsorbed FN from these surfaces that was utilized to create non-fouling biomimetic substrates.

Covalent-attachment of a short bioactive peptide (FN13) to a non-fouling background established a new class of biomaterial surface that actively promote the cell-mediated assembly of fibrillar ECMs. Cells cultured on these surfaces co-assembly FN and type I COL matrices, and show increased rates of proliferation. A defining characteristic to this surface is the threshold response of the peptide in promoting FN matrix assembly. Above a critical surface density of 0.009 pmol/cm^2, the effect on FN matrix assembly was saturated. This critical peptide density corresponds to a surface spacing of ~105 nm between FN13 peptides, which is nearly equivalent to the length of an extended FN dimmer (90-130 nm). Overall, this thesis makes important contributions to the development and design of biomimetic surface modifications that direct cell function for biomedical and biotechnology applications.

Recommendations for future experiments include many exciting possibilities. Further examination of the FN13-induced FN matrix effect on additional cell functions represents an excellent starting point for future work. Examination of gene and protein expression as well as mineralization will allow for evaluation of osteoblastic differentiation. FN is important for embryonic development and promotes differentiation of multiple cell types, while also playing a role in cancer metastasis. It would therefore be of interest to examine the effect that FN13 had on promoting FN matrix assembly in other cell types. Similarly, assembled FN matrices play a significant role in the co-assembly of

matrix proteins and the binding of soluble growth factors. The integrity of the FN13-induced fibrillar matrix could be further investigated by examining the ability to localize these soluble extracellular molecules. In addition, it could be of interest to move this 2-D model system toward a 3-D scaffold. Incorporation or attachment of FN13 peptide within a 3-D scaffold could promote matrix deposition within the scaffold, and promote cellular infiltration within the material. Finally, *in vivo* experiments with model surfaces should be conducted in order to address whether these surfaces similarly modulates cell response within the added complexity from being placed in the *in vivo* environment.

APPENDIX

The purpose of this appendix is to further supplement the experimental details that appear earlier in text. Previously mentioned experimental details were for journal submission. This appendix explains the finer details in a systematic fashion for each of the techniques utilized for the completion of this work.

In addition, a significant amount of time and effort was dedicated to the development of “mixed ligand” surfaces with presented both RGD and FN13 peptides. This immobilization of two peptides was done by sequentially tethering the RGD peptide for 30 min followed by the FN13 peptide for an additional 30 min. The original goal of this system was to identify possible synergistic or additive effects to surfaces that expressed both adhesion peptides to promote integrin-mediated initial adhesion, and the FN13 peptide that supports longer term effect in matrix assembly and cell proliferation (with the potential of additional functions). This work was the basis for the discovery that the anti-biotin antibodies were saturating on the surface before the peptides were. We were unable to determine absolute densities of each peptide within these mixed ligand systems, and were unable to find an additional function that was specific to these mixed-ligand surfaces that was not obtainable with any single ligand system. This was attributed to blindly guessing at what coating concentration we felt contributed to relative amounts of each peptide on the surface. Because of this, we felt that it was not worth adding the unfinished work to the thesis as its

own chapter, but felt that it would best serve future lab members in the appendix as a potential starting point to future work. For this reason, I am only including the data obtained from this system without additional write-ups. The experimental procedure is the same as other experiments except for the additional step in assembling monolayers. ENJOY!

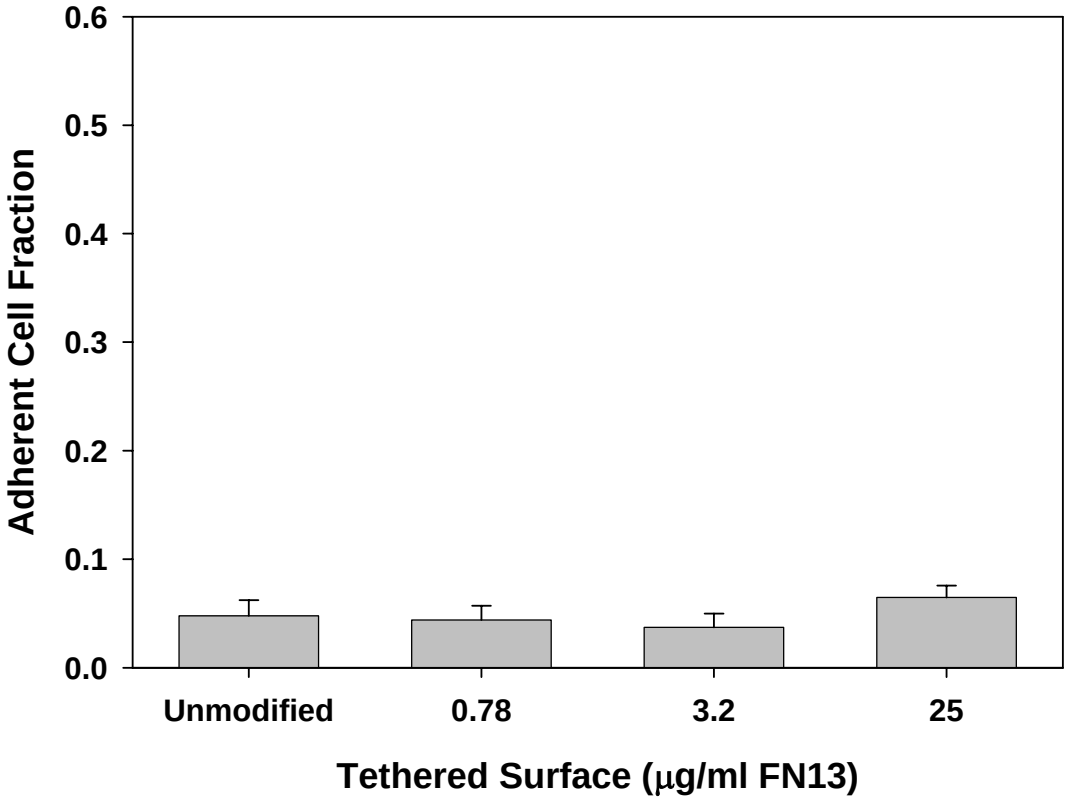

Results were analyzed by ANOVA using SYSTAT 8.0 (SPSS, Chicago, IL). If treatments were determined to be significant, pairwise comparisons were performed using Tukey post hoc test. A 95% confidence level was considered significant.

Within a given FN13 coating concentration, there were no significant differences in adherent cell fractions

Low initial adhesion to FN13 functionalized surfaces was the original reason for

exploring mixed ligand surfaces…

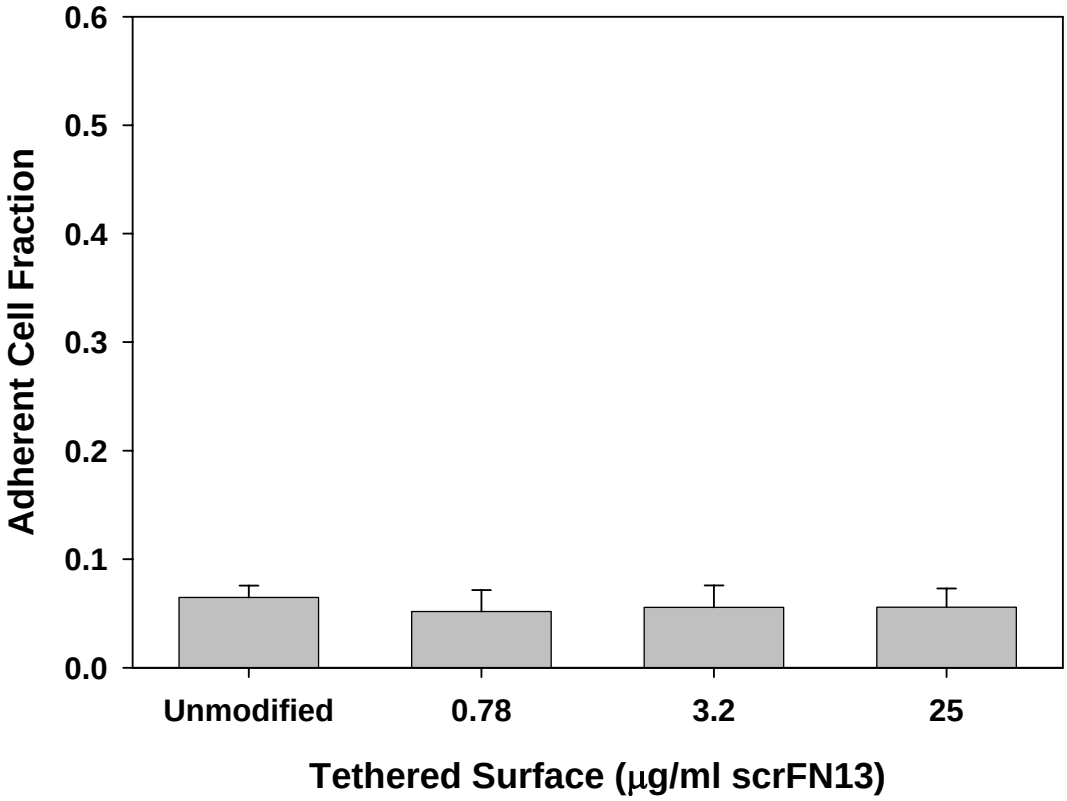

Results were analyzed by ANOVA using SYSTAT 8.0 (SPSS, Chicago, IL). If treatments were determined to be significant, pairwise comparisons were performed using Tukey post hoc test. A 95% confidence level was considered significant.

Within a given scrFN13 coating concentration, there were no significant differences in adherent cell fractions

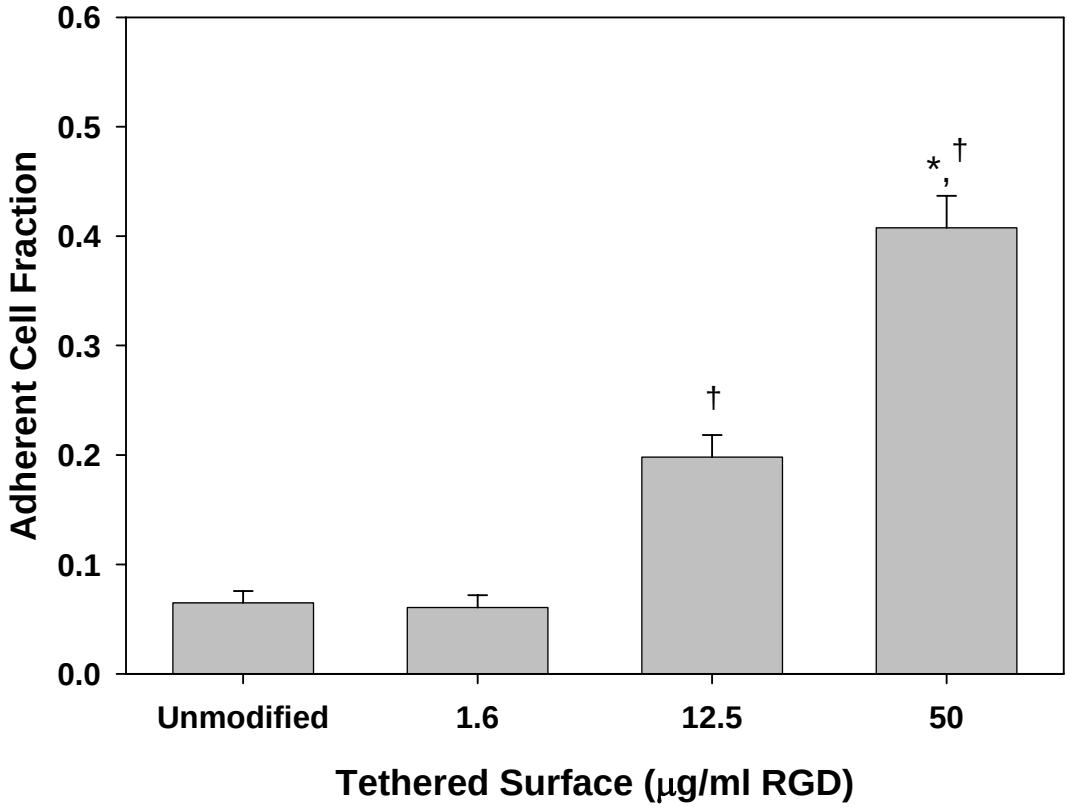

Results were analyzed by ANOVA using SYSTAT 8.0 (SPSS, Chicago, IL). If treatments were determined to be significant, pairwise comparisons were performed using Tukey post hoc test. A 95% confidence level was considered significant.

* vs. unmodified, ($p < 0.000008$)
† vs. 1.6 μg/ml RGD, ($p < 0.0025$)

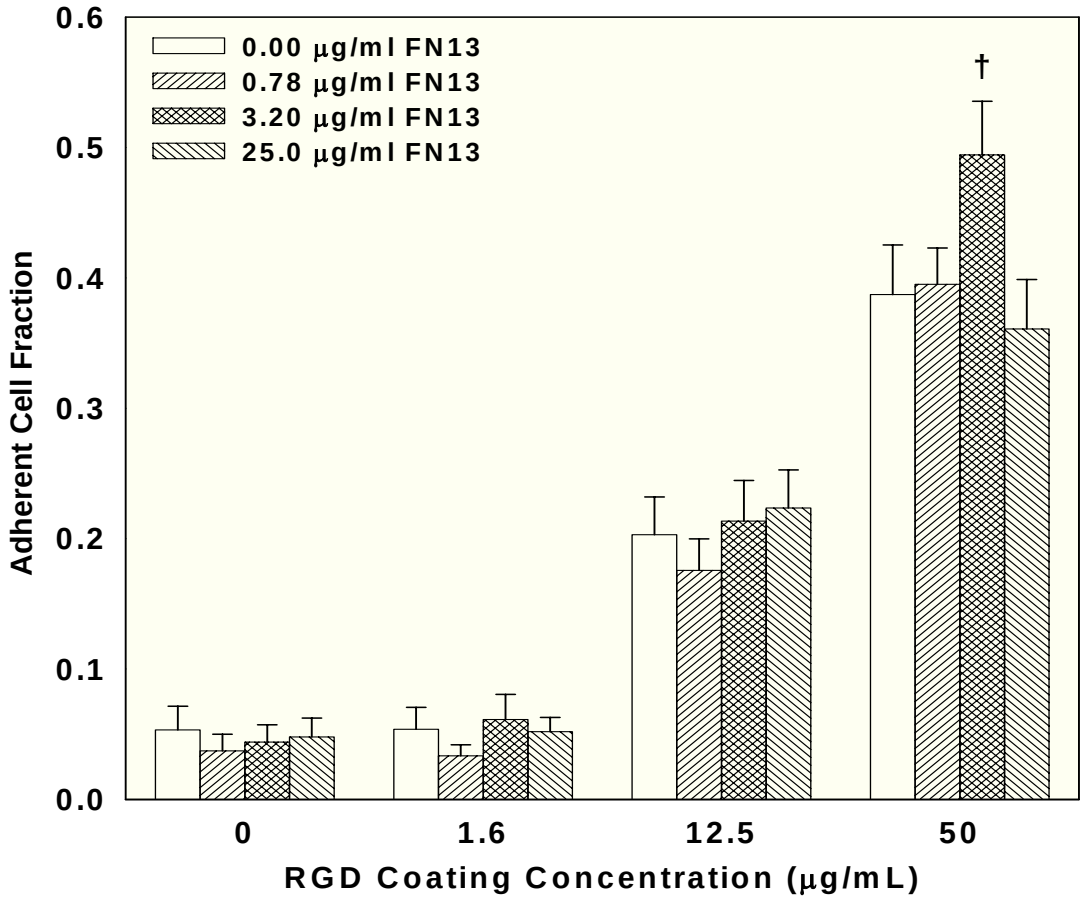

Results were analyzed by ANOVA within a given RGD concentration using SYSTAT 8.0 (SPSS, Chicago, IL). If treatments were determined to be significant, pairwise comparisons were performed using Fisher's Least-Significant-Difference Test. A 95% confidence level was considered significant.

For each RGD concentration, there were no significant differences in cell adhesion for between FN13 concentrations except for RGD = 50 μg/ml.

† RGD = 50 μg/ml vs. 25.0 μg/ml FN13 ($p < 0.02$)

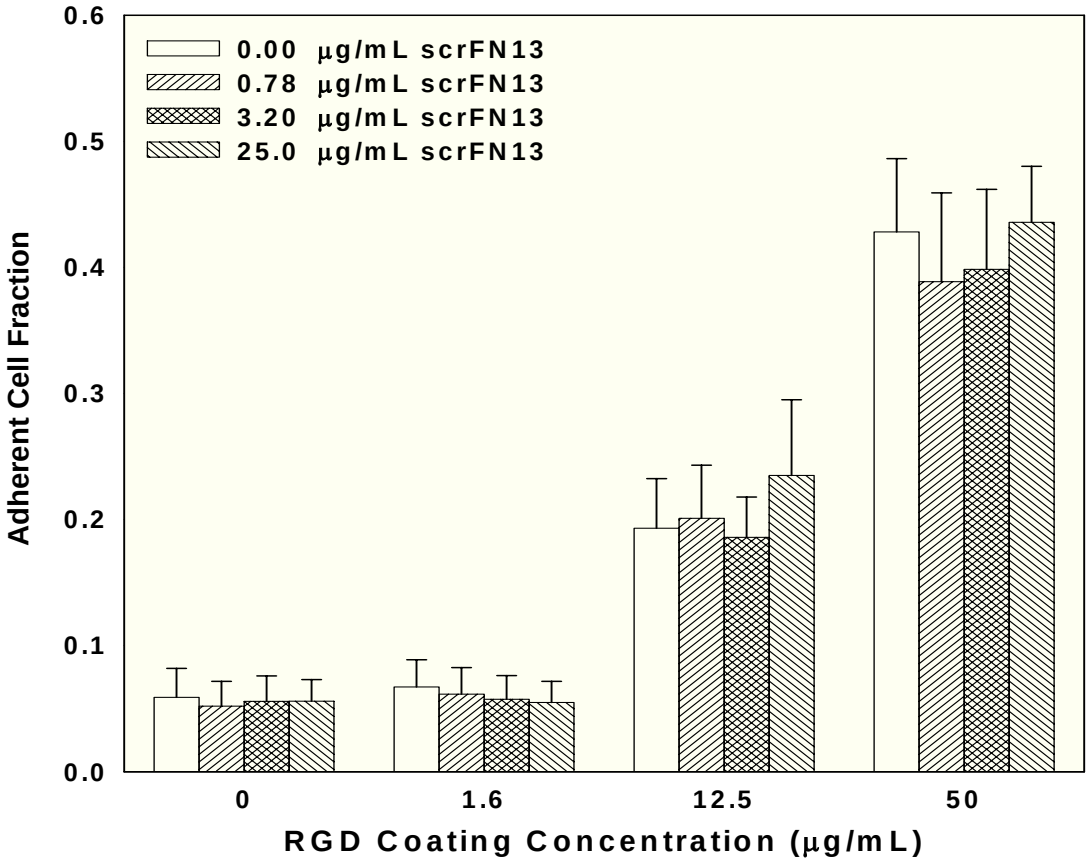

Results were analyzed by ANOVA within a given RGD concentration using SYSTAT 8.0 (SPSS, Chicago, IL). If treatments were determined to be significant, pairwise comparisons were performed using Fisher's Least-Significant-Difference Test. A 95% confidence level was considered significant.

For each RGD concentration, there were no significant differences in cell adhesion between FN13 concentrations.

Cell Adhesion Assay

Cell adhesion to SAMs was measured using a centrifugation assay that applies well-controlled detachment forces[1]. SAMs were assembled in Au-coated Lab-Tek chamber slides and functionalized with controlled densities of bioactive peptides, and then blocked in 1% BSA for 1 h to prevent non-specific adhesion. MC3T3-E1 osteoblast-like cells were labeled with 2 μg/mL calcein-AM and seeded at 200 cells/mm^2 in 10% FBS in α-MEM onto chamber slides for 45 min at 37 ^{o}C. Initial fluorescence intensity was measured to quantify the number of adherent cells prior to the application of force. After filling the wells with media and sealing with transparent adhesive tape, substrates were spun at a fixed speed in a centrifuge (Beckman Allegra 6, GH 3.8 rotor) to apply a centrifugal force corresponding to 92g. After centrifugation, media was exchanged and fluorescence intensity was read to measure remaining adherent cells. For each well, adherent cell fraction was calculated as the ratio of post-spin to pre-spin fluorescence readings.

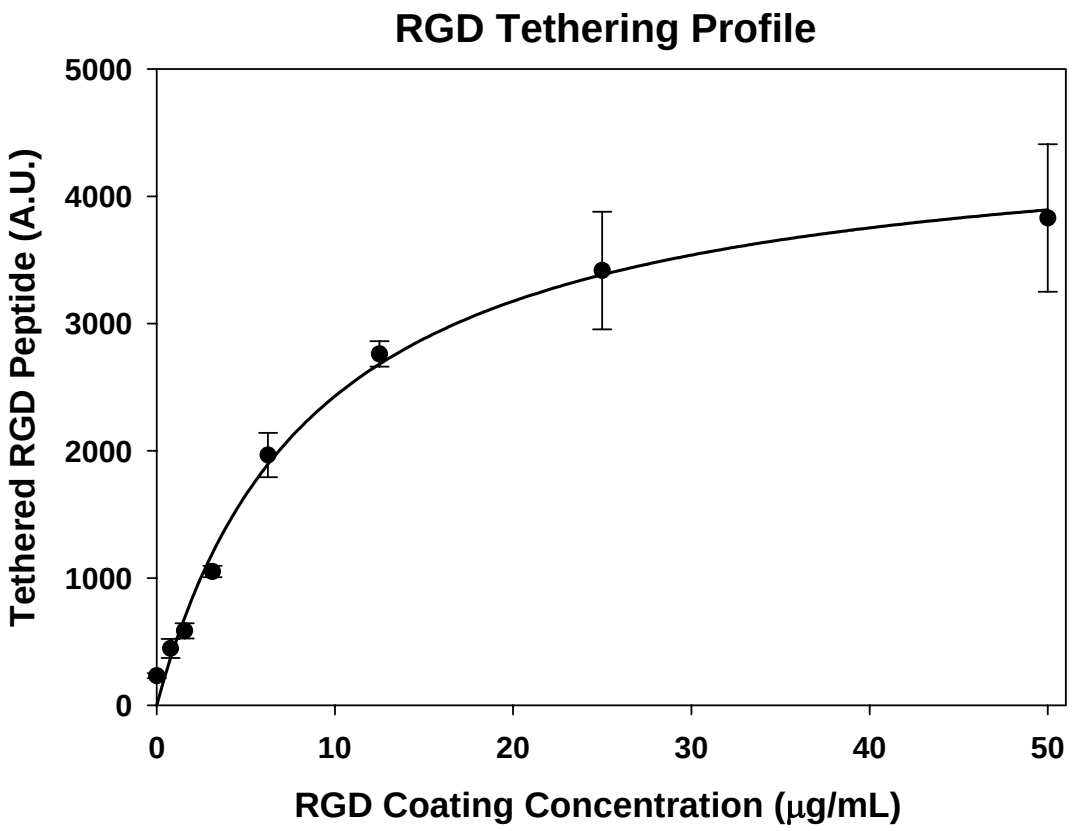

Curve Fit in Sigma Plot with modified hyperbola $R^2 = 0.99$

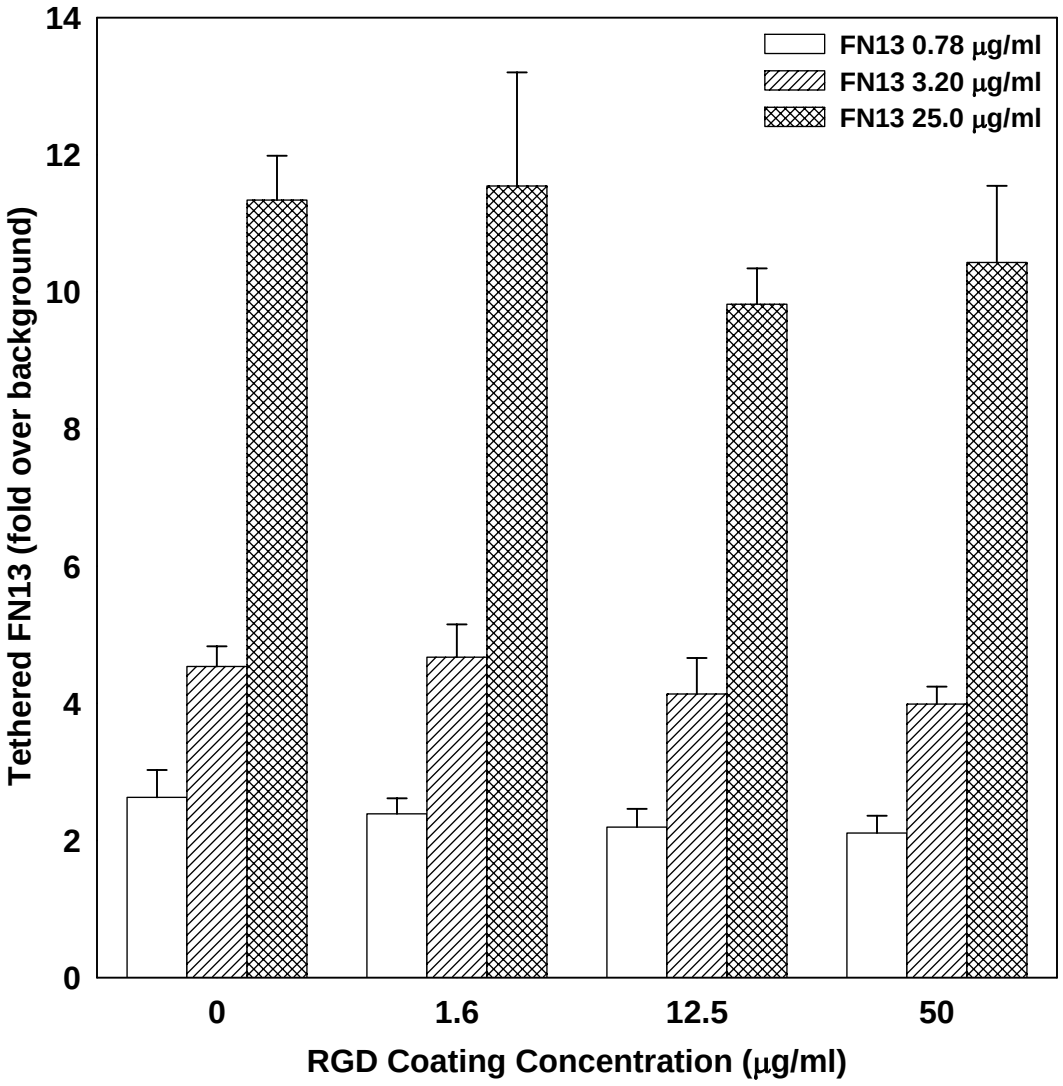

Results were analyzed by ANOVA using SYSTAT 8.0 (SPSS, Chicago, IL). If treatments were determined to be significant, pairwise comparisons were performed using Tukey post hoc test. A 95% confidence level was considered significant.

Within a given FN13 coating concentration, there were no significant differences between RGD concentrations

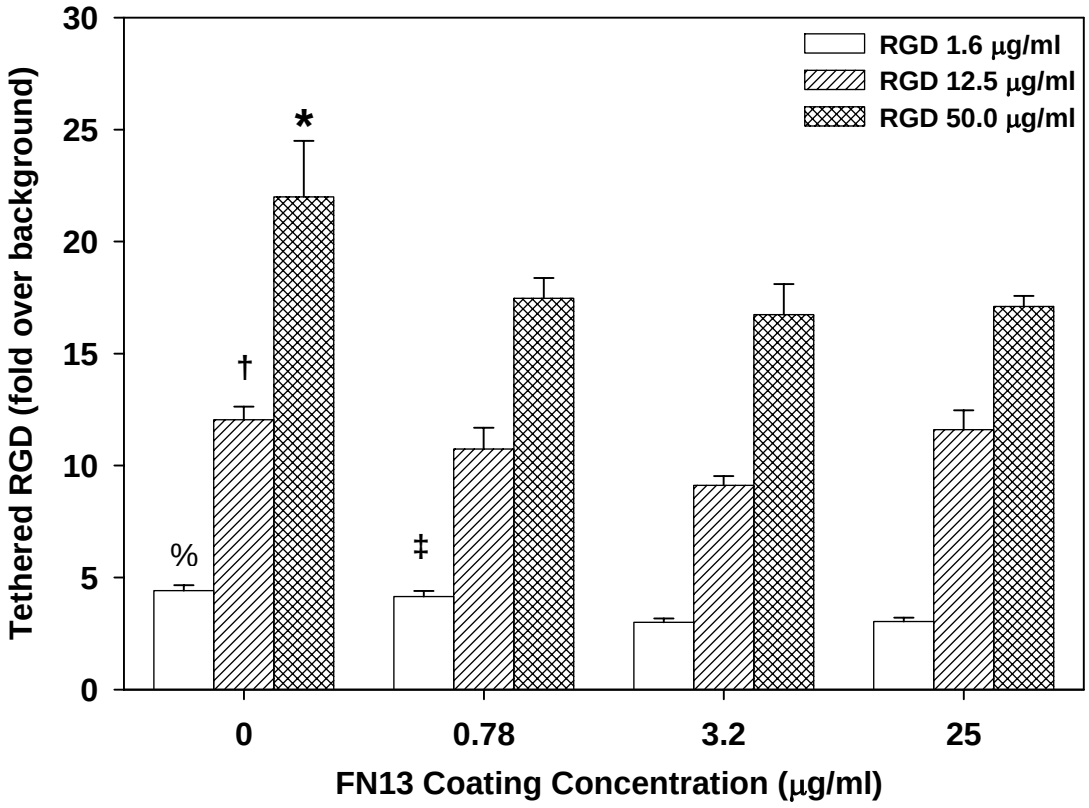

Results were analyzed by ANOVA using SYSTAT 8.0 (SPSS, Chicago, IL). If treatments were determined to be significant, pairwise comparisons were performed using Tukey post hoc test. A 95% confidence level was considered significant.

* RGD = 50.0 μg/ml vs. 0.78 μg/ml FN13, 3.2 μg/ml FN13, 25 μg/ml FN13, ($p < 0.020$)
† RGD = 12.5 μg/ml vs. 3.2 μg/ml FN13, ($p < 0.0049$)
% RGD = 1.6 μg/ml vs. 3.2 μg/ml FN13, 25 μg/ml FN13, ($p < 0.0009$)
‡ RGD = 1.6 μg/ml vs. 3.2 μg/ml FN13, 25 μg/ml FN13, ($p < 0.006$)

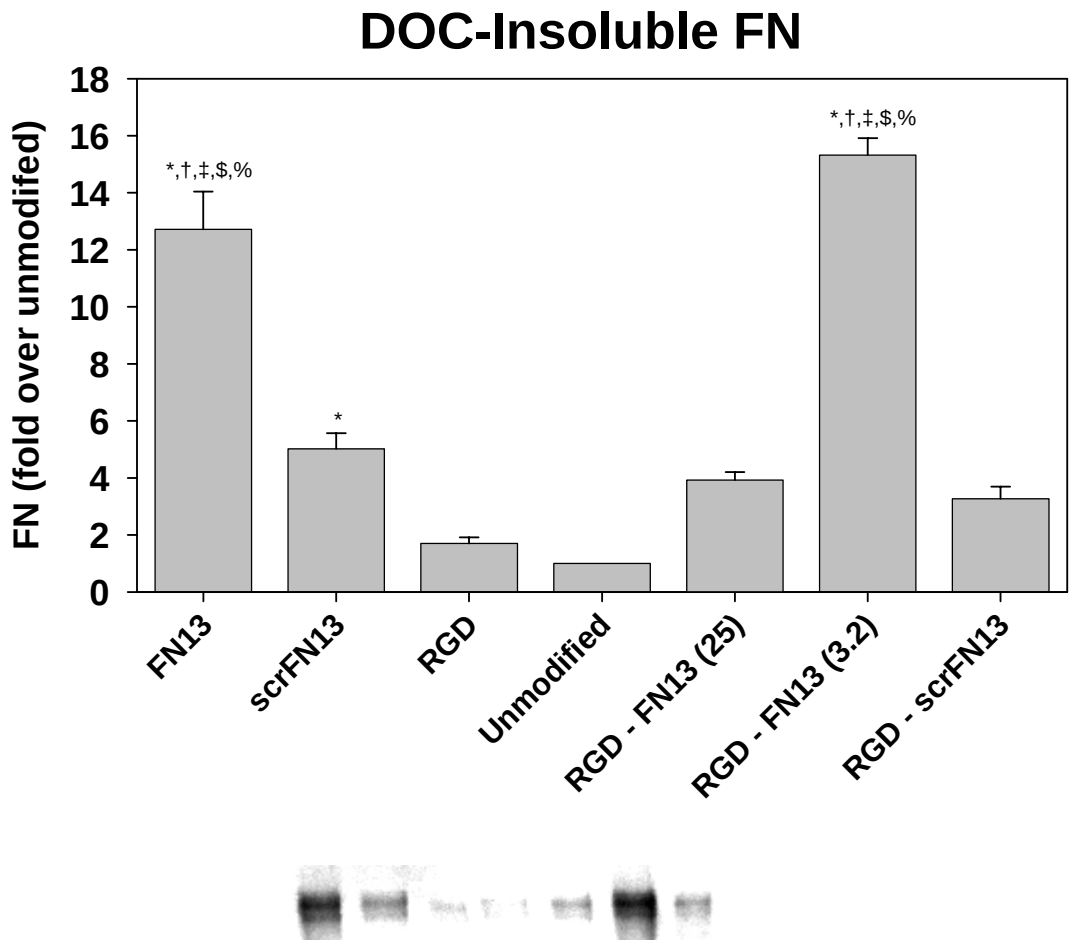

Order here is the same as plot above

Results were analyzed by General Linear Model using SYSTAT 8.0 (SPSS, Chicago, IL). If treatments were determined to be significant, pairwise comparisons were performed using Tukey post hoc test. A 95% confidence level was considered significant.

* vs. Unmodified, ($p < 0.02$)
† vs. RGD – FN13 (25), ($p < 0.0001$)
‡ vs. RGD – scrFN13, ($p < 0.00008$)
$ vs. RGD, ($p < 0.00003$)
% vs. scrFN13, ($p < 0.0003$)

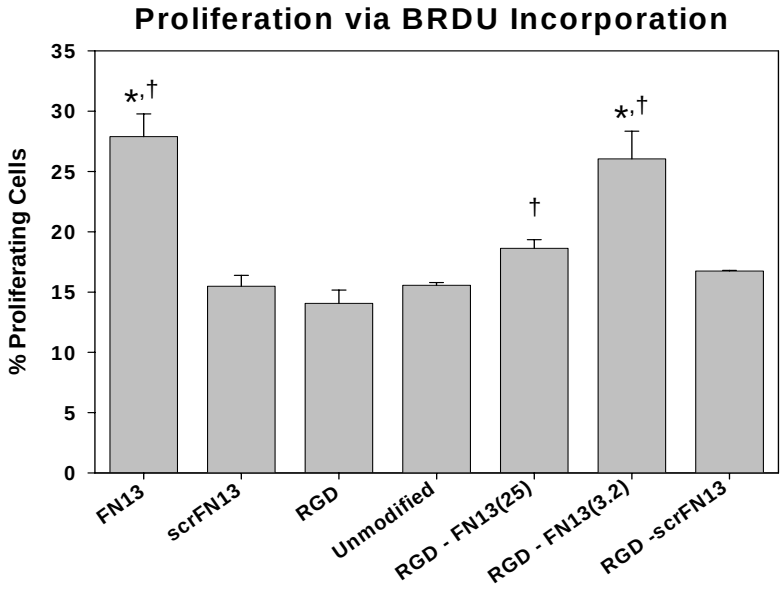

Trial #1 only trial # did not stain correctly and needs to be redone…

Results were analyzed by ANOVA using SYSTAT 8.0 (SPSS, Chicago, IL). If treatments were determined to be significant, pairwise comparisons were performed using Fisher's Least-Significant-Difference Test. A 95% confidence level was considered significant.

* Sig. vs. scrFN13, Unmodified, RGD-Fn13(25), and RGD-scr $p < 0.0006$

† Sig. vs. RGD $p < 0.02$

PROTOCOLS:

Preparation of substrates and gold deposition

There are two options when cleaning glass for gold deposition: 1) chemical cleaning, and 2) plasma Etching. Each has its pros and cons. Chemical cleaning has no limitations to size (of the glass) but if not rinsed vigorously, this time intensive procedure leaves at least half of the substrates unusable due to salt formation. However, this method obtains the cleanest glass when done properly. Cleaning with the plasma etcher is very simple, but this method does not clean the glass as well. Since the chemical cleaning can take the better part of a day, and it is obvious (slight dusty look on glass) when the plasma etched samples are not clean enough, I prefer the plasma etching technique.

Chemical Cleaning

1) Mix 70% H_2SO_4 w/ 30% H_2O_2 in beaker & place on hotplate heat (90 ^oC)
2) Place glass coverslips into solution and submerge all floaters
3) Let heat for 1 hour (check occasionally for floaters)
4) Pour solution down drain with running water (use drain in hood)
5) Rinse w/ diH_2O several times to remove all salts (most important step)
6) Rinse 2x in 70% EtOH AND 1x in 95% EtOH
7) Remove coverslips and place on Al-foil; put in oven (70 ^oC for 0.5-1.0 h)
8) Remove from oven and glue to TC dish lid with minimal ruber cement
9) Coat with Ti and Gold (thickness depends on the experiment)

Plasma Etching (first written by Kristen Michael)

1) With gloved hands, lift Pyrex cover at the handle. Place samples on metal sheet under cover being careful not to scratch the rubber gasket. Cover sample platform with Pyrex
2) Open Oxygen tank. The regulator pressure should be just above 30psi
3) Turn on “Vacuum Pump Power” switch. This switch turns on both the vacuum pump & the water-cooling sump-pump.
4) Adjust regulator pressure on controller to 20-30psi. Turn the “System Vacuum” switch to on (switch is 3-position so turn to top position). The vacuum gauge should read 30”Hg
5) Turn the “Gas Control” switch on
6) Adjust the flow meter to 2SCFH
7) Adjust the power knob on the right face of the microwave to 100%
8) Press “Time Cook” and set microwave timer to desired etch time (usually 2 – 5 min cycles with 5 minutes cooling)
9) Shut off “Vacuum Pump Power,” “Gas Control,” and “System Vacuum”

E-beam (first written by Kristen Michael)

1) Turn on water at the wall
2) Turn on main power, and display power
3) Open bell jar with switch.
4) With gloved hands:
    a. Remove holder being careful not to hit the detector.
    b. Add sample to holder (will melt plastic if at the center).

c. Replace holder in bell jar and close bell jar.

d. Close vent valve (labeled green, positioned behind bell jar).

5) Lower Bell Jar and close tight

6) Turn on mechanical pump power (will make a loud noise, pump down to < $2*10^{-6}$Torr).

7) Set metal position to Ti. (Set metal position by turning the rod at the right side of the bell jar.)

8) Turn on substrate to turn sample holder while depositing metal

9) Set controller to correct film and zero deposition thickness:

a. Prog, ^, ^, *film#* = 1, E*nter* (film# 2 for Au)

b. *Layer1* = 1, E*nter* (layer1 = 2 for Au)

c. Prog

d. Start, Stop quickly (back to back)

e. Reset (controller screen should say “Ready”)

f. Zero

10) Turn on the ion gun breaker switch and the ion gun emission controller

11) Rotate emission level so that when the shutter is open (w/ N_2), the deposition rate is ~ 2Å/sec

12) When you reach the desired deposition thickness, close the shutter and turn emission level to zero slowly.

13) After last metal, turn off shutter pump, deposition controller, and ion gun.

14) Wait ~4min for metal to cool

15) Turn off mechanical pump

16) Open vent valve at back of bell jar to return to 760 torr

For all experiments but FTIR, 100 Å Ti and 150 Å Au. For FTIR, 100 Å Ti and 2000 Å Au.

Reconstitution of Thiols

1) THIOLS ARE VERY AIR SENSITIVE AND SHOULD BE STORED UNDER NITROGEN IN FREEZER PRIOR TO AND AFTER RECONSTITUTION
2) MAKE ONLY ENOUGH TO USE AND DO NOT KEEP THIOLS IN SOLUTION LONGER THAN 2 WEEKS!!!
3) Make solutions of thiols 1mM in absolute EtOH (at desired ratio for mixed SAMs)

Monolayer Assembly

Monolayers were assembled differently for each type of surface.

Methyl and EG_3 Mixed Monolayers

1) Clean glass soaking in 95% EtOH for 30 min
2) Dry gold under stream of N_2 gas
3) Fill clean container with enough thiol solution to completely cover gold
4) Place gold into solution and let sit at room temp for 4 hours
5) Rinse excess thiol away with 95% EtOH and dry under N_2 gas

6) Soak in diH_2O for 15 – 30 minutes
7) Incubate in FN for 30 min
8) Block in BSA for 30 min
9) Elute in cPBS over night
10) Seed cells at desired density

EG_3 and EG_6-Acid Mixed Monolayers with Single Ligand

1) Clean Au by soaking in EtOH for 15 – 30 minutes
2) Assemble Mixed Monolayers of PEG_3 and PEG_6-Acid (solution = surface) for 4 hours on gold coated chamber slides
3) Rinse with EtOH and soak in diH_2O while preparing NHS solutions
4) Soak in NHS solutions for 30 min
    a. Activation Buffer: 0.1 M MES, 0.5 M NaCl, pH 6.0
    b. EDC = 0.039g per mL Buffer needed (2mM total)
    c. NHS = 0.0119 p per mL Buffer needed (5 mM total)
5) Add equal volume 40 mM solution of 2-mercapto ethanol (5 min, final 20 mM) to quench EDC
6) Tether ligands (peptide/ FN) to surfaces (30 min)
7) Aspirate and quench remaining NHS with 20 mM Glycine (5-10 min)
8) Aspirate and Block w/ 1% H.D. BSA (30 min)
9) Aspirate and incubate in complete PBS overnight (in incubator)

*** At this point, surfaces can be used for any of the experiments

EG_3 and EG_6-Acid Mixed Monolayers with Mixed Ligands

At this point of the project, it was a goal to remove the overnight incubation in cPBS for this mixed monolayer system. This treatment of the surfaces added an additional day to each experiment for the set-up. ELISAs were performed for different conditions including ranges in monolayer assembly time and elution in cPBS over night. It was determined that the thiols could be assembled overnight and the16 h PBS treatment could be removed.

1) Clean glass by soaking in EtOH for 15 – 30 minutes
2) Assemble Mixed Monolayers of PEG_3 and PEG_6-Acid (solution = surface) for 4 hours on gold coated chamber slides
3) Rinse with EtOH and soak in diH_2O while preparing NHS solutions
4) Soak in NHS solutions/ and or NHS Buffer for 30 min
    a. Activation Buffer: 0.1 M MES, 0.5 M NaCl, pH 6.0
    b. EDC = 0.039g per mL Buffer needed
    c. NHS = 0.0119 p per mL Buffer needed
5) Add 40 mM solution of 2-mercapto ethanol (5 min, final 20 mM) to quench EDC
6) Tether RGD (at various densities) to surfaces (30 min)
7) Tether either FN13 or scrFN13 to surfaces (various densities, 30 min)
8) Aspirate and quench remaining NHS with 20 mM Glycine (5-10 min)
9) Aspirate and Block w/ 1% H.D. BSA (30 min)
10) Aspirate and either seed cells or start ELISA

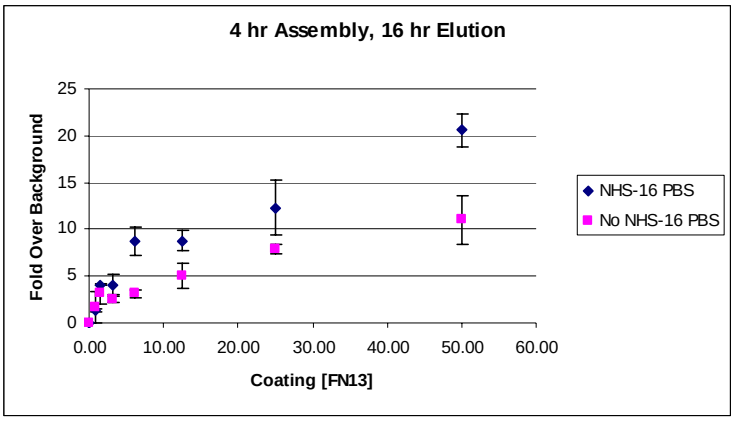

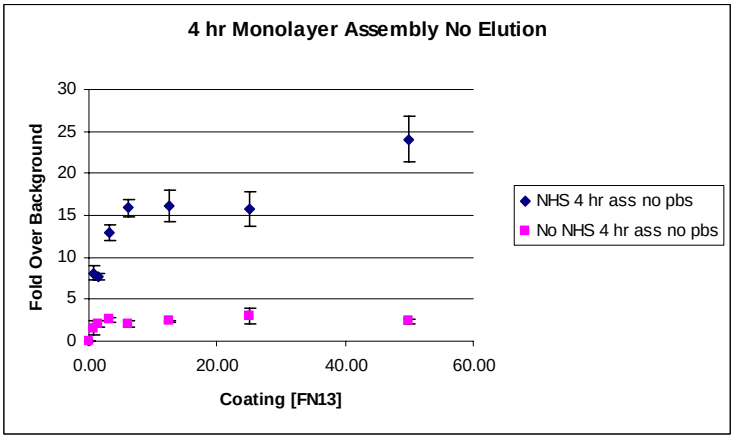

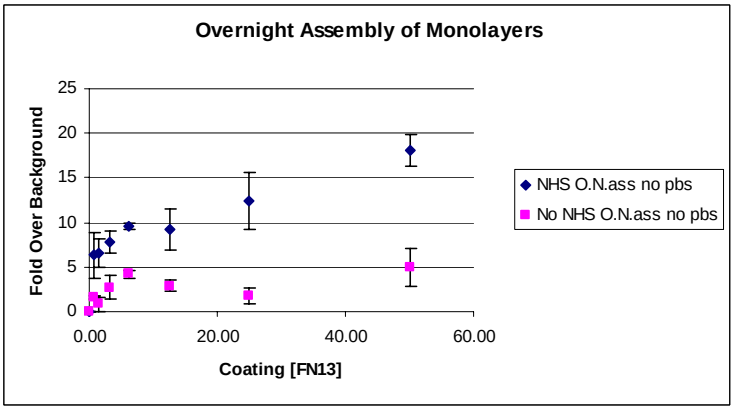

Surface Characterization

X-ray Photoelectron Spectroscopy (XPS) and contact angle measurements were described in the appropriate chapter.

FTIR On SAMs (Smart SAGA)

THESE EXPERIMENTS ARE VERY TRICKY AND SENSITIVE

1) Gold for monolayer assembly must be completely reflective so that the IR beam does not pass through and lose signal.
2) Coat VWR micro cover glasses 1 once, CAT NO. 48393 059; 22X50mm glass cover slips with 50 Å Ti and 2000 Å Au.
3) Treat gold in same manner as for other experiments in both storage and monolayer assembly (and for NHS formation).

FTIR Set Up

1) Open bench door and remove Sample holder
2) Insert Smart SAGA Accessory
3) The instrument should tell you that the SAGA was inserted and ask if you want to run checks…. Click **o.k.**
4) This will give you errors and tell you that it does not meet the required settings… click o.k. or cancel.
5) Go to Collect on dropdown menu and click on Experimental Setup
6) This menu has several tabs: Collect, Bench, Quality, Advanced, and Diagnostic. Make sure that they read as follows
    a. Collect:
        i. No of Scans = 1024
        ii. Resolution = 4
        iii. Final Format = % Reflectance

iv. Corrections = None

v. Check the box next to Auto Atmosphere correction

vi. Check the box next to Collect Background before each sample

b. Bench:

i. Set to **Auto Gain**

ii. Velocity = 0.1581

iii. Check the box next to min/max

iv. Sample Compartment = Main

v. Detector = DTGS KBr

vi. Beam splitter = KBr

vii. Source = IR

viii. Accessory = SMART SAGA

ix. Window Material = Ge

x. Range = 4000-600

c. Quality:

i. Check box next to spectrum

ii. Uncheck box next to “Use spectral quality checks”

d. Advanced and Diagnostic: No need to touch these!

7) Place clean gold sample w/o monolayer for a background scan. Aperture should be set to open and corresponding mask should be used

8) The bench will not give a reading unless gold is on holder (face down) to reflect the beam

9) Purge System for 2 hours before taking a background scan. Check bench purge; run a scan with less scan numbers on blank gold as background and sample. If spectra is straight line, then system is purged

10) Once purged, click on Collect on drop down menu and then on Collect Sample

11) This will ask you to name window… name it and click ok

12) Collection will take about 1h and 6 min. After finished, remove blank gold and place sample face down on SAGA. Let purge for almost one hour to remove introduced moisture and CO2.

13) Click ok on the box asking you to begin scan on sample.

14) After 1 h and 6 min. It will ask you to add it to the window that was in the drop down menu during the scan. Can't change after scan is complete!

15) Play with spectra as you like. Smooth, baseline correct, ect…

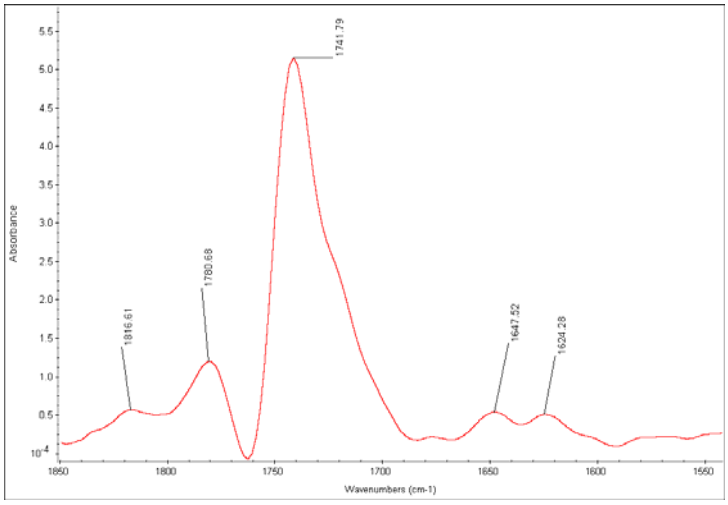

95% PEG_3 5% PEG_6-ACID converted to NHS

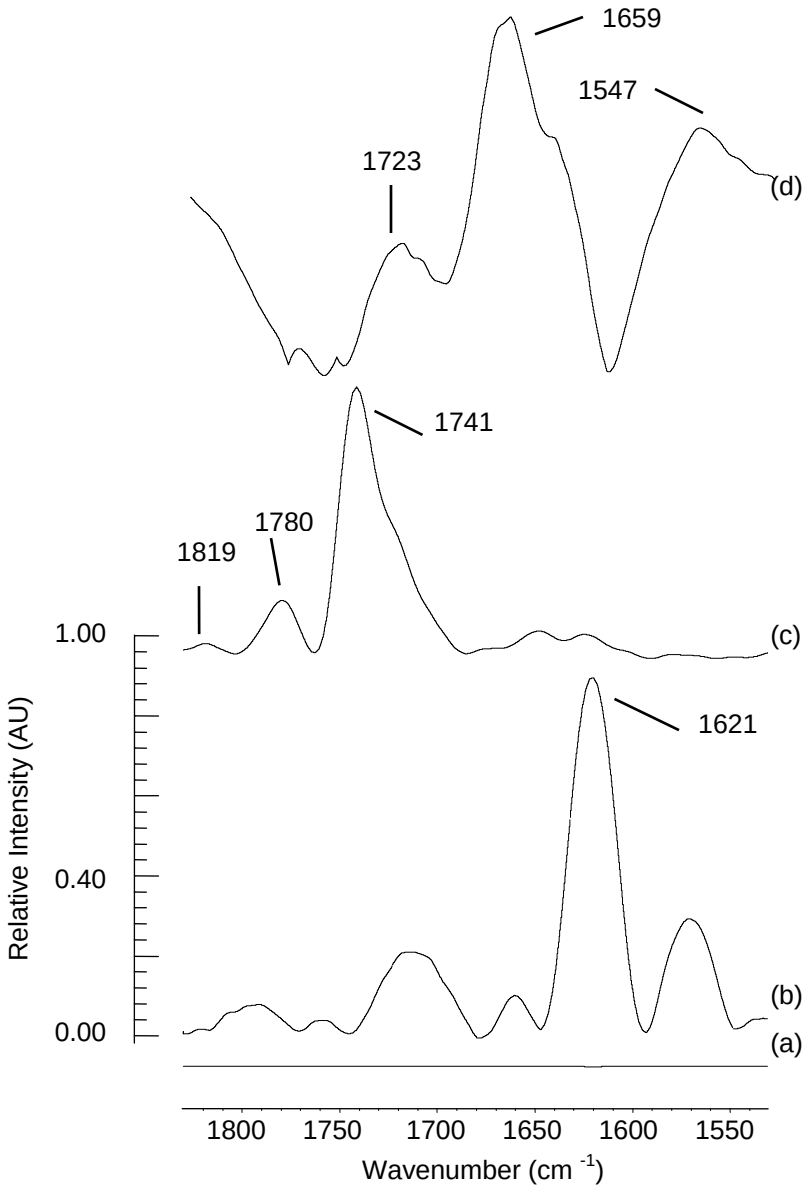

PIERS spectra acquired for (a) a confluent SAM of **1**, (b) a mixed SAM composed of **1** and **2** (χ (**1**) = 0.95), (c) a mixed SAM composed of **1** and **2** (χ (**1**) = 0.95) after activation with NHS and EDC to form the corresponding NHS ester.

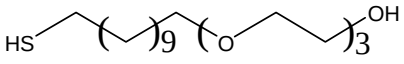

1

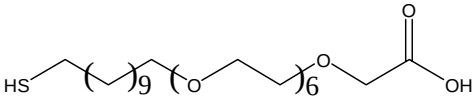

2

(a) No bands in this region, as expected for PEG surface

(b) The band at 1621 is assigned to the C = O stretch for carboxylic acid groups

(c) The band at 1741 is assigned to the asymmetric stretch of the NHS carbonyls, while the band at 1780 is assigned to the symmetric stretch of the NHS carbonyls, and the band at 1819 is assigned to the stretch from the activated ester carbonyl group.

(d) The band at 1723 is assigned to the C = O stretch for the carboxylic acid groups associated with hydrolyzed NHS esters, while the band at 1659 is assigned to the amide carbonyl stretch, and the band at 1547 is assigned to N-H bending.

Introduction of Bio-ligands and Proteins

For -EG_3 and –CH_3 terminated alkanethiol mixed monolayers, the bio-ligand of choice was FN. We used radio-labeled FN for ultra-sensitive measurements.

Quantification of Fibronectin on Monolayers (^{125}I-FN Study):

Iodinating FN with Bolton-Hunter Reagent (below):

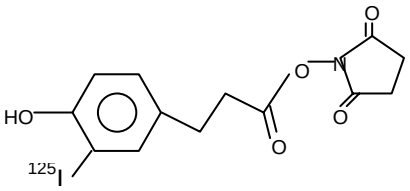

Day 1:

1) Make 0.1M NaB solution and pH to 8.5 (sterile)
2) Reconstitute 1g of FN with 100 μL of above solution

   Bring Bolton-Hunter Reagent to Radioactive center and in hood, behind lead…
3) Remove lid and insert 23-gauge needle (connected to charcoal trap) through the septum
4) A second needle is inserted through the septum with a gentle stream of Nitrogen to evaporate the benzene solvent (CAREFUL WITH FLOW TO PREVENT SPLASHING!!!)
5) Add 10 μL#2 above through the septum with a syringe and let incubate at 4^{o}C overnight (100 μg FN @ 10 μg/μL)

PREPARE Sephadex-25 Column:

1) Fill 50 mL conical vile with 0.5g sephadex-25 beads and add 1 mL 1%HD BSA, 1 mL 10% Azide, 20 mL di H_20. Place on rocking plate for several hours, then put into fridge overnight…. Incubate overnight to block for adsorption of the FN to the beads
2) Next day (packing column): Take 1 mL syringe and pull it apart.
3) Fill syringe up to the 0.9 mL make with the sephadex solution
4) Rinse 5X with complete PBS to remove excess BSA

Day 2:

1) Quench the reaction by adding 50μL of 0.2 M glycine in the 0.1 M NaB buffer (pH = 8.5)
2) Set up sephadex-25 column on stand and let eluant run off until level with top of beads.
3) Load the solution from the reaction vial.
4) Let six drops collect into one tube, then begin collecting 2 drops/ fraction
5) Collect fractions until get two spike in radioactivity with Geiger counter
6) 1^{st} spike if the labeled FN and second is the unreacted Bolton-hunter reagent (column is size exclusion so that the small gets trapped in the sephadex and comes off slower)
7) Combine early fractions with high signal. (mine = 220 μL)

Specific Activity:

1) Take 1 μL and drop entire pipette tip into a glass test tube
2) Run **Protocol #6 FN ADSORPTION** on above and empty test tube

Specific Activity = CPM / μg reading from above is CPM / μl

Ex: reading = <u>1170416 CPM / μl</u>

0.613 μg / μl (concentration from nano-orange)

S.A. = 1.9×10^6 CPM / μg

Other calculations are needed for safety sheet and are on page 95 of book 01-2

<u>*Nano Orange (Protein Quantification Technique):*</u>

Perform 1st on BSA as test of technique and of Nano Orange's Efficiency

*** Follow protocol from Molecular Probes Sheet

1) Mix 9 μl Component **A**, 450 μl Component **B** in 4.05 mL di H_2O
2) 4.5 μl (2 μg/ μl BSA, **C**) in 895.5 of #1

Put 225 μl of #2 into four vials…

Two are at 10 μg/ μl the other two are used to make serial dilutions

Leave in the vials and put in water bath @ 90 ^{o}C for 10 min

Centrifuge down and pipette 200 μl into black dish

Read on plate reader: Gain = 70 Absorbance = 470 Emission = 570

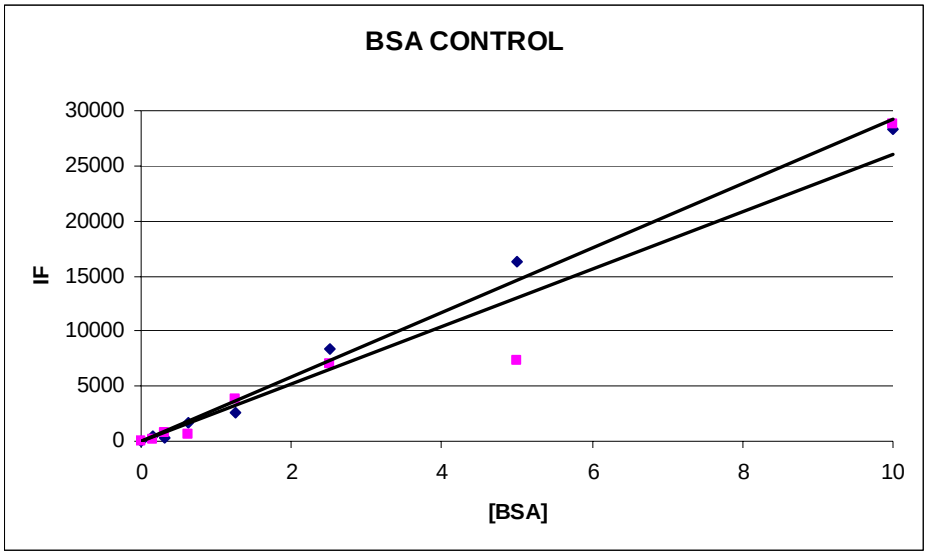

Nano Orange on "HOT" FN-^{125}I

1) Mix 9 μl Component **A**, 450 μl Component **B** in 4.05 mL di H_2O

2) 8.0 μl (1 μg/ μl cold FN) in 792 of #1 [diluted 1: 100 gives 10 μg/ mL]

3) Make serial dilutions of #2 about (10, 5, 2.5, 1.25, …)

4) Place 200 μl / well into black dish…

5) Take 2 μl of unknown concentration of HOT—FN and add 198 μl #1.

6) Read in plate reader at Gain = 60, Absorbance = 470 Emission = 570

7) Fit unknown into curve to determine the 1:100 diluted concentration

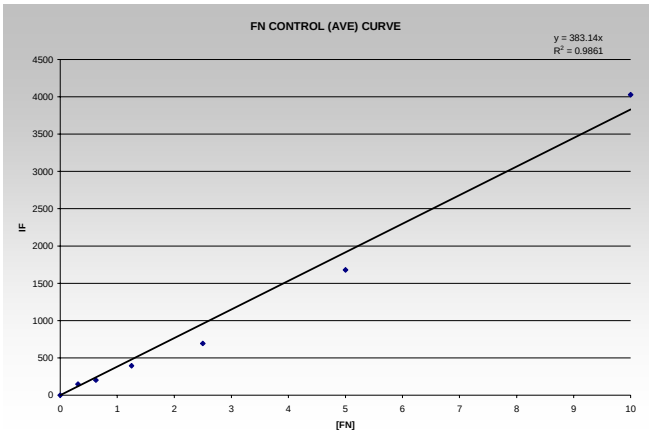

To demonstrate that the iodination procedure did not alter the activity of the protein, control adsorption experiments with different ratios of labeled and unlabeled protein were performed. (see page 102 of 01-02)

1) Make 5 μg/ ml solution of FN at varied ratios of hot to cold FN and read radioactivity adsorbed to glass following protocol for FN adsorption.
2) Ratio of signals should correspond to the ratio used in solution

FN Adsorption to SAMs:

1) SAMs were assembled on Au-coated 9 mm^2 glass cover slips and pre-soaked in diH_2O for 30 min.
2) Samples were then immersed in ^{125}I-FN solutions (mixed with unlabeled FN in PBS) for 1 h.
3) After removing FN solutions, samples were immersed in 1% BSA (1 h).
4) Samples were transferred to clean tubes and radioactivity was measured using a gamma counter.
5) Adsorbed ^{125}I-FN was quantified as radioactive counts (cpm) and converted to adsorbed FN surface densities (ng/cm^2).

6) For FN elution studies, samples were coated with FN and BSA as described above, then incubated in PBS or 10% NCS in DMEM for 1 h or 16 h, and the remaining FN adsorbed on the sample was quantified.

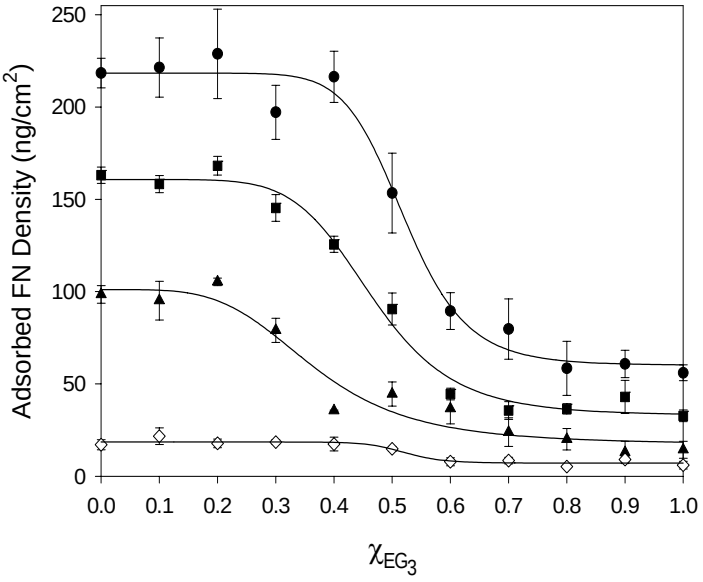

ELISA for Immobilization of Peptides to Mixed -EG_3 and -EG_6-Acid SAMs:

Example: Biotinylation of KGGGFN13

Use Pierce EZ-Link ™ PEO-Maleimide Activated Biotin

Reagents:

1) Phosphate/EDTA Buffer – 100 mM sodium phosphate, 5 mM EDTA; pH 6.0
2) Phosphate Buffered Saline (PBS) – 0.1 M sodium phosphate, 0.15 M NaCl; pH 7.2, 1 mM EDTA
3) Make 1 mg/ mL solution o peptide in # 1 above
4) Make a 10 mM solution of PEO-Biotin in # 2 above

5) Add 50 mL of # 4 above to # 3 above and let sit in dark at room temperature over night

FN 13 tethering to SAMs protocol:

1) Assemble Mixed Monolayers of PEG_3 and PEG_6-Acid (solution = surface) for 4 hours on gold coated chamber slides
2) Rinse with EtOH and soak in diH_2O while preparing NHS solutions
3) Soak in NHS solutions/ and or NHS Buffer for 30 min
    a. Activation Buffer: 0.1 M MES, 0.5 M NaCl, pH 6.0
    b. EDC = 0.039g per mL Buffer needed
    c. NHS = 0.0119 p per mL Buffer needed
4) Aspirate and quench EDC with 20 mM solution of 2-mercapto ethanol (5 min)
5) Tether FN13 peptide to surfaces (30 min) use serial dilutions of both “hot” and “cold” in complete PBS
6) Aspirate and quench remaining NHS with Glycine (5-10 min)
7) Aspirate and Block w/ 1% H.D. BSA (30 min)
8) Aspirate and incubate in complete PBS overnight (in incubator)
9) Rinse with diH_2O 3X and aspirate
10) Incubate in 60 μl of α-biotin-alkaline phosphatase (1:10,000) in 5% FBS – azide blocking buffer (1 h @ 37^oC in incubator)
11) Rinse 3X in diH_2O then block for 10 min in FBS buffer

a. FBS buffer = 5 mL FBS, 1 mL 10% NaN_3, fill to 100 mL with PBS

12) Rinse 3X with diH_2O add 60 μl 1X DEA solution while preparing substrate (at least 10 min)

a. 1X DEA = 2 mL 5X DEA (stock in fridge), 8 mL diH_2O

b. 5X DEA = 600 μl diethanol amine, 0.0519g $Mg{\cdot}6H_2O$

i. bring to 100 ml w/ di H2O (sterile)

ii. pH to 9.5 w/ 1N HCl and store at 0 ^oC

13) Aspirate and add 60 μl MUP solution to each well

a. 8 mL MUP solution = 6.0 mL diH_2O, 400 μl $NaCO_3H$, 2 mL 5X DEA, 19.2 μl MUP substrate

i. MUP substrate = make 25 mg MUP (stored in -20) with 1 mL of 1X DEA solution

14) Use multi-well pipette to suck off as much as possible and place into black dish (store chamber slides in dark in buffer while reading)

15) Read on plate reader:

a. Parameters:

i. Fluorescence; Plate definition = dynex96black.pdf

ii. Excite 360, Emission 465

iii. Gain 40, manual, read from top

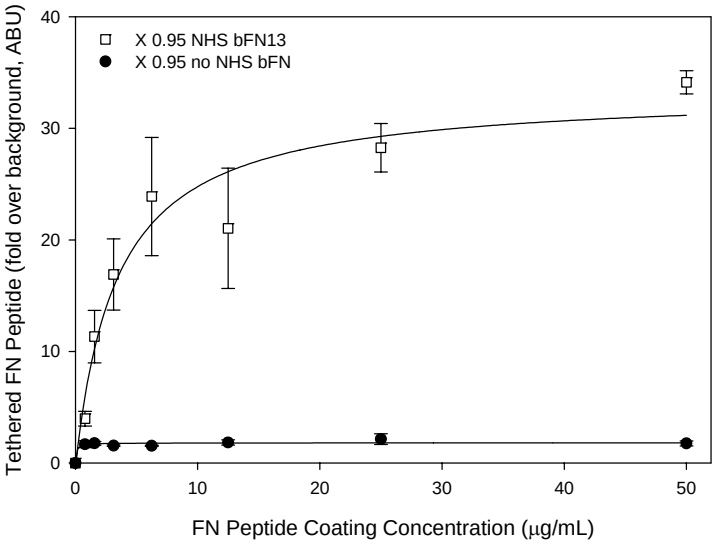

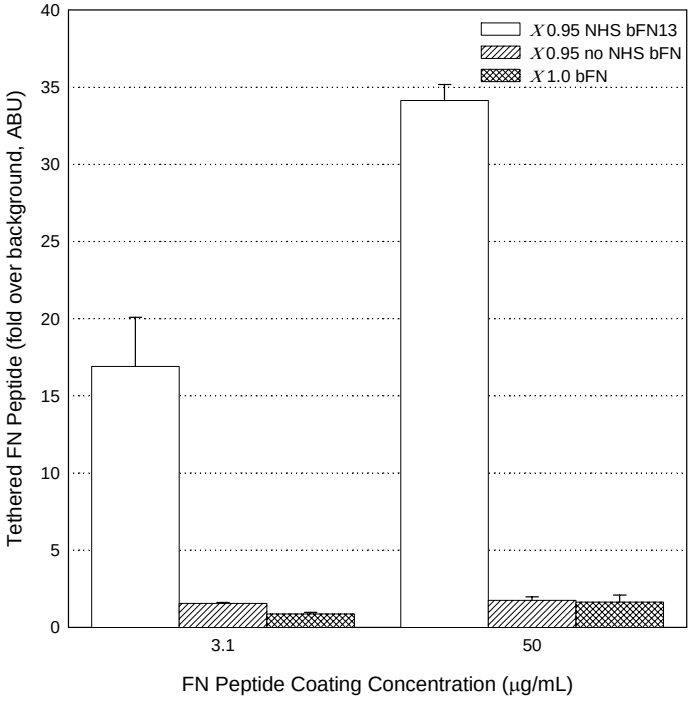

Radio labeling Peptides for Absolute Measurements of Immobilized Peptides to Mixed -EG_3 and -EG_6-Acid SAMs:

Iodination of FN peptides (KGGGAHEEICTTNEGVMY, and GRGDSPCY) using $Na^{125}I$ (Anal. Chem. 187, 292-301 (1990)).

Synthesis involves 1mCi (for each peptide) of ^{125}I-containing $Na^{125}I$ reagent (Amersham Biosciences, Piscataway, NJ). Iodination will be preformed according to protocol using IODO-GEN® Pre-Coated Iodination Tubes. Iodination and purification will be performed in NNRC RCZ and purified ^{125}I-FN peptides will be transported to 107 SSTC in a sealed tray with lid.

1. Two IODO-GEN® Pre-coated reaction tubes were wet with 1ml of High Tris Buffer (0.125 M Tris•HCl, pH 6.8, 0.15 M NaCl), and decanted.

2. 100 μl of Tris Buffer was added to the first tube as a reaction solvent.

3. 10 μl (1 mCi) of $Na^{125}I$ (Amersham IMS-30, in 50 μM NaOH) was added to the first IODO-GEN tube to activate Iodine (6 minutes at room temperature, flick every 30 sec.).

4. The full reaction volume was transferred to the second IODO-GEN® Pre-coated reaction tube and 6 minute flicking was repeated.

5. 55 μl (0.50 mCi) added to each peptide solution = React for 10 min at room temp with gentle flicking every 30 seconds, then let react overnight @ 4 ^{o}C.

6. peptide solutions =
    - FN13-Y = 321 μl of a 1.09 mg/ml solution in TRIS buffer (350 μg)
    - RGD-Y = 101 μl of a 1.58 mg/ml solution in TRIS buffer (160 μg)
    - Each peptide received 55 ul of Iodine solution to bring their final concentrations to around 1 mg/ml

7. Reaction is NOT QUENCHED with adding tyrosine since tyrosine gives background signal in the spec when determining peptide concentration and it is not successfully separated from the peptides on the columns.

8. add 0.38 ul of TFA to FN13 to bring to 0.1% TFA before loading onto column add 0.16 ul of TFA to RGD to bring to 0.1% TFA before loading onto column

9. Labeled FN peptides (^{125}I labeled peptide) were separated from the unreacted $Na^{125}I$ by reverse phase column chromatography using a Sep Pak C_{18} Light column (Waters, Milford, MA). Fractions will be collected and examined for radioactive counts.

COLUMNS

1) wash with 3 ml MeOH
2) stabilize with 4 ml TRIS Iodination Buffer with 0.1% TFA
3) load sample slowly in 0.1% TFA (drops and let creep onto column)
4) rinse with 3-4 ml TRIS buffer (w/ 0.1% TFA)
5) 2 ml each Eluant (collect all 2 ml as one fraction)
   Eluants:
   a) 10 % MeOH : 89.9 % Water; 0.1% TFA
   b) 20 % MeOH : 79.9 % Water; 0.1% TFA
   c) 30 % MeOH : 69.9 % Water; 0.1% TFA
   d) 40 % MeOH : 59.9 % Water; 0.1% TFA
   e) 50 % MeOH : 49.9 % Water; 0.1% TFA
   f) 60 % MeOH : 39.9 % Water; 0.1% TFA
   g) 70 % MeOH : 29.9 % Water; 0.1% TFA
   h) 80 % MeOH : 19.9 % Water; 0.1% TFA
   i) 90 % MeOH : 9.9 % Water; 0.1% TFA
   j) 99.9 % MeOH : 0.0 % Water; 0.1% TFA
   k) 100 % MeOH

Scan each fraction for radioactivity, pull vacuum on open vials to remove as much MeOH as possible before determining concentration with spec, or activity with gamma counter

Spec each fraction with UV Vis @ 280

Spicy RGD RDG-Y extinction coeff = 1.14
FN13-Y extinction coeff = 0.74

This column was unable to completely remove free iodine from the reaction mixture, and lead to very large background signal that swamped out tethering profiles. GOOGLE lead me to a company called Millipore (Billerica, MA). The have a filtration system called the “Stirred Cell”(cat no. 5125, 3 mL volume) which can use filters with a 500 Da cut off (cat no. 13012). Since the filter membranes have a 10% alcohol limit, samples were diluted to decrease % MeOH from first column. After loading 3 mL at a time (running down to 0.80 mL before reloading), and washing with 20 + mL of water in the same manner, 34 μg of the 110 μg loaded were recovered. This fraction had a S.A. of over 280,000. It was used for both single ligand-tethering profiles, and for mixed ligand systems in which Hot RGD was tethered first and cold FN13 second. There was a slight amount of free iodine left, so control surfaces of EG_3 were included for each coating concentration to subtract out free iodine binding to gold.

The FN13 peptide had high levels of free iodine after a first pass through the Millipore filters. The first run recovered 110 μg of the 300 + μg loading. The S.A. was a rather poor 28,000. A second attempt at removing the free iodine from the

FN13 fraction resulted in complete loss of the peptide to the filter. U.V. spec analysis showed no detectable levels of FN13 in any fraction off the column, or in the filter bed. Since the filter is reading very HOT, it suggests adsorption to the filter membrane.

I would only suggest using these membranes if large levels of high S.A. peptides are expected, and if the sample has no alcohol to require dilution (*Membranes also not compatible with NaOH).

Cell Culture

NIH 3T3 Mouse Fibroblast:

Media:

10 mL NCS, 1 mL P+S, fill bottle to 100 mL w/ DMEM

Split ratio varies depending on cell proliferation rate.

HT1080

Media:

10 mL FBS, 1 mL P+S, fill bottle to 100 mL w/ DMEM

Split ratio varies depending on cell proliferation rate.

MC3T3-E1 Osteoblast like cells

Media:

10 mL FBS, 1 mL P+S, fill bottle to 100 mL w/ DMEM

Split ratio varies depending on cell proliferation rate. **IT IS VERY IMPORTANT THAT CELLS SIT IN TRYPSIN FOR 1 MINUTE AND BANG PLATE TO REMOVE. THIS ALLOWS FOR MAXIMUM FN ON THE SURFACE OF THE CELL TO AIDE IN INITIAL ADHESION TO SURFACES.**

Immunofluorescent Staining:

This section is a general description of the immunofluorescent staining process, and meant to supplement specific procedures within chapters.

Solutions / Buffers:

Blocking Buffers:

1) 1 % H.D. BSA (use when staining for ECM proteins)
    a. 100 mL 1 % H.D. BSA solution
    b. 1 mL 10 % Sodium Azide (keeps sterile by interfering with the electron transport system)
2) 5 % NCS (use when not staining for ECM proteins)
    a. 5 mL NCS
    b. 1 mL 10 % Sodium Azide
    c. Fill to 100 mL line with PBS complete
3) 5 % FBS (use when not staining for ECM proteins)
    a. 5 mL FBS
    b. 1 mL 10 % Sodium Azide
    c. Fill to 100 mL line with PBS complete

Cross-linking / Fixing:

1) 3.6 % Formaldehyde (store in fridge in Al foil)
    a. 10 mL of the 36% Formaldehyde stock solution
    b. 90 mL PBS complete

2) CSK Solution

   a. 5 mL 1 M Tris –HCl

   b. 0.29 g NaCl

   c. 5.14 g Sucrose

   d. 61 mg $Mg{\cdot}Cl_2{\cdot}H_2O$

   e. pH to 6.8

   f. Fill to 100 mL line on bottle with di H_2O

3) CSK + Triton X Solution (chemical shelf, -20 ^oC on shelf, -20 ^oC 1D12)

   a. 10 mL CSK solution d. 350 μL 2mM PMSF

   b. 50 μL Triton-X-100 e. 200 μL Aprotinin

   c. 10 μL Leupeptin

Permeablize Cells:

1) Aspirate culture media
2) Add 1 mL CSK + Triton X Solution to each well/ sample (solution should be cold; 5-10 min then aspirate)
3) Add 0.5 – 1.0 mL of cold 3.6% CH_2O to each sample; incubate 5- 10 min
4) Block with appropriate blocking buffer for 5-10 min and aspirate
5) 1^o Anti bodies should be diluted to appropriate concentrations in blocking buffer and cover the sample with correct volume. Let incubate for 1 hour
6) Wash 3X with PBS and incubate for 5 – 10 minutes in blocking buffer
7) 2^o α-bodies diluted to appropriate concentrations in blocking buffer and cover the sample with correct volume. Let incubate for 1 hour in the dark

8) Wash 3X with PBS
9) Mount with Gel mount to slide with a cover-slip face up, and let dry
10) Nail polish edges of cover-slip with clear nail polish to prevent dehydration

Staining w/ anti-bodies:

1) 25 μL / 9mm^2 cover slip
2) FN = 1^o rb α-poly FN (1:400, -20 ^{o}C 1D11), 2^o α–rb Tx –Red (1:200, blue case 2nd shelf -20 ^{o}C)
3) α_5 = mouse $\alpha - \alpha_5$ (1:250, -20 ^{o}C), 2^o α– ms Alexa Fluor 488 (green) (1:200, blue case 2nd shelf -20 ^{o}C)
4) DNA = no primary, only 2^o Hoechst (1:10,000, fridge in Al foil)
5) Vinc = ms- α–Vinc (1:100, -20 ^{o}C 1D10), 2^o α– ms Alexa Fluor 488 (green) (1:200, blue case 2nd shelf -20 ^{o}C)
6) F-actin = No primary, 2^o rhodamine phalloidin (1:200, blue box -20)

Cell Adhesion Assay

Cell adhesion to SAMs was measured using a centrifugation assay that applies well-controlled detachment forces. SAMs were assembled in Au-coated Lab-Tek chamber slides. Cells (NIH-3T3 or MC3T3-E1) were labeled with 2 μg/mL Calcein-AM and seeded at 200 cells/mm^2 in serum containing media onto chamber slides for indicated times either at room temperature or 37 ^{o}C. Substrates were spun at a fixed speed in a centrifuge (Beckman Allegra 6, GH

3.8 rotor) to apply a centrifugal force. For each well, adherent cell fraction was calculated as the ratio of post-spin to pre-spin fluorescence readings.

Prepare Substrates

1) Chamber slides are disassembled by removing the chambers and treated as follows:
2) Pop chambers off of slide
3) With Razor Blade, remove extra PDMS from corners and from tall center spot
4) Place into Plasma Etcher and turn to 100% power
5) “COOK” for 5 min, rest 5 min, and “COOK” for 5 min more
6) Tape with Kapton directly onto sample holders in the ebeam
7) Coat with 100 Å Ti, and 150 Å Au

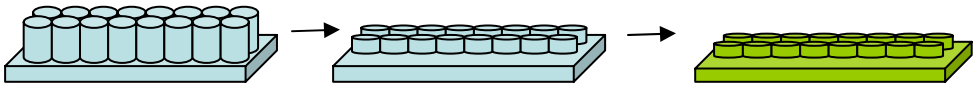

Protocol does not need to be sterile since adhesion for at most 1 h

1) Assemble monolayers according to surface type
2) Block with 1% H.D. BSA for 30 min

Cell Culture - Seeding

1) Aspirate Serum from cells
2) Rinse with complete PBS
3) Add 10 μl of Calcein-AM in 5 mL 2mM Dextrose PBS (1D9) for 100 mm dish
4) Let incubate for 20 minutes
5) Aspirate and detach cells from dish
6) Then seed cells in serum (NIH = 1 h @ 200 cells / mm^2, MC3T3 = 45 min @ 800 cells / mm^2) on bench top (60 μl / well).

Spinning

1) Glue chamber slides to the lid o a 96 well dish making sure that holes line up; try not to get glue under wells
2) Read plate on plate reader **Excite 494, Read 517** 10 min after seeding
3) After total adhesion time (45 min MC3t3 or 1 h for NIH), use vacuum grease to put chambers back on wells
4) Fill each well with cell culture media (240 μl)
5) Put transparent tape across the wells to seal in fluid
6) Place upside down into centrifuge and spin @ 92g (1000 rpm for 2 min, for MC3t3), (46g / 500 rpm for NIH)
7) Aspirate wells and add back 60 μL cell culture media to each well
8) Reread in plate reader
9) Record as **ADHERENT CELL FRACTION = post spin / pre spin**

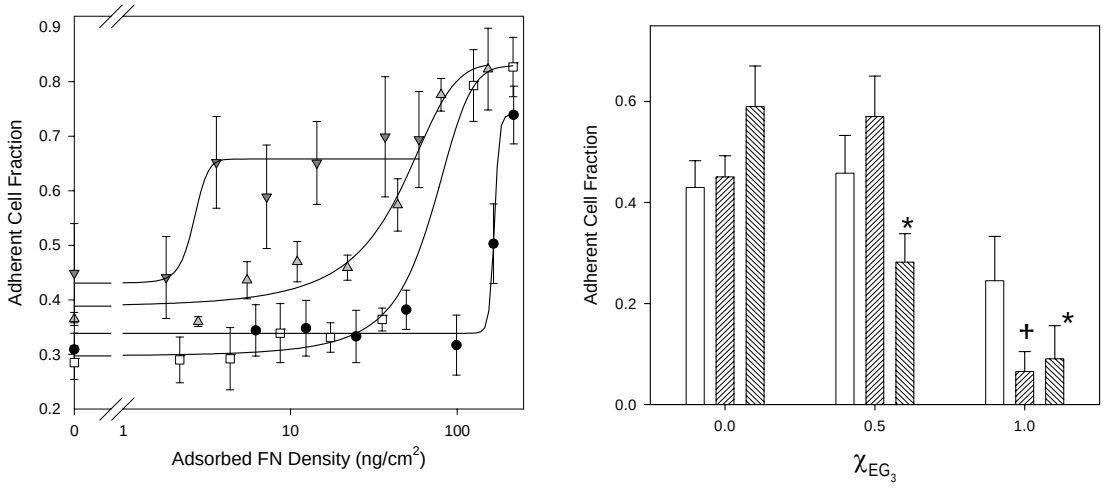

Cell Proliferation on Mixed Monolayers:

SYBR® Green:

This method for cell adhesion is very poor due to DNA "clumping"

1) 35 mm tissue culture dishes are taken directly from package and placed into e-beam
2) Coated with 50 Å Ti and 150 Å Au
3) Dishes and lids were placed into sterile hood, separated and placed face up
4) Lamp was turned on for 30 min to sterilize
5) Assemble monolayers as previously described
6) Seed cells (@ 150 cells/ mm^2 (144,317 cells / 35 mm dish, in 2 mL)
7) Have duplicate samples for each day interval tested
8) At each time point, take pictures of dishes (phase contrast)

9) Rinse 3X with **complete PBS** (***this needs to be more reproducible next time)

10) Take more pictures and aspirate

11) Add 120 μL of Lysis buffer to each dish and let incubate at rat. for 30 min

LYSIS BUFFER: 0.1 % SDS, 0.1 M Triton X in PBS (w/o ions)

12) Use cell scrapper to remove cells.

13) Harvest with pipette and store in micro centrifuge tube in the -80^{o}C freezer for analysis

Quantification of Cell Number:

1) Make a standard curve to correlate absorbance on plate reader to cell number

   a. Seed controlled number of cell onto 35 mm TC dish for 30 min (1/2 million)

   b. Once cells are stuck to dish, treat as about to harvest DNA of control number of cells

   c. Take 40 μL of the ½ million cell's DNA stock (from steps a & b) add to it 160 μL TE buffer (10 mM Tris-HCl, 1.0 mM EDTA in di H_2O, pH 8.0)

   d. Make serial dilutions from step C above putting 100 μL into each well on black dish and adding 100 μL of TE buffer back to dilute cell count in half (perform in triplicate for stats and error)

2) Sample preparation

   a. Place 20 μL of stored cell lysates into each well on black dish (perform in triplicate for each sample)

   b. Mix TE and stock SYBR Green® (80:1.2) and place 81.2 μL of solution into each well containing sample

   c. Place 1.2 μL of SYBR Green® into wells containing standards

3) Read in Plate reader **Excite = 497 Emission = 520**

ALAMAR Blue:

This method for cell proliferation is very simple, but is indirect. It also interferes with other processes within the cell and can alter the natural cell cycle. Should try another means for proliferation.

1) Monolayers assembled as previously described on 25 mm round cover slips each in a TC six well dish
2) Next day, transfer cover slips to Ultra-Low Adhesion TC dishes
3) Seed Cells (MC3T3-E1) in 10% FBS, 1% PS, α MEM @ 25 cells/mm^2 (Use area of 35 mm dish (A=962.11 mm^2) for seeding area.)
4) Add ALAMAR BLUE dye to make 10% of final volume in well (add 200μL to 2 mL seeding volume) five minute after seeding. This should ensure that all cells are about at the same state since there are different cell attachment rates.

5) Have well with no cells, but same ratio of media to dye to obtain background and track self degradation of dye
6) After 30 minutes, read the entire 6 well dish in the plate reader. (d(0))
    a. Fluorescence mode, Gain 40 or 60, Excite 485, Emission 595
7) Read again at d1, d2, and d3. Any longer and cell metabolic activity can decrease since no media changes.

BrdU Incorporation:

I found that this method for measuring cell proliferation was the best combination of ease of experiment and directness of the measurement.

1) Monolayers were assembled overnight on 25 mm circles coated with 100 Å Ti, and 150 Å Au (done in triplicate for each condition).
2) Assembled SAMs were treated as previously described to tether controlled densities of peptides, and block with BSA prior to cell seeding.
3) MC3T3-E1 cells were seeded at 50 cells/ mm^2 (cells had been synchronized by growing to confluence, then exchanging culture media with 0.5% BSA, 1% P+S, in αMEM for 3 day prior to seeding).
4) After 16h in culture, media was gently exchanged with media supplemented with BrdU at a final concentration of 3.1 μg/mL (from 1000x stock in water).
5) Cells were pulsed with BrdU for 3.5 h, then washed 2x with cPBS
6) Fix for 10 min with cold 70% EtOH

7) Wash 2x with cPBS

8) Denature DNA with 4 N HCl for 20 min, followed by 2x cPBS wash

9) Block with 1% H.D. BSA for 10 min

10) Stain, 1^{o} ms anti-BrdU (Becton Dickinson, Cat # 347580) (dilute 1:3.5 in 1% BSA), 45 min in incubator.

11) Rinse 2x with cPBS

12) 2^{o} = anti-ms IgG (Alexa Fluor 488, Molecular Probes) 1:200; and Eth Homo Dimer-2 1:1000 (Molecular Probes)

13) Rinse and Mount

14) Visualize and take 15-20 representative pictures per sample

15) Use Image Pro to separate green and red channels and count nuclei

16) Report as fraction of proliferating cells (over that 3.5 h time point).

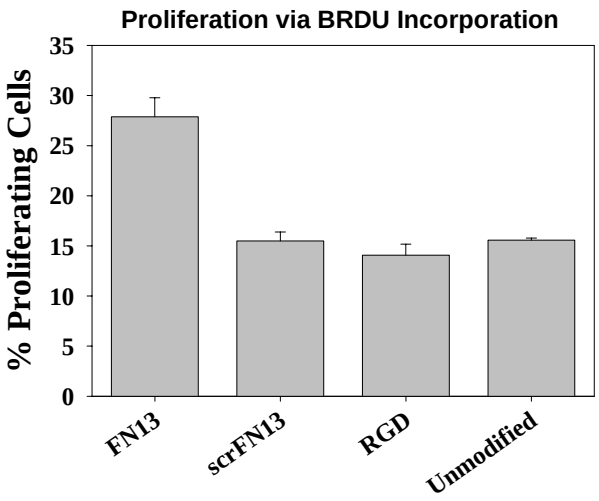

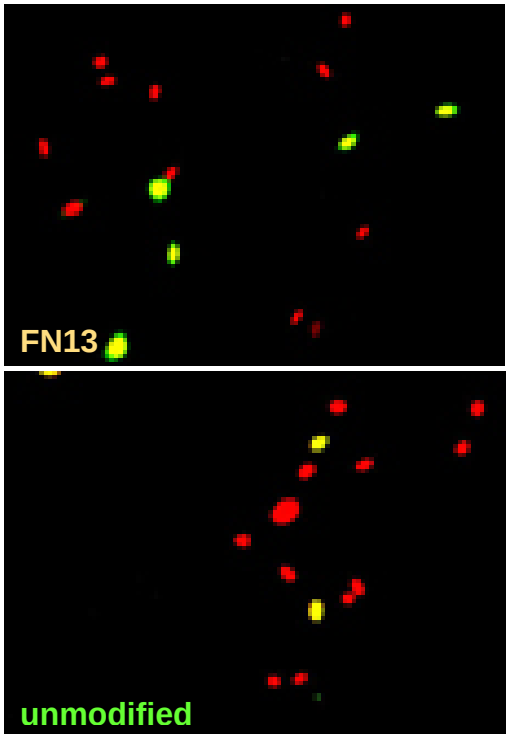

Quantification of Assembled FN Matrix by Western Blot

This is the best method to determine biochemically if FN has been incorporated into the insoluble ECM. DOC insoluble fractions under reduced conditions give the best result since they separate out soluble FN and reduced high molecular weight multimers so that they can run properly on the gel.

Day 0 (can also be same day cells are Lysed)

1. Make Buffers, Reagents and Gels
    a. DOC Lysis buffer
        i. 2% deoxycholate
        ii. 0.02 M Tris HCl (pH 8.8)
        iii. 2 mM PMSF
        iv. 2 mM EDTA
        v. 2 mM iodoacetic acid
        vi. 2 mM N-ethyl-Maleimide
    b. DOC Solubilizing Solution
        i. 1% SDS
        ii. 25 mM Tris-HCl (pH 8.0)
        iii. 2 mM PMSF
        iv. 2 mM EDTA
        v. 2 mM iodoacetic acid
        vi. 2 mM N-ethyl-Maleimide

c. Solutions for GELS

i. (A) 50% acrylamide/BIS (29:1)

1. 50 g 29:1 Bisacrylamide
2. bring to 100mL w/ water, store in fridge up to 2 months in foil

ii. (B) Separating GEL Buffer (1M Tris-HCl pH 8.8)

1. 30.3 g Tris-HCl in 150 mL water, pH 8.8
2. bring to 250 mL in water

iii. (C) 10 % SDS

1. 10 g SDS in 100 mL water

iv. (D) Stacking GEL Buffer (0.375M Tris-HCl pH 6.8)

1. add 11.4 g Tris to 150 mL water; pH to 6.8 and bring water to 250 mL

v. (E) Catalyst (make fresh on the day of use)

1. 100 mg of ammonium persulfate in 2 mL of water

vi. (F) 50% Sucrose

1. 50 g Sucrose; bring up to 100 mL with water

d. Prepare 6X Protein loading Buffers

i. Make 4X Tris-HCl SDS

1. 6.05 g Tris + 40 mL water → pH 6.8 bring to 100 ml with water; filter with 0.45 μm filter and add 0.4g SDS

ii. 6X Reducing Loading Buffer

1. 7 mL 4X Tris-HCl SDS; 3.8 g Glycerol, 1g SDS, 0.93 g DTT 1.2 mg bromo phenol Blue
2. bring up to 10 mL with water

iii. 6X NON-Reducing Loading Buffer

1. SAME AS ABOVE W/O DTT

e. 10 X Running Buffer

i. 240 mM Tris (base), 192 M glycine, 1% SDS in water

1. 29 g Tris (base), 144 g glycine, 10g SDS
2. bring up to 1 L with water

f. 10 X Glycine for Transfer Buffer

i. 30.3 g Tris Base, 144.1 g glycine; bring to 1 L with water

2. Preparing Separating Gels (makes 2.5 gels)

a. 5% Separating Gels

i. 2.5 mL (A); 9.4 mL (B); 250 μl (C); 4 mL (F); 8.3 mL water; 625 μl TEMED; 625 μl (E)

ii. fill cassette to the second from the top line and over lay with water to help release bubbles

iii. polymerize for 1-1.5h

iv. pour off water and add Stacking Gels

3. Stacking GELS 4%
    a. 1 mL (A); 125 μl (C); 4.2 mL (D); 6.3 mL water; 5 μl TEMED; 1 mL (E)
    b. fill to the top of the cassette with the stacking solution and insert a comb
    c. let solidify for 30 min
    d. can let sit on bench over night if using the next day, but stores in fridge for 3-4 d

SAMPLE COLLECTION (Day 1)

1. Aspirate media
2. Wash 2X with complete PBS
3. Add 250 μl of DOC lysing reagent to a 35 mm well; let sit for 10-20 min
4. Scrape with a cell scraper and collect lysates into a micro centrifuge tube
    a. Pipette up and down 25 times to shear DNA with the R-100 pipette
5. Centrifuge >14,000 g for 10 min (may need to spin 2X)
6. Remove DOC Soluble fraction and keep
7. WASH Insoluble fraction 3x with Lysing reagent to further purify
8. Solubilize DOC insoluble fraction in DOC Solubilizing Solution (50 μl)

Protein Quantification

1. Run micro-BCA Assay (see page 66 of lab book 03)

SDS-PAGE, TRANSFER (day 2)

1. prepare protein marker and FN positive control
    a. marker is kept by whom ever ran last gel
    b. FN control = load 1μg (1μl) concentrated pFN
    c. Put samples into Gel loading buffer (6X) if needed, add water to make up volume in behalf of sample, to dilute
    d. Boil samples for 10 min
    e. Prepare 500 mL 1X running buffer (dilute 5X w/ water)
    f. Assemble gel box (cassettes face inward with tape removed, there is a blank if running only one gel)
        i. Fill middle with running buffer and outer channel at least ½ way with buffer
    g. Load samples onto GEL with long GEL loading pipette tips
        i. Include marker and FN control
    h. Run Gel
        i. 90 V in Stacking Gel (~30 min)
        ii. 115-230 V in separating gel (few hours)

Protein Transfer

1. prepare transfer buffer
    a. 100 ml 10 X Tris Glycine, 2.5 mL 10% SDS, 150 ml MeOH, water up to 1L
2. prepare transfer member and filter paper

a. cut PVDF transfer membrane to size of gel (do not handle, use tweezers)
b. pre-wet membrane with MeOH for 30 sec, rinse in di water, soak in 50-100 mL transfer buffer for several minutes
c. cut filter paper to gel size and soak in transfer buffer before use

3. prepare blotting pads
   a. soak blotting pads in buffer before use and remove all bubbles before use

LOAD CATHODE CORE

For two gels

Anode core (+) TOP

Blotting pad (2)

Filter paper (2)

Transfer membrane

2nd gel

filter paper (2)

blotting pad

filter paper (2)

transfer membrane

1st gel

filter paper (2)

} for one gel, replace with blotting pad

blotting pad (2)

Cathode core (-) BOTTOM

- Align plate of chamber and hold over buffer chamber, squeeze together and place into chamber

- close the clamp

- fill chamber with transfer buffer

-attach lid and run at 30V for 90 min. SET TIMER!!!

-Prepare Blotto/Tween blocking buffer (store in fridge)

5% non-fat dry milk in PBS w/o ions + 0.02% azide + 0.2 % tween 20

1L: 50 g milk, 20 mL 1% azide; 2 mL tween

-dry membrane on paper towel for 5 min (protein facing up)

-mark ladder with a pencil

-rinse membrane several times with di water

-block over night with blotto/ tween in fridge (4^{o} C)

DAY 3 Antibody blotting, ECF imaging

Incubate in primary antibodies for 1h at room temperature, rocking (use 10 ml and save solution)

Rb α-FN 1:1000 min

Prepare tween for washing

10X TBS-Tween: 1L: 24.4 g Tris Base, 80g NaCl, pH to 7.6; 10 mL Tween 20, fill to 1L

Wash membrane 2X with TBS-Tween

Rock in TBS-Tween for 15 min

Rock in TBS-Tween 2X for 5 min each

Incubate in secondary antibodies

α- Rb AP 1:10,000 in blotto

Wash membrane 2X with TBS-Tween

Rock in TBS-Tween for 15 min; then Rock in TBS-Tween 2X for 5 min each

EFC imaging

--ECF substrate is stored in the -80C 1B6 (stock is 0.6 mg/mL)

--Use 1 mL per membrane

--Spread evenly on transparency (above my bench)

--Allow excess buffer to drip off membrane and lay face down onto the ECF. Careful to have no bubbles. DO NOT TRY TO MOVE ONCE DOWN, WILL CAUSE SMEARING!!!

-- let react for 5 min

--dry membrane on paper towel

--bring down to 1B to use core Fuji Film Phosophoimager (bring another transparency

--Use the FLA Fluoro 2340 plate (put into machine)

--place membrane face down on the upper left corner

--lay transparency over the membrane to flatten

Image software

--launch FLA 3000 from desktop

--Sample Mode: Fluor 473, Filter Y520

--16 bit gradation, 50 resolution, F10 sensitivity

modify in Image Ganger (??)

open file → image → range scope → move lines to modify contrast

save as bitmap file to a zip!

Example: DOC insoluble Reduced

FN13 scrFN13 RGD No Ligand

Collagen Assembly

The assembly of fibrillar COL matrices was examined using FITC-labeled type I collagen. This was the best method for examining COL assembly since anti-COL antibodies failed to stain properly. The COL antibodies that I tried were primarily for denatured COL and did not bind COL for IF staining. However, there is a wide body of literature using FITC-labeled COL to visualize COL matrix assembly. This can even be quantified real time with live cells. The biggest draw back to this procedure is that the COL must remain in acidic pH or it will self-assemble and form gels. At high concentrations (when added to media) this will also occur. I found this to be a problem as low as 5 μg/ml in media. To prevent self-assembly, to introduce FITC-COL to the culture media, a media change was required.

1) Following 24 h of culture, media was replaced with equal volumes of fresh culture media (37 ^{o}C) and culture media supplemented with FITC-labeled type I collagen (25 ^{o}C, Chondrex, Inc., Redmond, WA) to give a final concentration of 1 μg/ml.
2) Following additional 24 h incubation with FITC-collagen, substrates were fixed and stained for FN as described above.
3) 100X objective showed the best fibrillar images with co-assembly

Cell Differentiation:

1) Monolayers were assembled as described above on 25 mm circles
2) Low passage MC3T3-E1 osteoblasts were seed on functionalized monolayers and on COL-coated TC plastic @ 200 cells/ mm^2 (preferably in mineralized 10 % FBS, 1% PS, in α-MEM) seeding day = D(0)
3) On D(1), D(3), and D(5) media was exchanged with supplements; 50 μg/ml L-ascorbic acid and 2.1 mM sodium β-glycerophosphate.
4) On day 7, media was aspirated and and samples were washed 2x with cPBS (carefully, or cells will delaminate).

Alkaline Phosphatase Activity:

1) Add 500 ul of 50 mM Tris-HCl (pH 7.4) to each well.
2) Scrape and add to 3.5" plastic test tube
3) Sonicate each sample 2 x 10 sec @ 5.5-6.0 amps
4) Transfer to 1.5 mL epindorf tube
5) Centrifuge >10,000g for 5 min
6) Pellet will form on the bottom; transfer all but pellet to fresh tube
7) Run μBCA on each sample to use equal amounts of total protein for ALP activity assay

Micro BCA

1) Get 96 well TC plastic dish from TC room
2) Left three columns get serial dilutions of BSA (start with 1mg/ml)
3) Any well that will have sample gets 45 μl of diH_2O, and 5 ul sample (1:10 dilution)
4) From Pierce micro BCA kit, mix 25:24:1 part A:B:C with enough volume for 50 μl per well (including serial dilutions)
5) Put in incubator for 1 hr.
6) Read on Levenston plate reader with an absorbance of 562 nm.

APL Activity

1) In a 96 well black dish, make serial dilutions of ALP (stock in 3A5, -20 ^oC)
2) 2.5 ul of stock with 97.5 ul di H_2O; (gives 0.025 ug/ul)
3) 160 ul PBS with 40 ul of above to get 200 ul of 0.005 U / ul ALP (U = unit, 1 U = 1 umol / min)
4) 50 ul of #3 to each of the top three wells for serial dilution
5) 25 ul of PBS to all other wells of the serial dilution (and where sample goes), then do the serial dilution with 25 ul
6) Subtract volume need from sample from each sample well and add sample (in volume to give equal 2.5 ug of protein to each well)
7) 100 ul of MUP solution to each well (see ELISA for more details)
8) 1 h incubation under foil, in incubator if desired

9) Read in plate reader Excite = 360, Emission = 465; gain 40-60

Gene Expression

The procedure for the analysis of data and work up of samples takes multiple days and is broken up as so in the following protocol. Some days can be combined to save time, but days get very long with high sample numbers due to time intensive steps.

"Day #1 Cell Lysing"

1) Monolayers were assembled as described above on 25 mm circles
2) Low passage MC3T3-E1 osteoblasts were seed on functionalized monolayers and on COL-coated TC plastic @ 200 cells/ mm^2 (preferably in mineralized 10 % FBS, 1% PS, in α-MEM) seeding day = D(0)
3) On D(1), D(3), and D(5) media was exchanged with supplements; 50 μg/ml L-ascorbic acid and 2.1 mM sodium β-glycerophosphate.
4) On day 7, media was aspirated and samples were washed 2x with cPBS (carefully, or cells will delaminate).
5) In PRC room, add 350 μl of RLT Buffer: β-mercapto ethanol (100:1 mixture)
6) Scrape with cell scraper and put into purple two-part QIA Shedder tube.
7) Spin 2 min at max speed in centrifuge to homogenize
8) Remove purple top and replace lid; then place in freezer in -80 ^{o}C.

“Day #2 –RNA Purification”

1) Thaw tubes from above
2) Add 350 μl of 70 % EtOH (made with sterile water)
3) Pipette up and down to “homogenize” and then transfer to the RNeasy mini columns (pink)
4) Centrifuge 15 sec @ >10,000 rpm (only RNA should stay on column, but some DNA could)
5) Pour out what goes through the column
6) Add 350 μl RW1 to each tube and centrifuge for 15 sec at >10,000 rpm to rinse, toss what goes through
7) Make mixture of 10 μl DNase I stock with 70 μl RDD buffer per sample. Mix gently by inverting the tube several times.
8) Place 80 μl directly onto each membrane and let incubate at room temperature for 15 minutes.
9) Repeat step 6
10) Transfer columns to fresh collection tubes and put 500 μl RPE buffer onto each column and centrifuge for 15 sec @ >12,000 rpm, toss flow through
11) Add another 500 μl RPE buffer and spin 2 min @ > 12,000 rpm
12) Transfer column to lock-cap epindorph and add 40 μl RNAse free water directly to the filter. Spin 1 min > 12,000 rpm to elute RNA
13) Cap and store in the -80 ^{o}C.

"Day #3 Spec RNA to Determine the Concentration"

1) Use the Levenston U.V. Spectrophotometer to determine the concentration of each sample (DNA/ RNA spec at a wave length of 260 nm).

"Day #4 Real Time PCR"

1) Use template to determine how much RNA (volume) is needed for 1 μg RNA to make equal amounts of cDNA
2) Used B.K.'s standards and primers.
3) Set up a 96-well tube in PR trays w/ 8-joined tubes for each row
4) Columns 1-3 get 1 μl each of standard in the top spots and do serial dilutions
5) Rest of tubes get 1 μl of above cDNA 1 μg solution
6) Put 29 μl of MMA Solution in each well (Primers (F + R), Water, and Buffer)
7) Bring to PCR room

"In PCR Room"

1) Use the top computer (the MAC)
2) Sequence Detector V. 1.7a
3) New plate
4) Dye Layer → Sybr
5) Thermal Cycler Rxn (30 μl)

6) Sample Type Set up

a) All tabs = None

b) Except standard = sybr

c) Unknown = sybr

d) Temp = sybr

e) ☐ Quencher; None | OK |

7) Analysis → Analyze

8) Viewer: Rxn vs Cycle

9) Double click on the X- Axis

Max value > 15

Set baseline before first take of curve (before increase in the curve, baseline region)

-update calc.

Change threshold

Scroll screen, click, and drop

Click OK

Close

File → Export → Results → Desktop

*** Use template to determine amounts

Cell Differentiation: Von Kossa Staining for Matrix Mineralization

1) Following 14 days of culture, cells were fixed in 70% ethanol, rinsed and stained by von Kossa.

2) 5% $AgNO_3$ was added to each dish and plates were incubated under uniform light exposure for 30 min.

3) The stain was then fixed in Na_2SO_3 for 2 min, rinsed and dried.

4) Plates were scored for percent mineralization using Image Pro Plus image acquisition and analysis software (Media Cybernetics, Silver Springs, MD).

LIST OF PUBLICATIONS

Capadona, J.R., Petrie, T.A., Fears, K, Latour, R.A., Collard, D.M., & García, A.J. Surface-directed assembly of fibrillar extracellular matrices. *In Preparation* (2005).

Capadona, J.R., Collard, D.M., & García, A.J. Fibronectin adsorption and cell adhesion to mixed monolayers of tri(ethylene glycol)- and methyl-terminated alkanethiols. *Langmuir* **19**, 1847-1852 (2003).

Gallant, N.D., Capadona, J.R., Frazier, A.B., Collard, D.M., & García, A.J. Micropatterned surfaces to engineer focal adhesions for analysis of cell adhesion strengthening. *Langmuir* **18**, 5579-5584 (2002).

VITA

Jeffrey R. Capadona was born in 1978 in Oak Lawn, IL. He graduated from Saint Joseph's College in Rensselaer, IN after completing a B.S. in Chemistry. During his undergraduate years, Jeffrey was exposed to numerous areas of chemistry including plasma sprayed polymer adhesives while studying as a National Science Foundation Summer Undergraduate Research Program Fellow (NSF S.U.R.P). An interest in applying chemistry to fundamental applications in medical sciences led Jeffrey to graduate school at Georgia Institute of Technology in August of 2000. Jeffrey was co-advised by David Collard in the School of Chemistry and Biochemistry and Andrés García in the Woodruff School of Mechanical Engineering & the Petit Institute for Bioengineering and Biosciences. Jeffrey's research interests continue to fall on the cusp between applied chemistry and bioengineering.